IMPACT ASSESSMENT OF CLIMATE AND LAND USE CHANGE ON TIKUR WUHA RIVER

DIRIBA SHUMA

March 2015

E-Mail:- diribashuma@gmail.com

IMPACT ASSESSMENT OF CLIMATE AND LAND USE CHANGE ON TIKUR WUHA RIVER

BY: DIRIBA SHUMA

A Thesis Submitted to School of Graduate Studies Addis Ababa University in Partial Fulfillment of the Requirement for the Degree of Master of Science in Hydraulics Engineering

March 2015

E-Mail:- diribashuma@gmail.com

IMPACT ASSESSMENT OF CLIMATE AND LAND USE CHANGE ON TIKUR WUHA RIVER

A Thesis Submitted to School of Graduate Studies Addis Ababa University in Partial Fulfillment of the Requirement for the Degree of Master of Science in Hydraulics Engineering.

Members of examining board

1. DR. FANTAHUN ABEGAZ -------------- ----------
   Advisor signature Date

2. Dr. MEBRUK MOHAMMED -------------- -------------
   Internal examiner signature Date

3. Dr. AGIZEW NIGUSSIE -------------- -------------
   External examiner signature Date

4. ______________________ -------------- -------------
   Chairman signature Date

E-Mail:- diribashuma@gmail.com

CERTIFICATION

The undersigned certify that he has read the Thesis entitled **Impact Assessment of Climate and Land Use Change on Tikur Wuha River** and hereby recommend for acceptance by the Addis Ababa University in partial fulfillment of the requirements for the degree of Master of Science (Engineering).

____

Fantahun Abegaz (ph.D.)

(Supervisor)

____

Date

DECLARATION AND COPYRIGHT

I, Diriba Shuma , declare that this thesis is my own original work and that it has not been presented and will not be presented by me to any other university for Similar or any other degree award.

Signature: ______________________________

Date: __________________

E-Mail Address:- diribashuma@gmail.com

Abstract

The Specific objectives of this study are to asses impact of land use and climate change on Tikur Wuha River located at Awassa Lake catchment. Hydrologic model, HEC-HMS model was used to asses' impact of climate and land use change.

Orthorectified Landsat MSS, TM and ETM+ images covering the study area was classified by supervised image classification using maximum likelihood classifier (MLC). The sample set for the classification was created using the combination of bands 7, 4, 2 (for Landsat TM and ETM+ images of year 1986 and 2000, 2005,) and bands 4, 2,1 (for Landsat MSS image of year 1973). Result of image classification showed 28.77% reduction in forest cover, 3.6% reduction in lake cover, 23.49% increase in agricultural land, 3.6% increase in swamp and 5.3% increase in grassland within the span of 32 years from 1973 to 2005. Hydrologic impact assessment indicated that with the land-cover changes that have occurred, there is a change on the catchment runoff. This study reveals that watersheds run off was lower by 5.79 % in period 1973, 0.27% in 1986 compared to period of 2005 as reference.

Statistical Down-Scaling Model (SDSM) was used to derive local scale information from global climate scenarios generated by GCMs. Among four scenario families of Special Report on Emissions Scenarios (SRES), three of them (A1B, A2 and B1,) scenarios were used in this study. Historical weather data collected were used to calibrate and validate downscaling models. After calibration and validation, the downscaling model was used for computing future temperature and precipitation pattern. SDSM downscaled future precipitation was used in hydrologic model to asses impact of future climate change. The assessment showed that average mean flow increased in the future periods considered (2015 - 2035, 2040 - 2050 and 2080-2099). SDSM downscaling data resulted increase in the mean annual flow by minimum of 20.05 % and maximum of 51.67 % during time periods considered for three of emission scenarios considered.

Impact assessment of land use change showed that the runoff volume of Tikur Wuha River increases over past 32 years. Climate change impact analysis also showed that the river flow would increase in future.

Acknowledgement

First, thanks to almighty God for helps and all things done. I thank Debre Berhan University for sponsoring me to attend my education.

I am deeply indebted to my advisor Dr. Fantahun Abegaz for his passionate and unreserved support, guidance, encouragement and patience, which contributed to the success of this study.

I would like to thank Ministry of Water, Irrigation and Energy, National meteorological Agency (NMA), National map agency for providing me Hydrological, Meteorological data and topographic map for my study area. I would like to acknowledge the invaluable input of all individuals and organizations, in particular those who provided materials, climate and image data and who helped me a lot during the data collection period. I am highly indebted to my families and all my friends for their supports.

ACRONYMS

A2a - Medium-High Emissions Scenario

AGCM – Atmospheric General Circulation Model

CCCMA - Canadian Centre for Climate Modeling And Analysis

CGCM – The Canadian Global Coupled Model

CICS – Canadian Institute for Climate Studies

CN – Curve Number

DDC – Data Distribution Centre of IPCC

DEM - Digital Elevation Model

DN - Digital Number

DT - Decision Trees

ETM+ - Enhanced Thematic Mapper Plus

GCM - General Circulation Model

GFDL- Geophysical Fluid Dynamics Laboratory USA

GIS – Geographic Information System

GLCF - Global Land Cover Facility

GLWD - Global Lakes and Wetlands Database

HBV - Hydrologiske Byrån Avdeling För Vattenbalans

HEC- HMS - Hydrologic Engineering Center-Hydrologic Modeling System

HSG - Hydrological Soil Groups

IPCC – International Panel on Climate Change

ITCZ – Inter Tropical Convergence Zone

M.A.S.L – Meters above Sea Level

MLC - Maximum Likelihood Classifier

MPI - Max-Planck-Institute for Meteorology Germany

MSS - The Multispectral Scanner

NCAR - National Centre for Atmospheric Research USA

NCEP – National Centre for Environmental Prediction

NDVI - Normalized Difference Vegetation Index

NFS - Nile Forecast System

NIR - Near Infrared Or:

NN - Neural Networks

RCM – Regional Climate Model

RMS - Root Mean Square Error

RS - Remote Sensing

SCS – Soil Conservation System

SDSM - Statistical Downscaling Model

SMA - Soil Moisture Accounting

SRES - Special Report on Emissions Scenarios

SRTM - Shuttle Radar Topographic Mission

SVM - Support Vector Machines

SWAT – The Soil and Water Assessment Tool

SWIR - Short-Wavelength Infrared

TAR – Third Assessment Report

TM- Thematic Mapper

USACE - United States Army Corps of Engineers

UTM - The Universal Transverse Mercator

W.W.D.S.E-Water Works Design and Supervision Enterprise

WGEN – Weather Generator

Table of Contents

Appendixes

List of Figures

List of Tables

1 Introduction

1.1 Back ground

Tikur Wuha River is the primary affluent and major tributary of Lake Awassa draining from the eastern part of Lake Awassa watershed and covering a catchment area of 620 km^2. Tikur Wuha River starts from the small Cheleleka Lake, upstream of Lake Awassa where all perennial and some of the seasonal rivers drains into before going to Lake Awassa. The surface area of Lake Cheleleka was about 12 km^2 in 1972, but currently it has completely disappeared because of siltation. The lake floor, which once was covered by water, is now filled with sediments transported from the eastern highlands as a result of deforestation that has taken place over the last 30 years. Prior to the filling up of the basin with silt, Lake Cheleleka used to serve as a sediment trap for the Tikur Wuha River that flows into Lake Awassa. Because of losing this function as a sediment trap, water and sediment load to Tikur Wuha go now directly into Lake Awassa (W.W.D.S.E.2001).

Increased concentration of greenhouse gases is expected to alter the radiative balance of atmosphere, causing increases in temperature and changes in precipitation patterns and other climatic variables (Houghtonet al., 1990). One of the most important impacts on society of future climatic changes will be changes in regional water availability. Such hydrologic changes will affect nearly every aspect of human well-being, from agricultural productivity and energy use to flood control, municipal and industrial water supply, and fish and wildlife management. For example, larger reservoir spillways and drainage waterways will be required where runoff is expected to increase, and higher water supply storage needed where runoff is expected to decrease. The tremendous importance of water in both society and nature underscores the necessity of understanding how a change in global climate could affect regional water supplies.

(Water Resources Management, 1999.)

As per the IRI Technical Report 08-05: IRI Downscaling Report, assessments of climate change in Africa indicated some consensus of reduced winter rainfall in southern Africa, increased annual rainfall in east Africa and uncertainty for the rest of Africa.

In addition to climate change, the negative impacts of land-cover change to the natural environment especially in watershed ecosystems have been a widely recognized problem throughout the world. Changes such as forest cover reduction through deforestation and conversion for agricultural purposes can alter a watershed's response to rainfall events, that often leads to increased volumes of surface runoff and greatly increase the incidence of flooding and sedimentation of receiving water bodies (McColl.et.al, 2007 and Cebecauer.et.al, 2008). The detection of these changes is crucial in providing information as to what and where the changes have occurred and to analyzing these changes in order to formulate proper mitigation measures and rehabilitation strategies (Jojene.et.al,2011).This study cover the detection of land use change using satellite image analysis and assesses land use change impact using hydrologic model. Additionally, the study also analyses impact of climate change on water availability of the catchment.

1.2 General Objective

The general objective of the study is to assess the impact of climate and land use change on Tikur Wuha River for future development and management of sustainable water resources for the sub-catchment and down-stream users.

1.2.1 **Specific Objectives:-**

- To assess the impact of land use change on Tikur Wuha River
- To assess the impact of climate change on Tikur Wuha River

1.3 Statement of the Problem

From surface water resource point of view Lake Awassa is closed lake and fresh lake unlike most of the rift valley lakes. (Tenalem, 1998).Closed lakes are very dependent on the balance of inflows and evaporation and are very sensitive to change in either climatic variability, whether driven by climate change, or human interventions. This also means that they are very important indicators of climate change and can provide records of past hydro climatic variability over a large area (e.g., Kilkus, 1998; Obolkin and Potemkin, 1998). Small closed lakes are most vulnerable to a change in climate; there are indications that even relatively small changes in inputs can produce large fluctuations in water level and salinity in small closed lakes in western North America (Laird *et al*., 1996).

Therefore, assessing impact of climate and land use change on Tikur wuha river flow will help to maintain sustainability of Lake Awassa as Tikur wuha is a main tributary to this lake.

The majority of the settlement is found in this river catchment together with major socio-economic activities because of the suitable environmental conditions and natural resources availability. Therefore, Peoples negatively affect the land cover of the area. The negative impacts of land-cover change to the natural environment especially in watershed ecosystems have been a widely recognized problem throughout the world. The impact of land use change needs studies and measures have to be taken to protect water resources in the catchment. Many studies that address the effect of land cover changes on hydrological regimes were undertaken in experimental catchments of small scale (<1 km^2) (e.g. Bosch and Hewlett, 1982; Troendle and King, 1987; Lavabre et al., 1993; Iroum et al., 2005; Guillemette et al., 2005). However, water resources management often requires information on catchments of regional (>1000 km^2) or larger scale. Changes of land cover typically is a phenomenon at local or plot scale (e.g. 1 ha–1 km^2). Therefore, the impact of any disturbance will be minimal when catchments are of regional or larger scale. Therefore, when considering larger scale catchments, changes of land cover should be observable over larger domains and in essence is the premise to assess hydrological impacts of such changes. Changes in regional water availability will affect nearly every aspect of human well-being, from agricultural productivity and energy use to flood control, municipal and industrial water supply, and fish and wildlife management.

Daniel and Yonas (2010), Yemane (2004), reported recent studies with focus on the hydrology of the Lake Awassa catchment. Daniel and Yonas (2010) showed increase in cultivated land, natural vegetation and urban land use of the catchment. In addition, the study showed that the surface runoff will increase in future and lake water will rise due to land use change. During simulation of land use change the study uses linear regression from the percentage of land use in 1965 to 1998 to estimate future land use change. Yemane (2004) also showed increased trend of Lake Awassa water level. Both studies asses the catchment as a whole not specific to Tikur Wuha sub - catchment. The studies did not consider climate change impact and does not study the land use change impact specifically. However, both studies had recommended that further study is needed specific to Tikur Wuha sub - catchment with land use and climate change impact.

This study focuses on sub-catchment level to better understand impact of climatic and land use change as the water resource planning and managements were carried out at the sub- catchment level.

Therefore, understanding the mechanisms in space and time will help to manage water resources in sub-catchment and combat the potential damage that could be caused as a result of flooding and drought.

1.4 Research Questions

Questions to be answered by this study are:

Is there Land use land cover change in Tikur Wuha sub-catchment?

Does the Land use change have impact on the river flow?

Is there change on climate variable (Precipitation) in the past?

What is the trend of temperature and precipitation in the future?

Is there climate change impact on Tikur Wuha River in the future?

Is there increment or decrement on stream flow of Tikur Wuha River comparing present and future period Due to climate change?

2 Literature Review

The literature review were arranged in two parts which are; General science of the study and specific studies which were carried out on the study area.

2.1 Land Use Change Detection

Change detection is the use of remotely sensed imagery of a single region, acquired on at least two dates, to identify changes that might have occurred in the interval between the two dates. Those two dates can be years apart, for example to track changes in urbanization, or days apart, for example to track changes from a volcanic eruption.

Change detection has been applied to examine effects such as land use changes caused by urban and suburban growth, effects of natural disasters (such as floods, forest and range fires), and impacts of insect infestations upon forest cover, for example. Change detection requires application of algorithms that are specifically designed to detect meaningful changes in the context of false alarms changes that are, in reality, simply artifacts of the imaging process. In brief, the two images must be compatible in every respect: scale, geometry, resolution. Otherwise, the change detection algorithm will interpret incidental differences in image characteristics as changes on the landscape.

There has been much research devoted to evaluating alternative change detection algorithms. A basic distinction between pre-classification and post-classification comparisons captures a primary division in the natures of the approach. Post-classification change detection defines changes by comparing pixels in a pair of classified images (in which pixels have already been assigned to classes). Post-classification change detection typically reports changes as a summary of the “from-to” changes of categories between the two dates. Pre-classification change detection examines differences in two images prior to any classification process. Pre-classification algorithms typically permit the analyst to set thresholds for the magnitude of changes to be detected and highlighted. (Tammy E. Parece James B. Campbell, 2013).

A critical prerequisite for application of change detection by remote sensing is the identification of suitable pairs of images representing the same region. The analyst must assure that:

I. The two images register (that they match exactly when superimposed),

In case the image should be combined with data in another coordinate system or georeference, then a transformation has to be applied. This results in a ‘new’ image where the pixels are stored in a new row/column geometry, which is related to the other georeference (containing information on the coordinates and pixel size). This new image is created by applying an interpolation method called resampling. The interpolation method is used to compute the radiometric values of the pixels, in the new image based on the DN values in the original image. After this action, the new image is called geo-coded and it can be overlaid with data having the same coordinate system.

There are three different interpolation methods:

- Nearest Neighbor: In the nearest neighbor method, the value for a pixel in the output image is determined by the value of the nearest pixel in the input image
- Bilinear: The bilinear interpolation technique is based on a distance dependent weighted average, of the values of the four nearest pixels in the input image
- Bicubic: The cubic or bicubic convolution uses the sixteen surrounding pixels in the input image. This method is also called cubic spline interpolation.

II. That they were acquired during the same season, especially to track changes in vegetation, and

III. That there are no significant atmospheric effects.

The georeference formats employed by the Global Land Cover Facility (GLCF) for Landsat imagery include a UTM projection and a WGS84 datum and ellipsoid. In addition to this georeference information, a Landsat image file from the GLCF will have been processed using a resampling technique. Finally, the Landsat image may have been orthorectified, especially if it is a Landsat Geo-Cover image. All these characteristics are listed in the meta data file accompanying the scene.

Imagery from the Landsat satellites has been acquired since 1972, with a variety of characteristics to consider. There have been six operational Landsat satellites, with three different useful sensors, all of which are available through the GLCF. The Multispectral Scanner (MSS) sensor provides the oldest and lowest quality Landsat data, from 1972 – present. The Thematic Mapper (TM) sensor has improved quality and is available from 1984 – present. The Enhanced Thematic Mapper plus (ETM+) sensor on the Landsat 7 satellite was the best quality of all, until a mechanical anomaly occurred on the sensor in May 2003. Landsat 7 imagery is still being collected, even with this unfortunate defect. Landsat satellites acquire imagery in a regular, tiled fashion, (http://glcf.umiacs.umd.edu).

2.1.1 **Image classification**

2.1.1.1 **Supervised Classification**

In supervised classification, the user relies on her/his own pattern recognition skills and prior knowledge of the data to help the system determine the statistical criteria (signatures) for data classification. To select reliable samples, the user should apply information (either spatial or spectral) about the pixels that they want to classify. The location of a specific characteristic, such as a land cover type, may be known through field observations that acquire knowledge about the study area from first-hand observation, analysis of aerial photography, personal experience, etc. Field data are considered to be the most accurate (correct) data available about the area of study. They should be collected at the same time as the remotely sensed data, so that the data correspond as much as possible. However, all field data may not be completely accurate because of observation errors, instrument inaccuracies, and human shortcomings. Global positioning system receivers are useful tools to conduct ground truth studies and collect training sets. Training samples are sets of pixels that represent what is recognized as a discernible pattern, or potential class. The system will calculate statistics from the sample pixels to create a parametric signature for the class.

Not every pixel value can be assigned to a class. With training data, many of pixel values can be identified and assigned to a specific class. However, what happens with the unassigned pixels? In addition, some pixel values may fall into two classes. In supervised classification, you will choose the method/algorithm that decides how to assign these pixels.

ArcGIS provides four supervised classification options: Interactive, Maximum Likelihood, Class Probability, and Principal Components among the several classifiers available. The Maximum Likelihood Classifier (MLC) has been widely used to classify Remote sensing (RS) data and successful results of applying this classifier for land-cover mapping have been numerous (e.g., Cherill, Cingolani, et.al, 1994) despite the limitations due to its assumption of normal distribution of class signatures. Its use has also been effective in a number of post-classification comparison change detection studies .While recent studies have indicated the superiority of newly developed image classification techniques based on Decision Trees (DT), Neural Networks (NN) and Support Vector Machines (SVM) over MLC the advantage of MLC over these classifiers is significant owing to its simplicity and lesser computing time. This is crucial, especially for rapid land-cover mapping and change detection analysis of numerous multi-temporal images in a situation where time and computing resources are sorely limited. Moreover, the accuracy of any classifier is affected by the number of training samples and by selecting which bands to use during the classification. As reported by Huang et al., improved classification accuracies of MLC, DT, NN and SVM can be achieved when training data size is increased and when more bands are included. In the case of Landsat image classification, improvements due to the inclusion of all bands exceeded those due to the use of a better classifier or increased training data size, underlining the need to use as much information as possible in deriving land-cover classification from RS images. All these aspects were considered in the detection and analysis of land-cover change in the Landsat images of the study area.

2.1.1.2 **Evaluating Normality, Separability and Partitioning**

Normality, separability and Partitioning of the training classes were evaluated during image classification.

Each class's histogram was created, seen, and corrected until the distribution become normal. Using the scatter plot of the training data separability; if the training samples represent different spectral classes, of the training sample was seen. Training Samples were merged or deleted to avoid overlapping. Statistics shows measures that characterize your training data (such as mean, mode, etc.) and covariance.

Covariance evaluates the correlation of values in the different bands. Low values indicate that the values in a pair of bands tend to increase and decrease independently. High values indicate that the values in the two bands tend to increase and decrease together.

For effective classification, we prefer to see low covariance, indicating that the training data are providing independent information (i e., the data from the training fields are not replicating each other). (Tammy E. Parece James B. Campbell, 2013).

2.1.1.3 **Accuracy Assessment**

Accuracy Assessments were performed on classified images to determine how well the classification process accomplished the task. An accuracy assessment compares your classified image to an image, which is assumed correct (such as an aerial photo). This task was accomplished by compiling an error matrix. An error matrix is a table of values that compares the value assigned during the classification process to the actual value from an aerial photo. These were compared on a point-by-point basis. A random set of points was generated for the region covered by the area. Then using the aerial photos, the value for each point was identified. Then, these same random points were used to identify each point's known value in the classified image. The error matrix table was completed by comparing these two values. An important component of accuracy assessment, Cohen's kappa co-efficient was calculated from the error matrix. Kappa tells us how well the classification process performed as compared to just randomly assigning values, i.e. did we do better than random. (Tammy E. Parece James B. Campbell, 2013)

2.2 Climate Change Analysis

Assessing the impact of climate change on stream flows, soil moisture, ground water and other hydrological parameters essentially involves taking projections of climatic variables (e.g., precipitation, temperature, humidity, mean sea level pressure etc.) at a global scale. Downscaling these global-scale climatic variables to local-scale hydrologic variables, and computing hydrological components for water resources variability and risks of hydrologic extremes in the future are the major components. Projections of climatic variables globally have been performed with General Circulations Models (GCMs), which provide projections at large spatial scales.

Such large-scale climate Projections must then be downscaled to obtain smaller-scale hydrologic projections using appropriate linkages between the local climates. A number of studies have investigated downscaling methods for establishing a connection between coarse-resolution GCMs and hydrologic models (e.g. Wilby et al., 1998, 2000; Hay and Clark,2003; Wood et al.,2004; Benestad et al.2008).

2.2.1 **Downscaling**

Downscaling is the term for using models (statistical or dynamic) to increase the resolution of GCM output for a particular location. It may be performed to increase the temporal resolution (e.g., from monthly to daily values of Precipitation and Temperature) or the spatial resolution (e.g., from a GCM grid cell size down to the weather station scale). The two main approaches used for deriving local or regional scales information from the global climate scenarios generated by GCMs are dynamic downscaling, which involves a nested regional climate model (RCM) and statistical downscaling techniques which employs a statistical relationship between the large scale climatic state and the local variations derived from historical data. Dynamic downscaling primary contribution is through the inclusion of more realistic topography and land use/vegetation. Due to systematic errors that inevitably occur, RCMs require statistical corrections to provide realistic output. The main drawback of RCMs is that they are computationally costly complex models (Solman and Nunez1999). As such, RCM data is relatively scarce, fewer greenhouse gas emission scenarios are run and, except for a few inter-comparison studies, data from more than one model is rarely available for climate change uncertainty studies. Moreover, despite improvements, the output of RCMs is still too coarse for several practical applications, such as smaller watersheds and site-specific agricultural impact studies, which may need local and site-specific climate scenarios. Statistical downscaling utilizes relationships between GCM output and historical data to produce finer spatial and temporal resolution climate data at the regional level. They are typically as effective as and less expensive than dynamical downscaling. Especially useful for temporal downscaling (from monthly to daily values).

A diverse range of statistical downscaling techniques are available where each method lies, generally, in one of the three categories, namely regression (transfer function) methods , stochastic weather generators and weather classification schemes (Wilby et al., 2004).

Among the widely applied statistical downscaling techniques is the universally multiple linear regression models called Statistical Down-Scaling Model (SDSM).

Although there is no 'standard' approach to downscaling, i.e., obtaining finer resolution scenarios of climate change from the coarser resolution GCM output, there are two pieces of software available which can be used to undertake spatial and temporal downscaling: (Canadian Institute for Climate Studies, 1999-2005).

Those are:

I. **SDSM**, a **S**tatistical **D**own-**S**caling **M**odel, developed by Rob Wilby and Christian Dawson in the UK, and
II. **LARS-WG**, a stochastic weather generator developed by Mikhail Semenov, also in the UK.

Statistical downscaling methods involve developing quantitative relationships between large-scale atmospheric variables (predictors) and local scale surface variables (predictand) through the transfer functions (Wilby et al., 2004). The most common form has a predictand as a function of the predictors. The two frequently used terms in statistical downscaling are defined as follows as used in many publications. The predictor is the input data used in statistical models, typically a large-scale variable describing the circulation regime over a region. The predictor is also known as 'independent variable', or simply as the 'input variable', usually written as Predictand = f (predictors).The predictand is the output data, typically the small-scale variable representing the temperature or rainfall at a weather/climate station. The predictand, is also known as 'dependent variable',' response variable', 'responding variable', or simply as the 'output'. Statistical downscaling is computationally inexpensive, and thus can be easily applied to the output of different GCM experiments (Wilby and Dawson, 2007). Additionally, it can be used to provide local information, which could be most needed in many climate change impact applications.

2.2.1.1 **Spatial Downscaling**

Spatial downscaling refers to the techniques used to derive finer resolution climate information from coarser resolution GCM output. The fundamental bases of spatial downscaling are the assumptions that it will be possible to determine significant relationships between local and large-scale climate (thus allowing meaningful site-scale information to be determined from large-scale information alone) and that these relationships will remain valid under future climate conditions. The spatial resolution of most GCMs is between about 250 and 600 km. The forcing and circulations which affect regional climate, however, generally occur at much finer spatial scales than these and can lead to significantly different regional climate conditions than are implied by the large-scale state.

Spatial downscaling may be able to incorporate some of these regional climate controls and hence add value to coarse-scale GCM output in some areas - although its usefulness will be very much dependent on the region and climate data available. Each case will be different and may necessitate the investigation of a number of different downscaling techniques before a suitable methodology is identified and in some cases, it will not be possible to improve upon the coarse-scale scenarios of climate change by downscaling.

There are a number of general recommendations concerning spatial downscaling, which if followed, should facilitate the process:

- The GCM being used for spatial downscaling should be able to simulate well those atmospheric features, which will influence regional climate, e.g., jet streams and storm tracks.
- The downscaling technique should be based on a climate variable which does not exhibit large sub-grid scale variations, i.e., it is better to use a variable such as mean sea level pressure rather than one such as precipitation.
- The variables used in the downscaling process should also ideally be primary model variables, i.e., they are direct model output (e.g., sea level pressure) and are not based on parameterisations involving other model variables, as is the case with precipitation

Spatial downscaling techniques can be divided into empirical/statistical, statistical/dynamical methods and higher resolution modeling, e.g., regional climate modeling.

1. Empirical/statistical and statistical/dynamical methods

These techniques refer to methods in which sub-grid scale changes in climate are calculated as a function of larger-scale climate and can be broadly categorized into three classes:

- **Transfer functions**: - statistical relationships are calculated between large-area and site-specific surface climate, or between large-scale upper air data and local surface climate.
- **Weather typing**: - statistical relationships are determined between particular atmospheric circulation types (e.g., anticyclonic or cyclonic conditions) and local weather.
- **Stochastic weather generators**: - these statistical models may be conditioned on the large-scale state in order to derive site-specific weather.

The fundamental assumption behind all these methods is that the statistical relationships, which are calculated using observed data, will remain valid under future climate conditions.

Figure 2.1 illustrates the transfer function approach to empirical/statistical spatial downscaling. Blue arrows indicate steps based on observed climate data. Red arrows indicate the application of GCM data to determine site values corresponding to a particular future period.

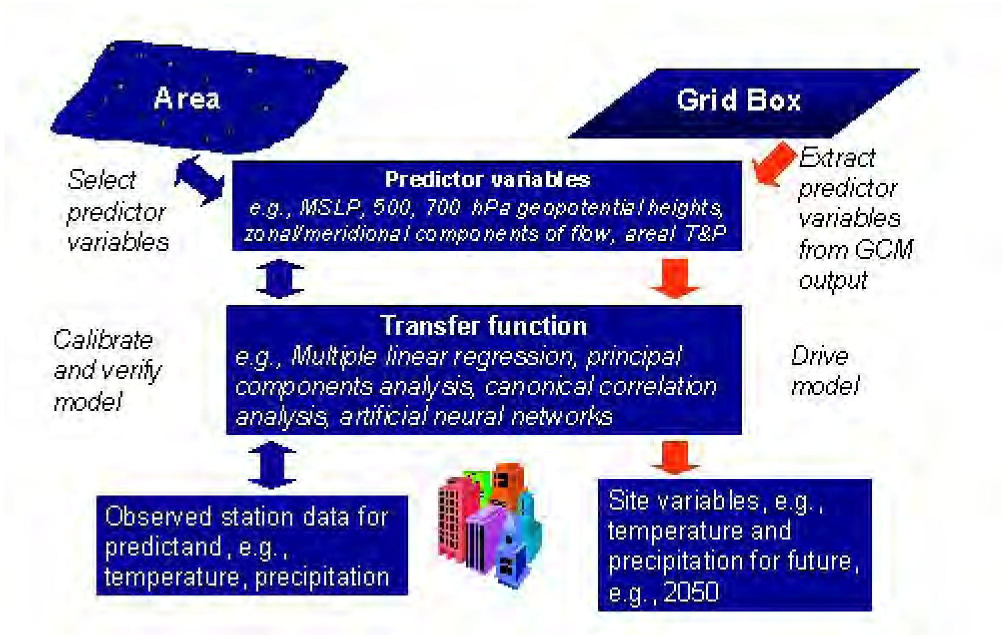

Figure. 2.1: The transfer function approach to spatial downscaling. (Adopted from Canadian Institute for Climate Studies)

The downscaling procedure using statistical/dynamical techniques is very similar to that described above for empirical/statistical methods. In this case, weather types, or atmospheric circulation patterns, are used rather than large-scale predictor variables and statistical relationships between the types, or patterns, and observed station data are calculated (see Figure 2.2). Blue arrows indicate steps based on observed climate data. Red arrows indicate the application of GCM data to determine site values corresponding to a particular future period. The first step in this process is the identification of the weather types, or atmospheric circulation patterns, usually from atmospheric pressure information. These types or patterns may be based on existing subjectively-derived weather classes, e.g., the Lamb weather types in the UK (Lamb, 1972; Jones *et al*., 1993) or the European Grosswetterlagen (Hess and Brezowsky, 1977), or they may be objectively derived using techniques such as principal components analysis or artificial neural networks. Once the weather types have been identified, then statistical models between the types and local station data are calibrated and then verified. If it is possible to develop models, which perform satisfactorily, then they can be used in climate change studies.

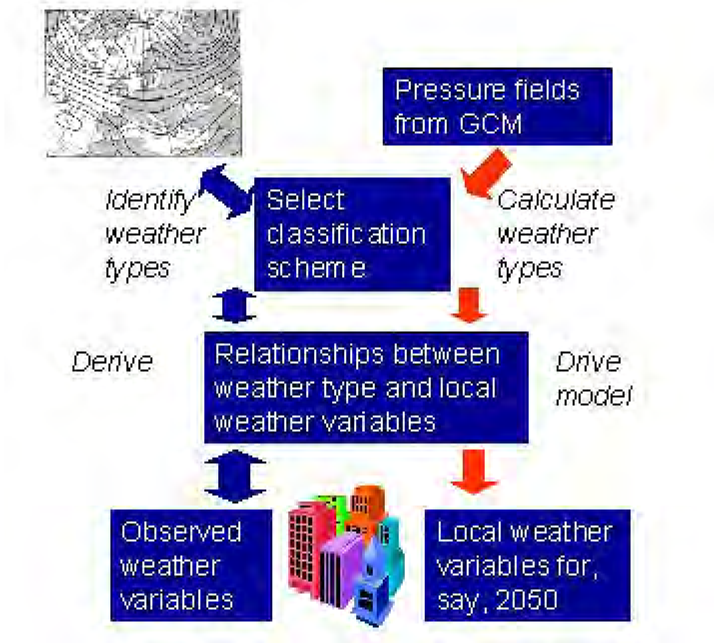

Figure 2.2: The weather typing approach to statistical downscaling. (Adopted from Canadian Institute for Climate Studies)

The caveats concerning model calibration, verification and use in climate change studies, detailed previously for the empirical/statistical techniques, are also valid for the statistical/dynamical methodologies. The advantages and disadvantages common to both empirical/statistical and statistical/dynamical spatial downscaling techniques are summarised as follows:

Advantages:

- these techniques may be able to provide more realistic scenarios of climate change at individual sites than the straight application of GCM-derived scenarios to an observed climate data set
- these techniques are much less computationally demanding than physical downscaling using numerical models
- ensembles of high resolution climate scenarios may be produced relatively easily
- statistical/dynamical techniques are based on sensible physical linkages between climate on the large scale and weather on the local scale

Disadvantages:

- large amounts of observational data may be required to establish statistical relationships for the current climate
- specialist knowledge may be required to apply the techniques correctly
- the relationships are only valid within the range of the data used for calibration - future projections for some variables may lie outside of this range
- it may not be possible to derive significant relationships for some variables
- a predictor variable which may not appear as the most significant when developing the transfer functions under present climate may be critical for determining climate change
- for statistical/dynamical downscaling the fundamental assumption may not hold - differences in relationships between weather type and local climate have occurred at some sites during the observed record (Wilby, 1997)
- for statistical/dynamical downscaling, the scenarios produced are relatively insensitive to future climate forcing - using GCM pressure fields alone to derive weather types and thence local climate does not account for the GCM projected changes in, for example, temperature and precipitation, so it may be necessary to include additional variables such as large-scale temperature and atmospheric humidity.

2.2.1.1.1 **Use of Stochastic Weather Generators in Spatial Downscaling**

Although stochastic weather generators are more widely used in temporal downscaling, they may also be used for spatial downscaling (Wilks, 1999a). The first step in the use of a stochastic weather generator is its calibration using observed daily weather data. Parameter files, which contain information about the statistical characteristics of the observed data, result from the calibration process and are subsequently used to simulate artificial weather data which have the same statistical characteristics as the observed data, but which differ on a day-to-day basis. For spatial downscaling, a weather generator can be calibrated using 'average' weather data for a particular region, roughly corresponding to the size of an appropriate GCM grid box, with the resulting parameter file describing the statistical characteristics of that region's weather.

This 'average' weather is calculated using a number of stations from within the relevant region. The weather generator is also run at each of these individual stations, resulting in a suite of individual station parameter sets.

Daily GCM data for the grid box corresponding to the area-average weather data are also used in the weather generator and another parameter file produced. The difference between the area-average and GCM grid box parameter sets are then applied to the individual station parameter files thus allowing the generation of synthetic data, corresponding to the period of the GCM, for each station within the area. This process is described in more detail in Wilks (1999a). Spatial downscaling using stochastic weather generators is not a straightforward process, may require access to the program code for the weather generator being used, and requires a large amount of observed station data, which may or may not be readily available.

2.2.1.2 **Temporal downscaling**

Temporal downscaling refers to the derivation of fine-scale temporal data from coarser-scale temporal information, e.g., daily data from monthly or seasonal information. Its main application is in scenario studies, particularly for the derivation of daily scenario data from monthly or seasonal scenario information. Monthly model output is available from many GCM experiments, whilst only a small number of experiments have archived daily model output. In addition, daily model output is not considered as robust as model output at the monthly or seasonal time scales and so is not generally recommended for use in scenario studies without more detailed investigations being undertaken. The simplest method for obtaining daily data for a particular climate change scenario is to apply the monthly or seasonal changes to a historical daily weather record for a particular station. However, this method maintains the current observed climate variability and the same sequences of, for example, wet and dry days and hot and cold spells. There is also only one time series available for each scenario, which limits the type of analyses for which the daily data can be used.

The most useful way of obtaining daily weather data from monthly scenario information is to use a stochastic weather generator i.e. a statistical model which generates time series of artificial weather data with the same statistical characteristics as the observations for the station in question (Wilks and Wilby (1999, Semenov *et al*. (1998)).

The fundamental assumption of stochastic weather generators is that the statistical correlations between the climate variables, derived from observed data, are valid under a changed climate. After calibrating the weather generator using observed daily data, a parameter file is produced which contains a statistical description of the characteristics of the climate at the site under examination. The monthly scenario changes in, for example, mean temperature, precipitation amount and solar radiation, can be incorporated by simply perturbing the appropriate parameters by the relevant amount. It is also possible to perturb climate variability by applying changes to the standard deviation of temperature or to the length of wet and dry spells (in the case of LARS-WG, one of the more widely-used weather generators). Daily GCM output can be used to determine changes in these components of climate variability, or arbitrary changes may be imposed. The stochastic component within a weather generator is controlled by the selection of a random number - by varying this random number completely different weather sequences can be generated. This means that it is possible to generate many sequences of daily weather for a particular scenario - the statistical characteristics of each sequence will be very similar, if not identical, but the day-to-day values will vary. In this way, it is possible to generate sufficient data to undertake risk analyses.

A point worth noting about stochastic weather generators is that they are designed for independent use at individual stations. Although it is possible to spatially interpolate the parameters from many individual stations and thus undertake spatial analyses, 'off-the-shelf' weather generators ignore the observed spatial correlation of climate.

This means that if a weather generator was used at two neighboring stations A and B; it would be able to simulate particular events, which would be expected to occur at both sites. That is to say the occurrence of three (3) prolonged droughts in a 30-year time series, but the occurrence of the events would not necessarily coincide at both sites, that is, the drought years at site A would differ from those at site B. So while the weather generator may provide an accurate statistical representation of the observed situation at each individual site, taken together the events are not simultaneous and thus result in a less severe aggregate impact on, for example, water resources or agriculture, than would be expected in the real situation where widespread drought affects a large area. Methods for incorporating spatial correlations in stochastic weather generation have been considered for both WGEN (Wilks, 1998; 1999b) and LARS-WG (Semenov and Brooks, 1999), the two most widely used weather generators. However, in both cases these techniques have not been incorporated into the versions of these models, which are generally available.

The advantages and disadvantages associated with the use of stochastic weather generators are briefly summarized as follows:

Advantages:

- the ability to generate time series of unlimited length
- the opportunity to obtain representative weather time series in regions of data sparsity, by interpolating observed data
- the ability to alter the weather generator's parameters in accordance with scenarios of future climate change - changes in variability may be incorporated as well as changes in mean values

Disadvantages:

- seldom able to describe all aspects of climate accurately, especially persistent events, rare events and decadal- or century-scale variations
- designed for use independently at individual locations and few account for the spatial correlation of climate

2.2.1.3 The climatological baseline

In order to characterize the present-day or recent climate in a region, good quality observed climatological data are required for a given baseline period. Issues to consider in selecting the climatological baseline include the types of data required, duration of the baseline period, sources of the data and how they can be applied in an impact assessment.

2.2.1.3.1 Baseline period

The baseline period is usually selected according to the following criteria (IPCC, 1994):

- Representative of the present-day or recent average climate in the study region;
- Of a sufficient duration to encompass a range of climatic variations, including a number of Significant weather anomalies (e.g. severe droughts or cool seasons);
- Covering a period for which data on all major climatological variables are abundant, adequately distributed over space and readily available;
- Including data of sufficiently high quality for use: A popular climatological baseline period is the non-overlapping 30-year "normal" period as defined by the World Meteorological

Organization (WMO). The current WMO normal period is 1961-1990. As well as providing a standard reference to ensure comparability between impact studies,

Other advantages of using this baseline period include:

- The period ends in 1990, which is the common reference year used for climatic and non-climatic projections by the IPCC in the First, Second and Third Assessment Reports.
- It represents the recent climate, to which many present-day human or natural systems are likely to have become reasonably well adapted (though there are exceptions, such as vegetation zones or groundwater levels that can have a response lag of many decades or more relative to the ambient climate).
- In most countries, the observed climatological data are most readily available for this period, especially in computer-coded form at a daily time resolution in evaluating impacts;
- Consistent or readily comparable with baseline climatologies used in other impact assessments.

2.2.1.4 The special report on emission scenarios (SRES)

In 1996, the IPCC began the development of new set of emission scenarios, effectively to update and replace the well-known IS92 scenarios. The approved new set of scenarios is described in the IPCC special report on emission scenarios (SRES). Four different narrative storylines where developed to describe consistently the relationship between the forces driving emission and there evaluation and to add context for the scenario quantification. The resulting set of 40 scenarios cover the wide range of the main demographic, economic and technological driving forces of the future greenhouse gas and sulpher emission. Each scenario represents the specific quantification of one of the four storylines. All the scenarios based on the same storyline constitute a scenario ‘family‘‘ which briefly describe the main characteristics of the four SRES storylines and scenario family (IPCC-TGICA, 2007).

A1. The A1 storyline and scenario family describe a future world of very rapid economic growth, global population that peaks in mid-century and declines thereafter, and the rapid introduction of new and more efficient technologies. Major underlying themes are convergence among regions, capacity building and increased cultural and social interactions, with a substantial reduction in regional differences in per capita income. The A1 scenario family develops into three groups that describe alternative directions of technological change in the energy system.

The three A1 groups are distinguished by their technological emphasis:

- Fossil intensive (A1FI)
- Non - fossil energy sources (A1T), or
- Balance across all sources (A1B)

(balanced is defined as not relying too heavily on one particular energy source, on the assumption that similar improvement rates apply to all energy supply and end use technologies).

A2. The A2 storyline and scenario family describe a very heterogeneous world. The underlying theme is self-reliance and preservation of local identities. Fertility patterns across regions converge very slowly, which results in continuously increasing population. Economic development is primarily regionally oriented and per capita economic growth and technological changes are more fragmented and slower than in other storylines.

B1. The B1 storyline and scenario family describe a convergent world with the same global population, that peaks in mid-century and declines thereafter, as in the A1 storyline, but with rapid change in economic structures toward a service and information economy, with reductions in material intensity and the introduction of clean and resource-efficient technologies. The emphasis is on global solutions to economic, social and environmental sustainability, including improved equity, but without additional climate initiatives.

B2. The B2 storyline and scenario family describe a world in which the emphasis is on local solutions to economic, social and environmental sustainability. It is a world with continuously increasing global population at a rate lower than A2, intermediate levels of economic development, and less rapid and more diverse technological change than in the B1 and A1 storylines. While the scenario is also oriented towards environmental protection.

2.2.1.5 **Criteria for selecting climate scenarios**

Five criteria that should be met by climate scenarios if they are to be useful for impact researchers and policy makers are suggested in Smith and Hulme (1998):

- **Criterion 1:** Consistency with global projections. They should be consistent with a broad range of global warming projections based on increased concentrations of greenhouse gases. This range is variously cited as 1.4°C to 5.8°C by 2100 (IPCC, 2001a), or 1.5°C to 4.5°C for a doubling of atmospheric CO2 concentration (IPCC, 1990; 1996 - otherwise known as the "equilibrium climate sensitivity" - IPCC, 2001a).
- **Criterion 2:** Physical plausibility. They should be physically plausible; that is, they should not violate the basic laws of physics. Hence, changes in one region should be physically consistent with those in another region and globally. In addition, the combination of changes in different variables (which are often correlated with each other) should be physically consistent.
- **Criterion 3:** Applicability in impact assessments. They should describe changes in a sufficient number of variables on a spatial and temporal scale that allows for impact assessment. For example, impact models may require input data on variables such as precipitation, solar radiation, temperature, humidity and wind speed at spatial scales ranging from global to site and at temporal scales ranging from annual means to daily or hourly values.
- **Criterion 4:** Representative. They should be representative of the potential range of future regional climate change. Only in this way can a realistic range of possible impacts be estimated.
- **Criterion 5:** Accessibility. They should be straightforward to obtain, interpret and apply for impact assessment. Many impact assessment projects include a separate scenario development component which specifically aims to address this last point.

2.2.1.6 **Selecting model outputs**

Many climate change experiments have been performed with GCMs. Therefore, if GCM-based scenarios are to be constructed, it is not easy to choose suitable examples for use in impact assessments. There have always been some limitations on the breadth of choice: some experiments may not have been fully archived in an accessible and public form, in some cases, the required variables have not been available and in many cases the impact assessors have simply not been aware of the potential sources of information. However, several research canters now serve as repositories of GCM information (e.g. the National Center of Atmospheric Research, USA; the Climatic Research Unit, UK; the Commonwealth Scientific and Industrial Research Organization, Australia). Some of these have also developed software for extracting, displaying and comparing information from different GCMs (e.g. see Hulme et al., 2000; Jones, 1996). The IPCC Data Distribution Centre complements these existing sources.

Thus, assuming that the user is in a position to select from a large sample, which results should be chosen? Four criteria for selection are suggested in Smith and Hulme (1998): vintage, resolution, validity and representativeness of results.

2.2.1.6.1 **Vintage**

In general, recent model simulations are likely (though by no means certain) to be more reliable than those of an earlier vintage. They are based on recent knowledge, incorporate more processes and feedbacks and are usually of a higher spatial resolution than earlier models. Therefore, it is of some concern that results from equilibrium experiments conducted as long ago as the early 1980s are still occasionally adopted in impact assessments without reference to more recent experiments. Moreover, one of the problems often encountered in evaluating impact studies is knowing exactly which version of a GCM has provided the scenario information. Part of this is due to poor reporting by the impact analysts, but part can also be attributed to confusing documentation of the model outputs. For instance, there are many sets of results available from different experiments conducted by the same modeling group, and quite often, these have been denoted using the same model name or acronym.

2.2.1.6.2 **Resolution**

As climate models have evolved and computing power has increased, there has been a tendency towards increased resolution. Some of the early GCMs operated on a horizontal resolution of some 1000 km with between 2 and 10 levels in the vertical. More models that are recent are run at nearer 250 km spatial resolution with perhaps 20 vertical levels (more in some ocean models). However, although higher resolution models contain more spatial detail (i.e. complex topography, better-defined land/sea boundaries, etc.) this does not necessarily guarantee a superior model performance.

2.2.1.6.3 **Validity**

A more persuasive criterion for model selection is to adopt the GCMs that simulate the present-day climate most faithfully, on the premise that these GCMs would also yield the most reliable representation of future climate. Several large impact assessment projects have used this approach (e.g. Smith and Pitts, 1997).

2.2.1.7 **How reliable are the Models Used to Make Projections of Future Climate Change?**

There is considerable confidence that climate models provide credible quantitative estimates of future climate change, particularly at continental scales and above. This confidence comes from the foundation of the models in accepted physical principles and from their ability to reproduce observed features of current climate and past climate changes. Confidence in model estimates is higher for some climate variables (e.g., temperature) than for others (e.g., precipitation). Over several decades of development, models have consistently provided a robust and unambiguous picture of significant climate warming in response to increasing greenhouse gases.

2.2.1.8 **SDSM Model Calibration and Validation**

The User specifies the model structure: whether monthly, seasonal or annual sub–models are required; whether the process is unconditional or conditional. In unconditional models, a direct link is assumed between the predictors and predictand (e.g., local wind speeds may be a function of regional airflow indices).

In conditional models, there is an intermediate process between regional forcing and local weather (e.g., local precipitation amounts depend on the occurrence of wet–days, which in turn depend on regional–scale predictors such as humidity and atmospheric pressure).

Once the transfer functions have been calculated, verification of the statistical models should be undertaken. This is usually carried out using a set of independent data, i.e., data withheld from the calibration process. Ideally, sufficient observed data will be available to enable at least 20 years of data to be used to calibrate a spatial downscaling model, with a further 10 years of data (ideally more) being available for model verification. Although this is not always possible, it is strongly recommended that some subset of the observed data be withheld to allow verification of the model using independent data.

The verification process compares the model-predicted station data values (calculated using the independent predictor variable data set) with the actual observed station data for the same period.

The predictor - predictand relationships vary from season to season and from (geographic) region - to - region, following the spatio-temporal variations of the atmospheric circulations (Karl et al., 1990). Therefore, the sets of potential predictors also vary spatio-temporally.

2.2.1.9 **Predictor variables**

The first step in SDSM process is the definition of the statistical relationships based on observed climate data .This requires the identification of the large-scale climate variables (also known as the independent or predictor variables) to be used in the transfer function(s). These predictor variables may be large-scale variables, such as mean sea level pressure (MSLP), or it may be necessary to calculate area-average values for a region, roughly corresponding to the size of the relevant GCM grid box, using station data. Candidate predictor variables should be (Wilby *et al*., 2001):

- Physically and conceptually sensible with respect to the site variable (the dependent variable or predictand),
- Strongly and consistently correlated with the predictand,
- Readily available from archives of observed data and GCM output, and
- Accurately modeled by GCMs

In practice, the choice of predictor variables is often constrained by data availability from GCM archives.

Once suitable predictor variables have been identified, and then the transfer functions can be calculated. In most spatial downscaling studies, the predictor data used are first normalized with respect to the period mean and standard deviation, rather than the actual data themselves being used. This facilitates the use of GCM data in the climate change component of downscaling, since GCM-derived scenarios of future climate change are expressed as changes with respect to a particular baseline time period in an attempt to overcome any shortcomings a GCM may have in simulating current climate conditions.

There are a number of methods which can be used to calculate the transfer functions (model calibration), e.g., multiple linear regression, principal components analysis and artificial neural networks.

There is no 'standard' method used for spatial downscaling - the selected procedure will depend very much on the situation and data available. However, researchers must be aware of the constraints associated with whichever method is selected. For example, if multiple linear regression is used, and then the predictor variables should be independent, i.e., the correlation between them should effectively be zero. If this is not the case, the regression coefficients will not be a true estimate of the contribution of each of the predictor variables to the variance of the predictand. In a linear regression model, if the predictor variables are correlated then they are attempting to explain the same thing and, as a result, the variance between the predictors may be split in a manner that is insignificant - this is known as multicollinearity.

In whichever statistical method is selected, however, the resulting transfer functions should explain a large percentage of the variance in the site data, i.e., the regional forcing (as defined by the predictor variables) should explain a large amount of the variability in the local station data. The error associated with the statistical transfer functions, usually defined by the standard error, should also be less than the projected future changes in the variable in question, if these functions are to be used to determine future climate at the location in question. If this is not the case then it cannot be determined whether the statistical model sensitivity to future climate forcing is greater than the model accuracy.

2.2.2 **Model Efficiency Evaluation**

The determination of model performance is rather subjective and will depend on the study location and the data available. For example, it is highly likely that spatial downscaling will not be as successful in mountainous regions, particularly for variables such as precipitation, as it would be in regions of less complex topography. Local forcing factors will play a much larger role in the determination of local climate characteristics (compared to the role of large-scale forcing factors) in these topographically complex regions than they do in areas of more homogeneous terrain.

If the model calibration and verification processes accomplished with satisfactory results, then the statistical models may be used for climate change studies. In this case, the relevant large-scale predictor variables are extracted from GCM output and then used to drive the statistical models calculated earlier using observed data, with the result being station data for the time period corresponding to that of the GCM input data.

It must be remembered that the statistical models have been calibrated using observed data and are therefore valid only for the data range used in the model calibration process. For some variables, such as temperature, it is highly likely that the GCM-derived values will lie outside of the data range used for model calibration. If this is the case, then it is technically incorrect to use the statistical models for downscaling.

2.2.3 **Bias-correction**

Although GCMs are regarded as the best tools available for projection of climate into the future, there are biases in GCM outputs. GCM bias is simply explained as the deviation of GCM outputs from the observations (Salvi et al., 2011). However, in more elaborated terms, incorrect reproduction of extreme temperatures, prediction of excess number of wet days with low-intensity rainfalls, under or over-prediction of climatic variables, incorrect seasonal variations and so on are some of the forms of biases prevailing in GCM out-puts (Teutschbein and Seibert, 2012). Chenet al.(2011) defined GCM bias as a time-independent component of the error in GCM outputs. According to Ojha et al.(2012), GCMs often incorrectly estimate the occurrences and intensities of precipitation. The limited understanding of the atmosphere and the simplified representation of the atmospheric processes in GCMs are regarded as the main causes of GCM bias (Liet al., 2010). In general, prognostic variables of a GCM contain relatively less bias than the diagnostic variables that are derived from the prognostic variables. Since prognostic variables do not always show good relationships with the predictands of interest, diagnostic variables are also used in developing the downscaling models despite their larger bias. The correction of bias is performed in two distinct ways: (1) the correction of bias in GCM outputs and (2) the correction of bias in the predictands (e.g. precipitation) which were downscaled from GCM outputs. However, neither of the above approaches is capable of correcting the inherent physics and thermodynamics of the GCM simulations, as bias-correction has no direct connection with the internal functions of the GCM.

There are number of different bias-correction techniques in use, which are applicable to GCM outputs and also to the predictands downscaled from GCM outputs.

Bias correction techniques can be applied not only to GCM outputs, but also to the outputs of downscaling models, irrespective of whether the downscaling approach is dynamic or statistical. Ghosh and Mujumdar (2008) used the quantile mapping technique for the removal of bias in streamflows, which were statistically downscaled from GCM outputs. Teutschbein and Seibert (2012) used multiple bias-correction techniques (linear scaling, local intensity scaling, power transformation, variance scaling, quantile mapping and delta-change approach) on dynamically downscaled precipitation and temperature. The major advantage of applying the bias-correction techniques on the downscaled (either statistically or dynamically) hydroclimatic outputs is that, this process is computationally much cheaper than bias correcting each GCM output individually, prior to downscaling. The advantage of applying a bias-correction to each GCM output separately (before introducing to the downscaling model) is that the bias in each variable is individually corrected. However, this procedure is useful only if the bias-correction was capable in adequately correcting the time series of each GCM output, rather than just their statistics (Sachindra et.al.2014).

2.3 Hydrologic Modeling

2.4 Hydrologic Model Selection Criteria

There are numerous criteria, which can be used for choosing the right hydrologic model. These criteria are always project dependent, since every project has its own specific requirements and needs. Further, some criteria are also user dependent, such as personal preference for computer operation system, input/output management and structure, or users add on expansibility. Among the various project-depended selection criteria, there are four main common, fundamental ones that must always be considered (Cunderlik 2003):

I. Required model outputs important for the needed purpose and therefore to be estimated by the model:- Does the model predict the variables required by the project such as peak flow, event volume and hydrograph, long term flows?

II. Hydrologic processes that need to be modeled to estimate the desired outputs adequately:- is the model capable of simulating regulated reservoir operation, single event or continuous processes?
III. Availability of input data: - can all the inputs required by the model be provided within the time and cost constraints of the project?
IV. Price: - does the investment appear to be worthwhile for the objectives of the project?

HEC-HMS which is a comprehensive hydrologic model, developed by Hydrologic Engineering Centre (HEC) of United States Army Corps of Engineers (USACE), was used in this study. HEC-HMS model is selected for this study due to the following reason:

- The program uses various models and input data requirement is moderate;
- HEC-HMS facilitates many currently available hydrologic modeling algorithms
- Parameters in HEC-HMS can be efficiently prepared by the use of GIS tools, such as the HEC-GeoHMS or ArcHydro, in a semi-automated process
- The model is tested for impact of climate change on hydrological study in different part of the world including Ethiopia and
- The availability of the model

HEC-HMS is designed to simulate the precipitation-runoff processes of dendritic watershed systems. It is also designed to be applicable in a wide range of geographic areas for solving the widest possible range of problems. This includes large river basin water supply, and flood hydrology, and small urban or natural watershed runoff (HEC, 2006). The current version of HEC-HMS (3.5.0) is a highly flexible package. It includes different methods to simulate infiltration losses, transforming excess precipitation, base-flow estimation.

2.4.1 **HEC-HMS Model Setup**

HEC-HMS Model setup consists of 4 main model components: basin model, meteorological model, control specifications and input data (time series, paired data and gridded data). The Basin model for instance, contains the hydrologic element and their connectivity that represents the movement of water through the drainage system (HEC, 2006).

The sub basin physical characteristics such as longest flow lengths, centeroidal flow length and slopes derived from DEM are used for estimating the hydrologic parameters. Longest flow path information, for example, was used for estimating time of concentration

The background maps provide a spatial context for the hydrologic elements composing basin model. They are commonly used for showing the boundaries of a watershed or the location of streams. Terrain pre-processing, Basin processing and HMS model support are the main functionalities of HEC-GeoHMS.

In the terrain pre-processing DEM is used as input and a series of steps consisting of computing the flow direction, flow accumulation, stream definition, stream delineation, watershed delineation, and watershed aggregation are performed step by step to derive the drainage networks. The basin processing step gives capability of merging, editing and subdividing of basins and rivers whereas the HMS model support produces a number of hydrologic inputs that are used directly in HMS.

The meteorological component is also the first computational element by means of which precipitation input is spatially and temporally distributed over the river basin.

2.4.2 SCS runoff curve number

Runoff volume models used in HEC-HMS are initial and constant rate model,SCS curve number (CN),Gridded SCS CN ,Green and Ampt , Deficit and Constant rate, Soil moisture accounting(SMA) and Gridded SMA.

SCS CN is simple, predictable, and stable method. It relies on only one parameter, which varies as a function of soil group, land use and treatment, surface condition, and antecedent moisture condition.

In addition, its features readily grasped and reasonable well-documented environmental input. SCS CN is well established method, widely accepted for use in US and abroad (Ponce and Howkins, 1996). Therefore, SCS CN was selected as runoff loss model in this study.

The major factors that determine CN are the hydrologic soil group (HSG) cover type, treatment, hydrologic condition, and antecedent runoff condition (ARC). Another factor considered is whether impervious areas outlet directly to the drainage system (connected) or whether the flow spreads over pervious areas before entering the drainage system (unconnected).*(* United States Department of Agriculture Natural Resources Conservation Service; Conservation Engineering Division Technical Release 55 ,June 1986).

2.4.2.1 **Hydrologic soil groups**

Infiltration rates of soils vary widely and are affected by subsurface permeability as well as surface intake rates. Soils are classified into four HSG's (A, B, C, and D) according to their minimum infiltration rate, which is obtained for bare soil after prolonged wetting. (United States Department of Agriculture Natural Resources Conservation Service; Conservation Engineering Division Technical Release 55, June 1986).

2.4.2.2 **Cover type**

There are a number of methods for determining cover type. The most common are field reconnaissance, aerial photographs, and land use maps. Land use map developed from satellite images was used to determine land cover of the study area. Major land cover/Land use types identified were; Agricultural Land, Forest, Grass Land and Marshy Land.

2.4.2.3 **Treatment**

Treatment is a cover type modifier to describe the management of cultivated agricultural lands. It includes mechanical practices, such as contouring and terracing, and management practices, such as crop rotations and reduced or no tillage. As explained in strategic site action plan for conservation and sustainable use of lake Awassa biodiversity farming community of the area are reluctant to make long term investment in the form of terracing, tree planting and other activities that increase agricultural productivity and environmental control.

2.4.2.4 **Hydrologic condition**

Hydrologic condition indicates the effects of cover type and treatment on infiltration and runoff and generally estimated from density of plant and residue cover on sample areas. Good hydrologic condition indicates that the soil usually has a low runoff potential for that specific hydrologic soil group, cover type, and treatment. Some factors to consider in estimating the effect of cover on infiltration and runoff are (a) canopy or density of lawns, crops, or other vegetative areas; (b) amount of year-round cover; (c) amount of grass or close-seeded legumes in rotations; (d) percent of residue cover; and (e) degree of surface roughness.

2.4.3 **Estimating Base flow Model Parameters**

The program (HEC-HMS) includes three alternative models of base flow, which are: constant monthly-varying model, exponential recession model, linear reservoir volume accounting model. Linear reservoir accounting is used in conjunction with Continuous soil moisture accounting Model (SMA), which is runoff volume model. In this particular study, exponential recession model was used. It represents watersheds base flow (chow, Maidment, and Mays 1988). The recession model has been used often to explain the drainage from natural storage in a watershed (Linsley et al, 1982).The study area contains lake, which is natural storage so that the recession model was selected.

2.4.4 **Direct runoff model**

HEC-HMS uses different models to estimate direct runoff. This are, User-specified unit hydrograph(UH),Clark's UH ,Snyder's UH,SCS UH, ModClark ,Kinematic wave, User specified unit hydrograph(UH).

Choice of direct runoff model from amongst the included options depends upon:

- Availability of information for calibration or parameter estimation
- Appropriateness of the assumptions inherent in the model. Each of the models is based upon one or more basic assumptions; if this are violated, then avoid the use of the model. For example, the SCS UH model assumes that the water shade UH is a single-peaked hydrograph. If all available information indicates the shape of the watershed and configuration of the drainage network causes multiple peaks for even simple storms, then the SCS UH should not be used. Likewise, the kinematic wave model is not universally applicable: Ponce (1991) for example argues that because of numerical properties of the solution algorithms, the method "... is intended primarily for small watersheds (those less than 2.5 Km^2), particularly in the cases in which it is possible to resolve the physical detail without compromising the deterministic nature of the model." Thus, for larger watershed one of the UH models is perhaps a better choice.
- User preference and experience. A combination of experience and preference should guide the choice of models.

Snyder's UH relates hydrograph characteristics (peak flow rate, base time, etc.) to watershed characteristics (Snyder, 1938; Gray, 1961).SCS UH is derived based on dimensionless Unit hydrograph (Soil conservation service 1972). The Clark UH and the ModClark depends upon a quasi-conceptual accounting for watershed storage. To use ModClark model, a gridded representation of the watershed must be defined. In this study, Clark's UH was used.

Clark's UH derives a watershed UH by explicitly representing two critical processes: translation (movement of the excess from its origin throughout the drainage to the watershed outlet and Attenuation (reduction of the magnitude of the discharge, as the excess is stored throughout the watershed).

2.4.5 **Previous study on the Study Area**

Study on Effect of Land Use Change on the Hydraulic Regime of Lake Awassa giving emphasis to the estimation of runoff contribution from gauged and un-gauged catchments using the semi-distributed model known as SWAT. The inflow records were analyzed statistically to evaluate if changes in the land cover affected the hydrological response of the catchment. The results of the analysis indicate that the average inflow to Lake Awassa in 1998 was 3.15 m^3/sec or 99.34MCM, whereas in scenario year 2017 the average inflow is ascertained to be 3.5m^3/s or 110.38MCM. Because of the land cover change the flow will increase by 0.35m^3/s, that is, 11.04MCM. (Daniel Shewangizaw and Yonas Michael*, 20*10).

Another study done on Lake Awassa water balance using spreadsheet model shows, hydrological components that play an important role in the lake level fluctuation are known to be evaporation, rainfall and surface runoff. The correspondence of runoff values to the fluctuation of lake level shows the close relationship of lake level rise to catchment runoff. Although the lake level fluctuations mimic most to the fluctuation of surface runoff it is not possible to conclude whether land use or climatic change alone is the cause for the increase of the runoff. Therefore, the lake level rise is attributed to combined effect of land use and climatic changes. The study recommended "to explore impact of land use and climate change on catchment runoff better, water balance specific to Tikur wuha sub-catchment is vital by assessing the land use change in detail using remote sensing data. (Yemane Gebreegziabher 2004)

Study on “Climate Change Impact on Agricultural Water Resources Variability in the Northern Highlands of Ethiopia” used projected changes in precipitation and temperature in the basin for two future seasons (2046–2065 and 2080–2100) were analyzed using outputs from fifteen GCMs. The study then investigated how these changes in temperature and precipitation might translate into changes in stream flow and other hydrological components using SWAT model. Among the different Special Report on Emissions Scenarios (SRES), which were developed by the IPCC, this study used the AlB, A2 and B2 scenarios for this climate change impact study. This study followed the historical-modification procedure of Harrold and Jones (2003) which produces climate time-series and that have similar statistical properties to the observed datasets. (Shimelis G.et.al.2011).

Another study titled as” Application of Hydrological Models for Climate Sensitivity Estimation of the Atbara Sub-basin” was investigated. In this study, two hydrological models (Hydrologiske Byrån avdeling för Vattenbalans (HBV) and Nile Forecast System (NFS) are applied to the Atbara catchment, Nile River basin area to study the sensitivity of runoff to changes in rainfall and potential evapo-transpiration. The overall objective of this study was to study the sensitivity of the runoff from Atbara catchment area to changes in rainfall and potential evapo-transpiration.

3 Materials and Methods

3.1 Study area

Tikur Wuha River is the primary affluent and major tributary of Lake Awassa draining from the eastern part of Lake Awassa watershed and covering a catchment area of 620 km^2. Tikur Wuha River starts from the small Cheleleka Lake, upstream of Lake Awassa where all perennial and some of the seasonal rivers drains into before going to Lake Awassa. Its elevation ranges from 1681 to 2984 m +MSL. Figure 3.1 shows location of the study area.

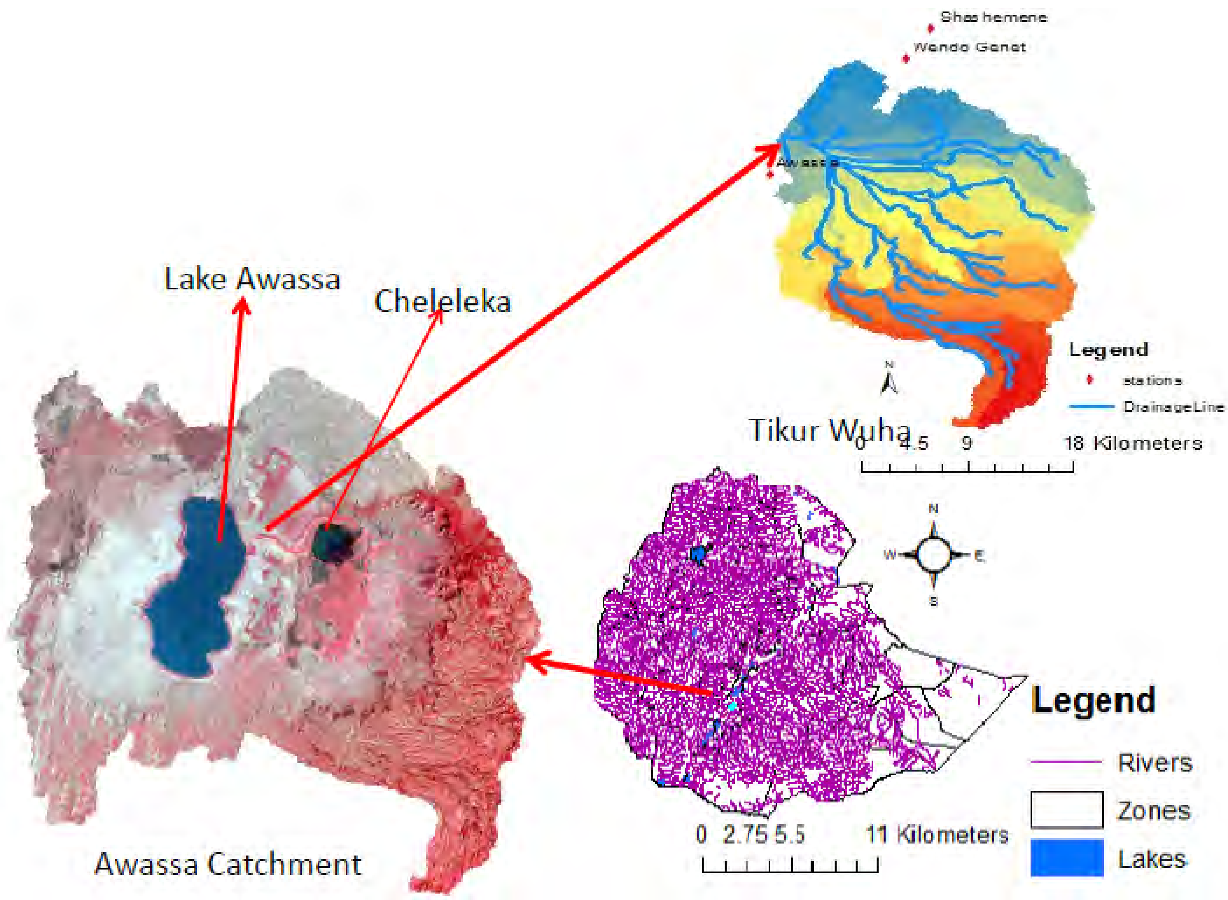

Figure 3.1 Location map of the study area

3.1.1 **Soil**

The soils of the Awassa sub-basin are primarily deep, medium and fine textured Chromic and Haplic Luvisols in the south and east on a rolling to hilly topography with mixed perennial and annual cultivation. In the centre of the sub-basin, extending into the Wendo Koshe Hills, the soils are Chromic and Eutric Cambisols, moderately deep-to-deep and medium textured with poorly drained, fine textured Vertic Cambisols in the Cheleleka wetlands. To the north and west of the lake, the soils are moderately deep-to-deep, well to excessively drained Vitric Andosols, with small areas of very shallow Leptosols.

3.1.2 **Hydrology**

Hydrologically, the surface water of the rift valley lakes basins are not connected though there is a considerable flow of ground water. Precipitation in the basins, as in the tropics, is very high although there is time - to - time variation in distribution. There is also high ground water recharge directly from precipitation.(site Action Plan For the conservation and sustainable use of the Lake Awassa Biodiversity (Rift Valley Lakes Project)).Rainfall and stream flow of Tikur Wuha River for selected periods are shown in Figure 3.2.

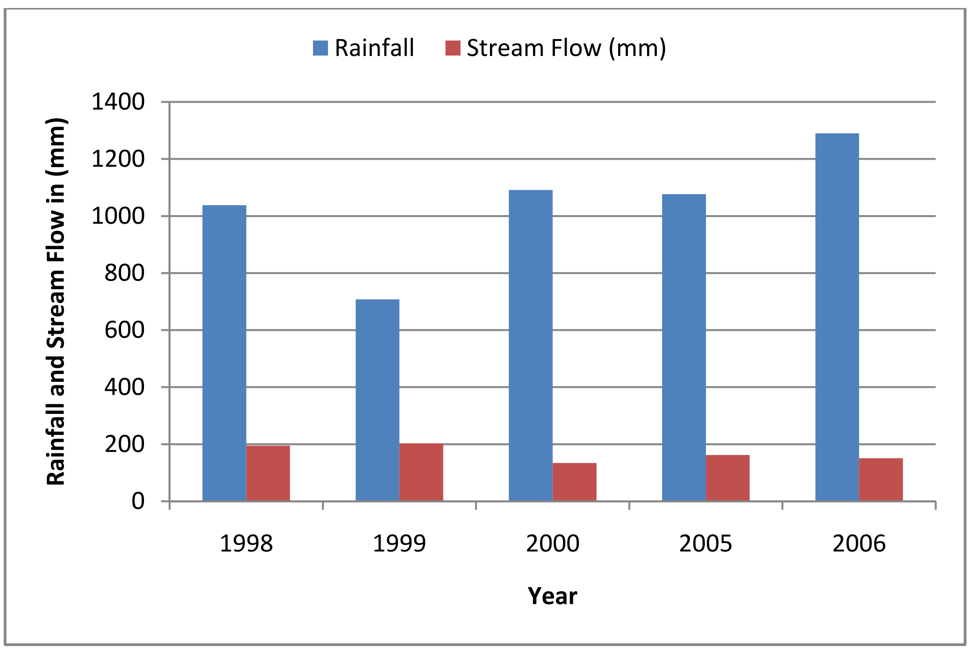

Figure 3.2 Rainfall and stream flow for some years in Tikur wuha sub-catchment

3.1.3 **Climate**

The moisture for precipitation in the area originates from south-west equatorial air stream, which moves northwards with intertropical convergence zone (ITCZ), (W.W.D.S.E, 2001).The annual rainfall in the watershed area at Wendo Genet station varied from 1,200 to 1,400 mm. This is the main source for Tikur Wuha discharge in to the lake. Mean annual rainfall of Awassa and the vicinities is 834 mm with 80 Rainy days.

Mean monthly temperatures varied between 17 and 22 ^{0}C with mean temperature of 17 ^{0}C and low in July. The maximum temperature is 33.8^{0}C and drops to 25.5 ^{0}C from May to November.

3.1.4 **Land use**

The humid escarpments in the northeastern part (Wendo Genet areas) comprise a patch of wet evergreen montane forest together with agro-ecosystem rich with coffee, enset and various fruit plants. The Shallo and Cheleleka swamps also lie at the foot of this escarpment extending to the east. In addition, irrigated vegetable cultivation and eucalyptus plantations practiced around the mouse of Tikur Wuha River. Dense woodland and trees around the lake used to support variety of wild life. Now, however, they are degraded due to their conversion to different land uses, viz., farmland, settlements etc.

3.2 Materials used

3.2.1 **Land use Change Detection**

A common approach in integrated RS-GIS-Modeling for event-based watershed runoff predictions usually involves; i) the derivation of land-cover related parameters of the models from remotely-sensed images, (ii) the use of GIS to prepare the model and to extract additional parameters, (iii) calibration and validation of the model using field measured data to test its efficiency, and then (iv) using the model to simulate runoff and use the simulated information to characterize the conditions of the watershed (O'Connell et.al,2007 Vafeidis,et.al,2007). For land-cover change impact predictions in watersheds, the same approach is generally followed, except that the model is run first for an initial land-cover condition, then the land-cover related parameters of the models are altered to reflect the change, and the model is re-run.

Approach followed for land use change impact assessment were:

I. The derivation of land-cover related parameters of the models from remotely-sensed images,
II. The use of GIS to prepare the model and to extract additional parameters,
III. Run HEC-HMS model first for an initial land-cover condition (use 2000 land use map)
IV. Calibration and validation of the hydrologic model-using field measured data
V. Then the land-cover related parameters of the models are altered to reflect the change, and re-run the model
VI. Using the model to simulate runoff and use the simulated information to characterize the Conditions of the watershed.

All Image analysis was undertaken using ArcMap 10.1 Image analysis tool.

3.2.2 **HEC-HMS Model**

HEC-HMS which is a comprehensive hydrologic model, developed by Hydrologic Engineering Centre (HEC) of United States Army Corps of Engineers (USACE), was used in this study. HEC-HMS is designed to simulate the precipitation-runoff processes of dendritic watershed systems. It is also designed to be applicable in a wide range of geographic areas for solving the widest possible range of problems.

HEC-GeoHMS, an Arc view extension developed by the U.S. Army Corps of Engineers (USACE) was used to create the basin model background map file and to delineate the sub catchments from the Digital Elevation Model (DEM).

3.2.3 **Down-Scaling Model (SDSM)**

SDSM permits the spatial downscaling of daily predictor-predictand relationships using multiple linear regression techniques. The predictor variables provide daily information concerning the large-scale state of the atmosphere, whilst the predictand describes conditions at the site scale. The software reduces the task of statistically downscaling daily weather series into a number of discrete processes.

3.3 Data Collection

The input data collected for this study were meteorological data, soil data, spatial data and satellite image data. The detail is explained as follows.

3.3.1 **Meteorological Data**

Required daily precipitation, maximum temperature and minimum temperature were collected from National Meteorology Agency. Four stations' data were collected for precipitation data and one station data for minimum and maximum temperature. Precipitation stations are Awassa station (from year 1973), Shashemene Station (from year 1980), Haisawita Station (from year 1970) and Wondo Genet station (from year 1965). Maximum and Minimum temperature was collected for Awassa Station starting from the period of 1974. Daily Stream flow data was also collected from Ministry of Water, Irrigation and Energy, Ethiopia. The stream flow data recorded from two-gage stations located Near Awassa Bridge and near Dato village were collected.

3.3.2 **General Circulation Models (GCMs)**

Along with observed meteorological data, the general circulation model (GCM) output of precipitation and temperatures for future time lines (2001 - 2100) were downloaded from Canadian Centre for Climate Modeling and Analysis (CCCMA) on daily basis. IPCC 20-th Century Experiment with CGCM3.1/T63 for period 1961 - 2000 was also downloaded for calibration and validation.

As shown in Figure 3.3, the study area (green shaded grids) is completely falls in between: upper left corner (I_1=13 J_2=36 (33.75^{o}E, 9.77^{o}N)), lower left corner: I_1=13 J_1=34 (33.75^{o}E, 4.18^{o}N), upper right corner: I_2=15 J_2=36 (39.38^{o}E, 9.77^{o}N), lower right corner: I_2=15 J_1=34 (39.38^{o}E, 4.18^{o}N)

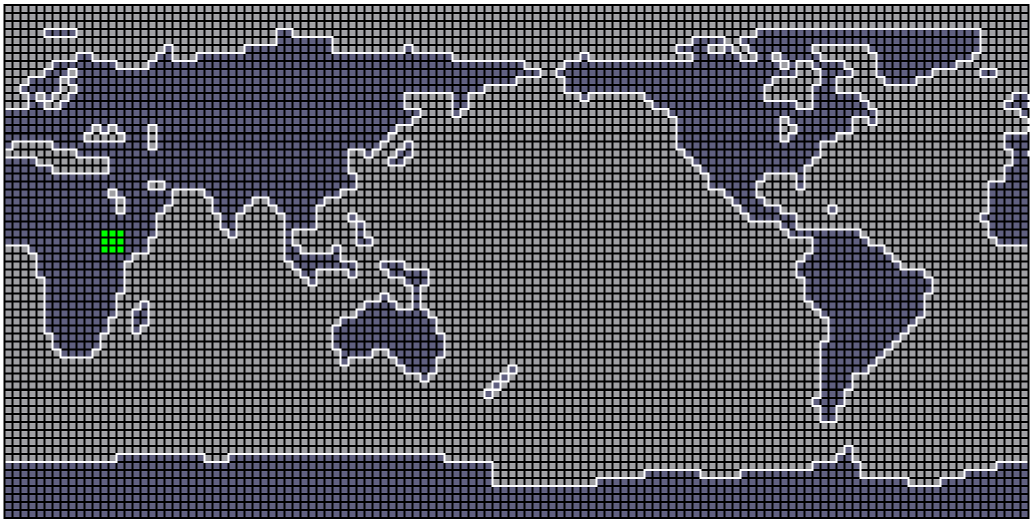

Figure 3.3. Window with 2.81° latitude x 2.81° longitude grid size from which the grid box for the study area is selected

Many climate change experiments have been performed with GCMs. Therefore, if GCM-based scenarios are to be constructed, it is not easy to choose suitable experiment for use in impact assessments. Four criteria for selection are suggested in Smith and Hulme (1998): vintage, resolution, validity and representativeness of results. Vintage and resolution of the downloaded data is shown in Table 3.1. From two model outputs shown in Table 3.1, climate variables obtained from CGCM3.1 (T63) model on daily basis was used in this study. The third version of the Canadian Centre for Climate Modeling and Analysis (CCCMA) Coupled Global Climate Model (CGCM3) makes use of the same ocean component as that used in the earlier. The Second Generation Coupled Global Climate Model, but it makes use of the substantially updated atmospheric component.

Table 3.1. IPCC identification (ID) along with the calendar year ('vintage') of the first publication of selected model output.

Model, ID, Vintage	**Sponsor(s), Country**	**Atmosphere Top Resolution a References**	**Ocean Resolution Z Coord.,Top BC References**	**SeaIce Dynamics, Leads References**	**Coupling Flux Adjustments References**	**Land Soil ,Plants, Routing References**
CGCM3.1(T47), 2005	Canadian Centre for Climate Modeling and Analysis, Canada	top = 1 hPa T47 (~2.8° x 2.8°) L31 McFarlane et al., 1992; Flato, 2005	1.9° x 1.9° L29 depth, rigid lid Pacanowski et al., 1993	rheology, leads Hibler, 1979; Flato and Hibler, 1992	heat, freshwater Flato, 2005	layers, canopy, routing Verseghy et al., 1993
CGCM3.1(T63), 2005	Canadian Centre for Climate Modelling and Analysis, Canada	top = 1 hPa T63 (~1.9° x 1.9°) L31 McFarlane et al., 1992; Flato 2005	0.9° x 1.4° L29 depth, rigid lid Flato and Boer, 2001; Kim et al., 2002	rheology, leads Hibler, 1979; Flato and Hibler, 1992	heat, freshwater Flato, 2005	layers, canopy, routing Verseghy et al., 1993

3.3.3 **Climate Change Scenarios**

Scenarios are images of the future, or alternative futures. They are neither predictions nor forecasts. Rather, each scenario is one alternative image of how the future might unfold. A set of scenarios assists in the assessment of future developments in complex systems that are either inherently unpredictable, or that have high scientific uncertainties (IPCC,2007).

The Special Report on Emissions Scenarios (SRES) (IPCC,2007) are grouped into four scenario families (A1, A2, B1 and B2) that explore alternative development pathways, covering a wide range of demographic, economic and technological driving forces and resulting GHG emissions.

From among the different Special Report on Emissions Scenarios (SRES), which were developed by the IPCC, this study used the AlB, A2 and B2 scenarios for this climate change impact study. These scenarios cover a range of future pathways, with respect to global vs. regional development, and environmental vs. economic emphases.

3.3.4 **Soil Data**

Soil data of the catchment was obtained from Ministry of water, irrigation and energy and Harmonized World Soil Database. Identified soil groups are Silt Loam, Sand,Sandy Loam and Loams as shown in Figure 3.4 .

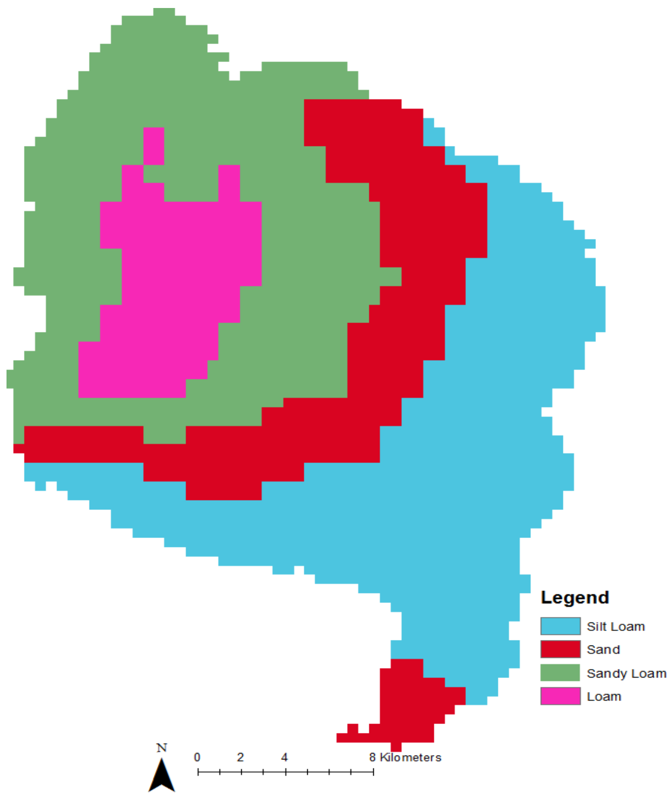

Figure 3.4 Soil Type of Tikur wuha Catchment

3.3.5 **Spatial Data**

To create the basin background map, delineation of the sub catchments Digital Elevation Model (DEM) was required. DEM are available by different organizations and could be downloaded. In this study, DEM was downloaded from the Consortium for Spatial Information, which provides the NASA Shuttle Radar Topographic Mission (SRTM) 90 m x 90 m resolution Digital

Elevation Data for the entire world. DEM Provided by ASTER GDEM was also downloaded for study area. Topographic map of the area for period of 1976 was obtained from Ethiopian National Map Agency.

3.3.6 **Satellite image data**

Orthorectified Landsat MSS, TM and ETM+ images covering the study area, were obtained from the Global Land-cover Facility (GLCF), University of Maryland (http://glcf.umiacs.umd.edu). Acquisition date, path and rows of images obtained are shown in the Table 3.2.

Table 3.2. The data sources for the analysis of land cover change.

Path/Row	sensor	Acquisition date	Resolution (m)	Provider
181/55	MSS	1973-01-31	57	✓ GLCF
168/55	TM	1986-01-21	28.5	✓ GLCF
168/55	ETM+	2000-02-05	28.5	✓ GLCF
168/55	ETM+	2005-12-03	28.5	✓ GLCF
169/55	TM	2010-01-30	28.5	✓ GLCF

3.4 Data Analysis

Data analyses were organized as: image data analysis, climate data analysis, hydrologic analysis and presented as follows.

3.4.1 **Image Data Analysis**

A critical prerequisite for application of change detection by remote sensing is the identification of suitable pairs of images representing the same region. Therefore, image transformation was applied to images obtained for this study. Geo-Coding was done using data management tool in ArcMap by which 1973 Image with 57m x 57m resolution was re-sampled to 2005 images and all images had the same resolution (30m x 30m),so that it is possible to overlay the images for change detection.

Image data, which were acquired during the same season, were checked, especially to track changes in vegetation. From meteorological point of view, there are three seasons in Ethiopia; Belg, Kiremt and Bega. The images used in this study were obtained in the same season as shown in Table 3.3 except image of year 2000.

Table 3.3 Meteorological seasons of Ethiopia and acquisition date of Images

Path/Row	sensor	Acquisition date	Season (metro)	Remark
181/55	MSS	1973-January-31	Bega	Dry Season
168/55	TM	1986-January-21	Bega	Dry Season
168/55	ETM+	2000-February-05	Belg	Small Rainy
168/55	ETM+	2005-December-03	Bega	Dry Season
169/55	TM	2010-January-30	Bega	Dry Season

3.4.1.1 **Landsat Image Pre-Processing**

Prior to any image pre and post processing, the geometric accuracy of the images was checked. For the Landsat TM image, twenty two (22) points identifiable on both the image and 1:50,000 topographic maps of the same area published by the National Mapping agency were used for the geometric accuracy assessment. These points were mostly road intersections. The Universal Transverse Mercator Zone 37N World Geodetic System 1984 (UTM 37 WGS84) grid coordinates of each point were determined both on the image and on the map. Comparison of grid coordinates of these points in the 1986 Landsat image with those in the topographic map was assessed. Root mean square error (RMS error) was found to be 6m, which is less than half a pixel (<14.25m).

The co-registration of the 1973, 1986 and 2000 Landsat image to the 2005 Landsat image was next performed. In this case, the 2005 Landsat image was the reference image (master image) where the UTM coordinates of points on the 1973, 1986 and 2000 Landsat image were compared. Images of time period 1973, 1986 and 2000 are slave images.

3.4.1.2 **Image classification**

The sample set for the classification is created using the combination of bands 7, 4, 2 (for Landsat TM and ETM+ images of 1986 and 2000,2005,) and bands 4, 2,1 (for Landsat MSS image of 1973) since these band combinations allow visualization of the images in their true color. Old topographic map of 1976 and Google Earth Images was used as a source of information for interpreting major land cover classes.

Creation of training sample set is also supported by derivation of Normalized Difference Vegetation Index (NDVI) and unsupervised classification of the images.

True Color: For the true color rendition, band 1 was displayed in the blue color, band 2 was displayed in the green color, and band 3 was displayed in the red color.

False-Color:-, also called Near Infrared or NIR: Short-Wavelength Infrared (SWIR) or "Pseudo Natural Color": In this SWIR image, band 2 was displayed in blue, band 4 was displayed in green, and band 7 (or 5) was displayed in red. Color combination and their indication on ground cover are shown in Table 3.4.

Table 3.4. Color combinations and their indication

Ground Cover Type:	**In Natural Color (3,2,1), appears:**	**In False Color: (4,3,2), appears:**	**In Pseudo Natural Color (7,4,2), appears:**
Trees and bushes	Olive Green	Red	Shades of green
Crops	Medium to light green	Pink to red	Shades of green
Wetland Vegetation	Dark green to black	Dark red	Shades of green
Water	Shades of blue and green	Shades of blue	Black to dark blue
Urban areas	White to light blue	Blue to gray	Lavender
Bare soil	White to light gray	Blue to gray	Magenta, Lavender, or pale pink

(Source: NASA; https://zulu.ssc.nasa.gov/mrsid/tutorial/Landsat%20Tutorial-V1.html)

By creating a composite image, images were displayed in color displaying bands in the Red, Green, and Blue (RGB) format. This allowed to see different features within a scene and become more familiar with the scene to identify urban areas, forests, agriculture, and water bodies, for example. To allow visual interpretation of the image in their true color, image enhancement was done. One of enhancement done was a vegetation index. The Normalized Difference Vegetation Index (NDVI) is a very important vegetative index. Healthy green leaves have a higher reflectivity in the near infrared band while stressed, dry, or diseased vegetation much less reflectivity. So, NDVI can be useful indicator of vegetation stress. It was done using equation (1).

$$\frac{\text{Landsat B4} - \text{Landsat B3}}{\text{Landsat B4} + \text{Landsat B3}} \quad \ldots\ldots\ldots\ldots\ldots\ldots\ldots\ldots\ldots\ldots\ldots\ldots\ldots\ldots\ldots\ldots\ldots\ldots\ldots\ldots\ldots \text{(1)}$$

Where:-Landsat B4 is landsat band four (Infrared)

landsat B3 is Landsat band three (Red)

3.4.1.3 Definitions used in classification of land cover

I. **Grass Land:-**This class includes any geographic area dominated by natural herbaceous plants (grasslands, prairies, steppes and savannahs) with a cover of 10% or more, irrespective of different human and/or animal activities, such as: grazing, selective fire management etc. Woody plants (trees and/or shrubs) can be present assuming their cover is less than 10%.

II. **Forest Land:-**area with high density of trees which include eucalyptus and coniferous trees, dense woodland.

III. **Agricultural Land: -** areas used for crop cultivation, and the scattered rural settlements.

IV. **Water: -** area which ponds water throughout the year, and rivers.

V. **Marshy (Swamp) Land: -** area which remains water logged and swampy throughout the year, and rivers.

3.4.1.4 Image Classification Method

Supervised classification used in this study was also supported by unsupervised classification. Therefore, both supervised and unsupervised image classification was done during image classification.

3.4.1.4.1 Unsupervised Classification

In unsupervised classification, pixels are clustered together based on spectral homogeneity and spectral distance. During unsupervised classification, eight (8) clusters were used.

3.4.1.4.2 Supervised Classification

Representative samples of each class were collected from the images for supervised image classification (Table 3.5). The maximum likelihood classifier (MLC) was selected since unlike other classifiers it considers the spectral variation within each category and the overlap covering the different classes. The supervised classification was supported by derivation of NDVI and unsupervised classification of the images.

The training sets comprised, as a minimum, a sample of typically 10–30 pixels per class per band, and were collected in such a way that the assumption of normal distribution of the MLC is satisfied.

Table 3.5: Land-cover classes identified from the Landsat MSS, TM and ETM+ images of the study area with number of samples pixel collected for classifier training

Land-Cover Class	1973 landsat Number of Pixels	1986 landsat Number of Pixels	2000 landsat Number of Pixels	2005 landsat Number of Pixels
Water	79603	79600	56244	-
Forest	4005	4008	3938	544
Agricultural Land	1032	1033	1661	8875
Grass land	15437	1932	14469	4247
Swamp	289	63	372	3129

For the Landsat image classification, selected bands, unsupervised classification and the derived NDVI image were subjected to classification. Polygons were drawn on identified scenes so that class name and class values are given by training sample manager tool. Training data selected are not only from one area of the scene; it was distributed across the entire scene. After training areas were selected, normality, separability and partitioning of the samples were evaluated. Training samples classified in the same class were selected and the histogram was drawn. Looking at the histogram drawn, the distribution of the color was seen if there is any overlap or normality of the distribution was evaluated. When there are images, which overlap, it shows that some samples have to be merged or deleted. Images, which overlap, were evaluated using scatter plots. Scatter plots plot the pixel values of training data in one band against those of another.

Viewed as scatter plots, the points should not overlap if the training samples represent different spectral classes. First, each individual class was seen if there is any overlap and any opportunities to merge or delete training samples. Once evaluation of classes was finished, all classes were compared to each other to see their separability. Before classification, last task done was evaluation of covariance of training data. Covariance evaluates the correlation of values in the different bands. For effective classification, covariance with low values is preferred. When covariance with high values obtained the training data were re-evaluated. This was done for all the classes until the satisfactory result was obtained. Training data obtained following the procedure explained above was saved and used in supervised image classification. Covariance between the bands were shown in appendix A. (Table A.9 - Table A.12).

3.4.1.5 **Accuracy Assessment**

For 1973 and 1986 image classification, accuracy assessment was done using topographic map of the study area prepared in 1976. About 30 random points were created for 1973 image classification of Awassa watershed and 35 points for 1986 image classification. Error matrix table was completed by comparing values of random points on classified image and topographic map as shown in Table 3.6. For year 2000 and 2005 image classification accuracy assessment was not done, because of lack of data.

During image classification, the following numbers were assigned for land cover types identified:

Water = 1, Forest = 8, Agricultural Land = 3, Grass Land = 6 and Swamp = 7

Table 3.6 Error matrix of 1973

	Water(1)	Forest(8)	Agricultural Land(3)	Grass land(6)	Swamp(7)	Total
Water(1)	5	0	0	0	0	5
Forest(8)	0	6	3	0	0	9
Agricultural Land(3)	0	1	10	0	0	11
Grass land(6)	0	0	0	0	0	0
Swamp(7)	0	0	0	0	0	0
Tot_col	5	7	13	0	0	21

Using the error matrix overall accuracy was calculated. Overall accuracy is the percentage of random points that are the same in both images (year 1973 classified image and topographic map). In error matrix of 1973, (Table 3.6) there are 21 points (5 water, 0 Grassland, 0 Swamp, 6 forests and 10 Agricultural lands). There are 28 random points created. So, overall accuracy was estimated by dividing number of point in error matrix by total random points. i.e. 21/28, which is 75%.

Calculation of Cohen's Kappa

Kappa provides us with insight into our classification scheme and whether or not we achieved results better than that would have achieved strictly by chance.

The formula for kappa is:

$$\frac{\text{Observed}-\text{expected}}{1-\text{expected}} \quad \text{.......... (2)}$$

Where: - Observed is overall accuracy. Expected is calculated from the rows and column totals.

Therefore, the product of the rows and columns was calculated first and shown in Table 3.7.

What would be expected based on chance was calculated by equation (3):

$$\frac{\text{Product matrix}}{\text{Cumulative sum of product matrix}} \quad \text{.......... (3)}$$

The product matrix is the sum of the diagonals from Table 3.7. Which is: 25 + 63 + 143 + 0 + 0 = 231

The Cumulative Sum is the summation of all product matrixes (Table 3.7), which is 25+35+65+45+63+117+55+77+143 = 625, ignoring zero values.

So Expected is 231/625 = 0.3696

Therefore, kappa (K) = $\frac{0.75-0.3696}{1-0.3696}$ = 0.603. This figure is interpreted as that the classification is 60.3% better than would have occurred strictly by chance.

Table 3.7 Product matrix

	Water column	Forest column	Agricultural Land column	Grass land Col	Swamp Col
Water row	5x5 = 25	5x7=35	5x13=65	5x0=0	5x0=0
Forest	9x5 = 45	9x7 = 63	9x13= 117	9x0=0	9x0=0
Agricultural Land row	11x5=55	11x7=77	11x13 =143	11x0	11x0=0
Grass land row	0x5=0	0x7=0	0x13=0	0x0=0	0x0=0
Swamp row	0x5=0	0x7=0	0x13=0	0x0=0	0x0=0

Following the same procedure of 1973 image classification accuracy assessment was done for 1986 image classification. For error matrix of 1986, that have 26 points and 35 random points, overall accuracy is 26/35 or 74.28%. Error matrix and product matrix of 1986 image classification is shown in Table 3.8 and 3.9 respectively.

Table 3.8 Error matrix of 1986

	Water(1)	Forest(8)	Agricultural Land(3)	Grass land(6)	Swamp(7)	Total
Water(1)	2	0	0	0	0	2
Forest(8)	0	8	6	0	0	14
Agricultural Land(3)	0	0	16	0	0	16
Grass land(6)	0	0	0	0	0	0
Swamp(7)	0	0	0	0	0	0
Tot_col	2	8	22	0	0	26

Table 3.9 Product matrix

	Water column	Forest col	Agricultural Land col	Grass land Col	Swamp Col
Water row	2x2=4	2x8=16	2x22=44	2x0	2x0
Forest row	14x5=70	14x8=112	14x22=308	14x0	14x0
Agricultural Land row	16x5=80	16x8=128	16x22=352	16x0	16x0
Gland row	0x5=0	0x8=0	0x22=0	0x0	0x0
Swamp row	0x5=0	0x8=0	0x22=0	0x0	0x0

What would be expected based on chance. Was calculated by :

$$\frac{\text{Product matrix}}{\text{Cumulative sum of product matrix}}$$

The product matrix is the sum of the diagonals: 4 + 112 +352+0+0 = 468

The Cumulative Sum is: 4+16+44+70+112+308+80+128+352 = 1114, ignoring zero values.

So Expected is 468/1114 = 0.42

Therefore, kappa (K) = $\frac{0.7428-0.42}{1-0.42}$ = 0.5565

This shows that the 1986 image classification is 55.65% better than would have occurred strictly by chance.

3.4.2 **Climate change Analysis**

Climatological baseline selection, climate change in the catchment ,climate downscaling model, temperature and precipitation downscaling calibration and validation, model efficiency evaluation and downscaling future scenarios were performed in this section and presented as follows.

3.4.2.1 **The climatological baseline**

Issues to consider in selecting the climatological baseline include the types of data required, duration of the baseline period, sources of the data and how they can be applied in an impact assessment. The baseline period is usually selected according to criteria given by IPCC (IPCC, 1994).Based on the criteria's Baseline period of 1961-1990 was used in this study.

3.4.3 **Climate change in the catchment**

To determine if there is climate change in the catchment in the past, the change on the rainfall of the area was analysed as it is used as input for HEC-MS model to determine the flow in the river. Climatological baseline (1961 - 1990) was used as past and periods of (1991 - 2010) were used as current. Summary statics of precipitation data for all station were calculated for both periods (past and current) using SDSM. Monthly mean of the past and current were used for comparison if there is change in rainfall of the area. Area weight determined from Theissen polygon were used to determine average rainfall of all stations.

3.4.4 **Down-Scaling Model (SDSM)**

The software reduces the task of statistically downscaling daily weather series into a number of discrete processes.

The following steps (I - VI) were procedures followed during downscaling.

I. Quality control and data transformation:

Model transform used for conditional process (Precipitation) was with a fourth root transformation and no transformation was applied for temperature downscaling for all stations. The transformation type is recorded in *.PAR and *.SIM files to ensure that data are consistently handled during subsequent scenario and data analysis routines.

Quality assessment was also done for both precipitation and temperature as shown in Table 3.10

Table 3.10 Quality assessment of observed data

Rainfall station (mm)	Period	Minimum	Maximum	Mean
Awassa	1973 - 2000	0	110.4	3.03
WondoGenet	1965 - 2000	0	99	3.125
Shashemene	1980 - 2000	0	68.5	2.59
Haisawita	1970 - 2000	0	79.2	3.137
Temp.Data (C^o)				
Max.Temp.	1974 - 2000	0	33.8	26.75
Min.Temp.	1973 - 2000	-2.8	19.5	12.28

II. Preliminary screening of potential downscaling predictor variables

This step identifies those large-scale predictor variables, which are significantly correlated with observed station (predictand) data. The probable predictors and the observed daily precipitation totals from 1961 to 2000 were split into two 20-year time slices; 1961-1980, and 1981-2000. The Pearson correlation coefficients between the probable predictors and the observed daily precipitation were calculated for all two time slices and the whole period (1961-2000), at each grid point in the atmospheric domain.

The probable predictors which showed good statistically significant correlations (at 95 % confidence level, p = 0.05) consistently over the two time slices and the whole period were selected as the potential predictors. This process was done on annual basis. Selected potential predictors are shown in Table 3.11.

Table 3.11: Selected potential predictors for All rainfall stations and temperature in study area.

Station	Pridictand	Pridictor
Awassa	precipitation	specific_humidity,surface_upwelling_shortwave_flux_in_air, , eastward_wind, 2m surface air temperature,
	Maximum temperature	toa_outgoing_longwave_flux,surface_downwelling_shortwave_flux_in_air, surface_upwelling_shortwave_flux_in_air, eastward_wind
	Minimum temperature	toa_outgoing_longwave_flux, eastward_wind, northward_wind
Wando Genet	precipitation	2m surface air temperature, specific_humidity ,northward_wind, air_pressure_at_sea_level
Shashemene	precipitation	northward_wind, 2m surface air temperature,specific_humidity , ,air_pressure_at_sea_level
Hasiwaita	precipitation	specific_humidity,surface_upwelling_shortwave_flux_in_air, eastward_wind, 2m surface air temperature, northward_wind,

III. Assembly and calibration of statistical downscaling model(s)

The large-scale predictor variables identified in (II) were used in the determination of multiple linear regression relationships between these variables and the local station data. Statistical models may be built on a monthly, seasonal or annual basis. Information regarding the amount of variance explained by the model(s) and the standard error is given in order to determine the viability of spatial downscaling for the variable and site in question. Assembly of the candidate predictor suite can be a far more involved process entailing data extraction, re–gridding and normalisation techniques. For this reason, SDSM is supplied with a prepared set of daily predictor variables for selected grid boxes covering globally for all land areas via the web http://www.cics.uvic.ca/scenarios/index.cgi?Scenarios.

For precipitation downscaling, the predictor suite contains variables describing atmospheric circulation, thickness, stability and moisture content. In practice, the choice of predictor variables is often constrained by data availability from GCM archives.

IV. Synthesis of ensembles of current weather data using observed predictor variables

Once statistical downscaling models have been determined, they can be verified by using an independent data set of observed predictors. The stochastic component of SDSM allows the generation of up to 100 ensembles of data which have the same statistical characteristics but which vary on a day-to-day basis. In this study, 20 ensembles of data were generated.

V. Generation of ensembles of future weather data using GCM Derived predictor variables

Provision of the appropriate GCM-derived predictor variables allowed the generation of ensembles of future weather data by using the statistical relationships calculated in (III).

VI. Diagnostic testing/analysis of observed data and climate change scenarios

The statistical characteristics of both the observed and synthetic data were calculated for comparison and thus determination of the effect of spatial downscaling.

SDSM Version 2.1 was demonstrated at the CCIS Workshop on Methods and Techniques for Constructing Regional Climate Scenarios held at the University of Laval, Quebec City, in November 2000. SDSM Version 2.2 was released in September 2001. SDSM Version 4.2 was used in this study.

3.4.4.1 **Awassa Maximum and Minimum Temperature Downscaling Calibration and validation**

Daily Temperature Calibration was done for Awassa station. The first 20 years of data (1973 - 1990) were considered during calibration and the remaining 9 years of data (1991 - 2000) were considered during model validation. Temperature calibration is unconditional process. In addition, P value during calibration is considered as P must be < 0.05 but if greater, the correlation between the predictand and variable is more likely by chance i.e. statistically the variable is not significant. During selection of potential variables the correlation of the variables with predictand were also considered and shown in Table 3.12.

The scatter plots for the predictors were also done and considered since the correlation values only do not show their dependency. Variables selected and used to downscale maximum temperature were, (RLUT, RSDS, RSUS, UAS) and (RLUT, UAS and VAS) to downscale minimum temperature.

Table3.12 Predictor variables and their correlation values with maximum temperature annually

Variables	Correlation value
surface_upward_sensible_heat_flux (hfss)	0.37
eastward_wind (uas)	-0.565
surface_upwelling_longwave_flux_in_air (rlus)	0.337
toa_outgoing_longwave_flux (rlut)	0.53
surface_downwelling_shortwave_flux_in_air (rsds)	0.44
surface_upwelling_shortwave_flux_in_air(rsus)	0.468
specific_humidity(huss)	-0.29
Evsp	0.158
surface_upward_latent_heat_flux (hfls)	0.223
precipitation_flux (pr)	0.087
surface_air_pressure (ps)	0.282
northward_wind(vas)	0.158

3.4.4.2 **Precipitation downscaling Calibration and validation**

Daily precipitation was calibrated for all stations of the study area. For Awassa station, the first 20 years of data (1973 - 1990) considered during calibration and the rest 9 years data (1991 - 2000) were considered during model validation. The period for model calibration is selected to make the calibration period similar to climate baseline selected (1961 -1990). Periods of 1961 - 1973 were given -999 to indicate missing value during calibration. Precipitation calibration is a conditional model as it depends on the occurrence of wet-days, which in turn depend on regional–scale predictors such as humidity and atmospheric pressure. The event threshold value is important to treat trace values during the calibration period. For daily precipitation calibration purpose, event threshold value was fixed to be 0.1 mm/day so that trace rain days below this threshold value will be considered as a dry day.

Table 3.13 Calibration and Validation period for Precipitation Model.

Station	Years of data	Calibration Period	Validation period
Awassa	1973 - 2013 (40 years)	1973 – 1990	1991-2000
Shashemane	1980 - 2011 (31 years)	1980 – 1990	1991-2000
Haisawita	1970 - 2010 (40 years)	1970 - 1990	1991 - 2000
Wando Genet	1965 - 2010 (45 years)	1965 – 1990	1991 - 2000

3.4.5 **Model Efficiency Evaluation**

Nash-Sutcliffe coefficient (E)

The Nash-Sutcliffe model efficiency coefficient (E) is commonly used to assess the predictive power of hydrological models. However, it can also be used to quantitatively describe the accuracy of model outputs for other things than discharge such as nutrient loadings, temperature, concentrations etc. (Water Science technical series, report no. 14.)

It is defined as:

$$E = 1 - \frac{\sum_{i=1}^{n} (X_{obs,i} - X_{model})^2}{\sum_{i=1}^{n} (X_{obs,i} - \overline{X_{obs}})^2} \text{..........} \quad \text{..........} \quad \text{..........} \quad \text{......}(4)$$

Where: X_{obs} is observed values and X_{model} is modeled values at time/place i.

$\overline{X_{obs}}$ mean observed value

3.4.6 **Bias-correction**

The precipitation downscaled by the SDSM model with GCM outputs was bias-corrected against the observed precipitation and temperature pertaining to the station of interest. The bias-correction was applied to the precipitation downscaled with GCM outputs as it was computationally efficient than bias-correcting each GCM output individually.

MBC (Monthly bias-correction) is a relatively simple bias-correction method used by Johnson and Sharma (2012). In that study, it was used to correct the mean and the standard deviation of the precipitation output of a GCM with those of the observed precipitation. In this study, it was employed to correct the mean and the standard deviation of the precipitation downscaled with GCM outputs against those of observed precipitation. Let monthly time series of precipitation downscaled with GCM outputs for a calendar month i beY_i,for the past climate. As a first step,Y_i was standardized with its monthly mean ($\mu_{GCM,i}$) and standard deviation ($\sigma_{GCM,i}$) according to Equation (1). This yielded the standardized time series Y_i' for each calendar month as follows:

$$Y_i' = \frac{Y_i - \mu_{GCM,i}}{\sigma_{GCM,i}} \text{---}(1)$$

Then this standardized precipitation time series for each calendar month i (Y_i') was transformed back with Equation (2), using the monthly mean ($\mu_{Obs,i}$) and standard deviation ($\sigma_{Obs,i}$) of observed precipitation pertaining to the past climate. Equation (2) provided the monthly bias-corrected time series of precipitation downscaled with GCM outputs (Z_i). This bias-corrected time series of downscaled precipitation has the monthly mean and standard deviation of the observed precipitation.

$Z_i = Y_i'. \sigma_{Obs,i} + \mu_{Obs,i}$ ---(2)

For the correction of bias in future precipitation, the precipitation downscaled with GCM outputs for future were standardized with their means and standard deviations corresponding to the past climate following Equation (1), and transformed back with those of past observed precipitation according to Equation (2). In MBC, it is assumed that the bias in the mean and the standard deviation of the precipitation downscaled with GCM outputs for past climate (with respect to past observations) remains the same in the future.

3.4.7 Downscaling future scenarios

After calibrating the SDSM model, using observed data and large-scale predictors originating from CGCM3.1/T63, the same empirical relationship with predictors, supplied by GCMs, were tuned to downscale the future climate change scenario simulated by GCMs.

Scenario Generator operation produced 20 ensembles of synthetic daily weather series given atmospheric predictor variables supplied by CGCM3.1/T63 climate model. The predictors were downloaded on daily basis for period (2001 - 2100), for emission scenarios A2, A1B and B1. The scenarios were analysed for future periods of 2020's (2015 -2035), 2050's (2040 - 2060) and 2080's (2080 - 2100).

3.5 Hydrologic Analysis

HEC-GeoHMS develops a number of hydrologic inputs for HEC-HMS. Background shape files, basin model file, meteorological model and HMS project files were created for study area and shown in appendix C.

3.5.1 Terrain preprocessing

3.5.1.1 Tikur Wuha Sub-catchment Delineation

DEM downloaded from ASTER GDEM on 12-march-2014 and SRTM were used in the analysis. Both Obtained data were used to compare terrain pre-processing result. Terrain pre-processing was started by filling sinks. When sink was filled and compared with published data of the catchment, the area near the lake was filled with (equaled) a large area especially around the city, which gives incorrect watershed. Therefore, deranged polygon option was used. i.e. A "Deranged Polygon" was used to define areas that will not be filled. The Awassa lake polygon was extracted from global lakes and wetlands database (GLWD). Then, the terrain was filled except the region of the lake. Delineated Awassa catchment and Tikur Wuha sub-catchment are shown in Figure 3.5.

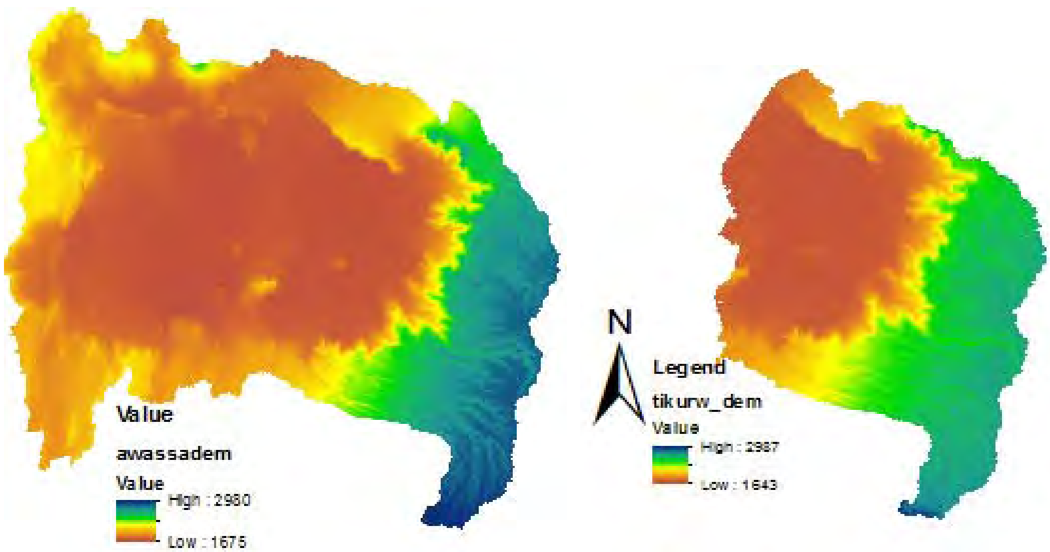

Figure 3.5 A Awassa Catchment DEM Figure.3.5.B.Tikurwuha Subcatchmnet DEM

After Awassa watershed was delineated from the downloaded DEM, by using steps in terrain preprocessing, the result was compared with the published maps. Then, Tikur-Wuha sub-catchment was again extracted from the DEM, by using watersheds delineated in delineation of Awassa catchment. Extracted Tikur-wuha DEM was processed following the Terrain preprocessing steps (filling sink, flow direction, flow accumulation, stream definition, stream segmentation, catchment grid delineation, and catchment polygon processing).

3.5.1.2 **Flow direction and Flow accumulation**

Flow direction was done after filling sink. The values in the cells of the flow direction grid indicate the direction of the steepest descent from that cell. Then flow accumulation was done next to flow direction.

3.5.1.3 **Stream definition**

This step classifies all cells with a flow accumulation greater than the user-defined threshold as cells belonging to the stream network. The user-specified threshold may be specified as an area in distance units squared, e.g., square kilometers, or as a number of cells. The flow accumulation for a particular cell must exceed the user-defined threshold for a stream to be initiated. The default is one percent (1%) of the largest drainage area in the entire DEM. The smaller the threshold chosen, the greater the number of sub basins delineated in a following step. In case we take default value (The default is one percent (1%) of the largest drainage area in the entire DEM) it gives us about 29 sub catchments. To minimize the reaches of the segment user specified threshold values were taken for stream definition.

3.5.1.4 **Stream segmentation and Catchment Grid delineation**

Stream definition was used for stream segmentation. Catchment grid delineation was done following stream segmentation.

3.5.1.5 **Catchment Polygon Processing**

The three functions Catchment Polygon Processing, Drainage Line Processing and Adjoint Catchment Processing used to convert the raster data developed so far to vector format.

3.5.1.6 **HMS Data Check**

This step checks the datasets for consistency in describing the hydrologic structure of the model. For example, the program checks to make sure unique names were used for river reaches and sub basins. In addition, the program checks that rivers reaches and centroids are contained within a sub basin. This is needed for placement of the hydrologic element names and the hydrologic element connectivity. In general, the program keeps track of the relationship between the stream segments, sub basins, and outlet points. These checks are necessary because the relationships between hydrologic elements may have been broken by unintentional use of subdivide and merge tools. The program produces a text file, “SkelConsChk.txt”, which contains the summary of the data check and its summary was shown below.

HMS Consistency Checking Log

CHECKING SUMMARY

****

Unique names - no problems.

River containment - no problems.

Center containment - no problems.

River connectivity - no problems.

VIP relevance - no problems.

3.5.1.7 **Stream and Sub-basin Characteristics**

HEC-GeoHMS computes several topographic characteristics of streams and sub-basins that can be used for estimating hydrologic parameters. The user should compare and verify the physical characteristics with published information prior to estimating the hydrologic parameters. The stream and sub-basin physical characteristics are stored in attribute tables, which can be exported for use with a HEC-HMS and other programs.

3.5.1.8 **Project Area:-**

The project area layer is used to show the upstream drainage area for the outlet point and the project point layer shows the location of the outlet point. Project area for this study is about 627.47Km^2.This was using project point at gage near Dato village. The Control point used was at coordinate, Latitude: 7^0: 6': 0" N and Longitude: 38^0:30': 0" E. HEC-HMS developed for the study area was shown in Figure 3.6.

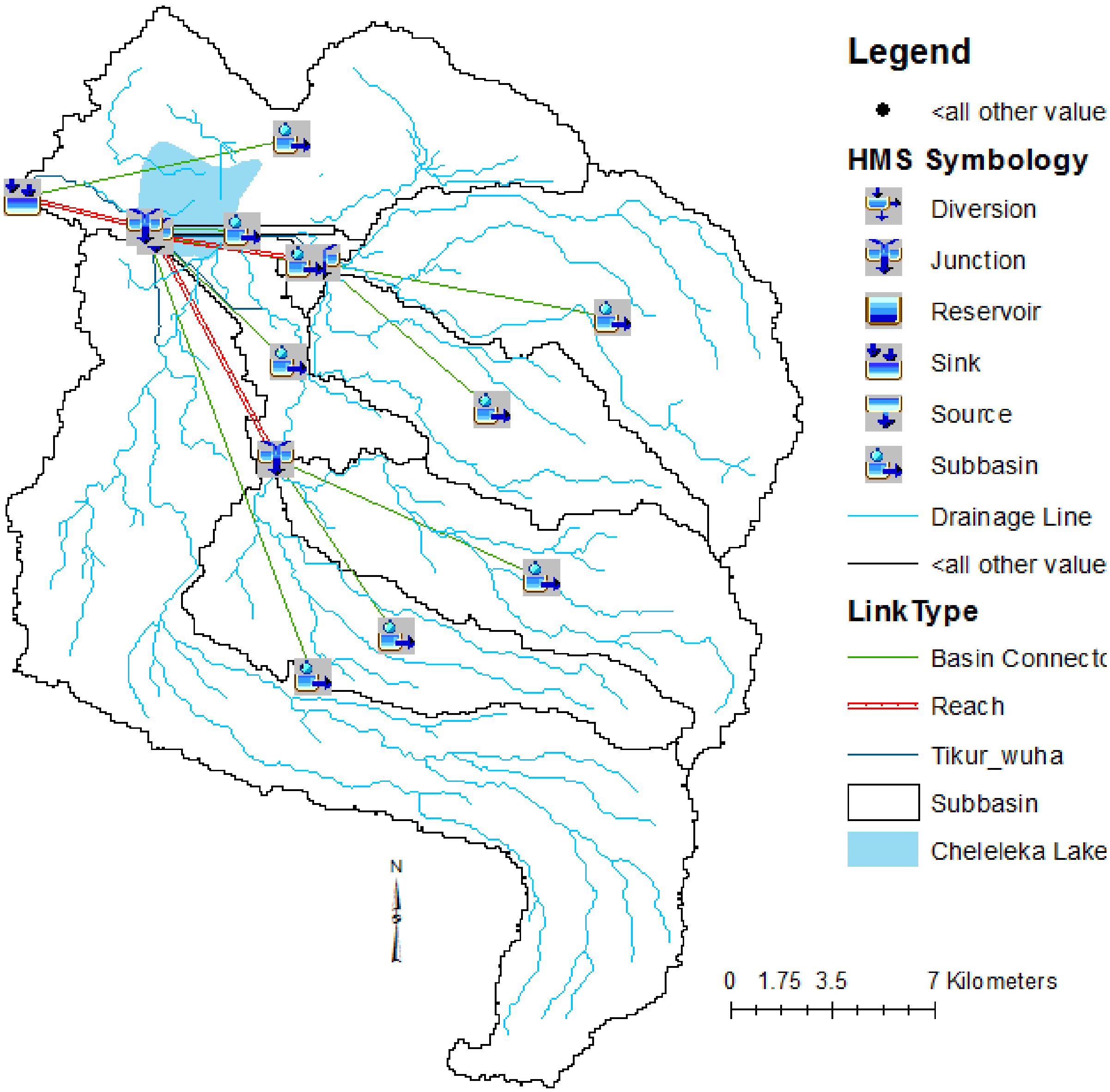

Figure 3.6 HEC - HMS project developed

3.5.2 **HMS Project Setup**

The HMS Project Setup menu is responsible for extracting data that will be used to develop the necessary information to create HEC-HMS project. The approach for extraction involves specifying a control point at the downstream outlet. This location represents the downstream boundary for the HEC-HMS project. After defining the downstream outlet, HEC-GeoHMS extracted data from the datasets created using the terrain preprocessing tools for the drainage area upstream of the outlet. Then HEC-GeoHMS was used to refine the sub basin and stream delineations, extract physical characteristics of sub basins and streams, estimate model parameters, and prepare input files for HEC-HMS.

3.5.2.1 **HEC-HMS Inputs**

HEC-HMS Model setup consists of 4 main model components: basin model, meteorologic model, control specifications and input data (time series, paired data and gridded data).

The basin model includes, runoff Loss method, runoff transform and baseflow model. Runoff loss models needs initial abstraction, curve number and percentage of impervious. Parameters for runoff transform includes time of concentration and storage coefficient and base flow model parameters are initial discharge, recession constant and threshold flow.

Even though long records of time series data are available, a concurrent data set for both of the stations used from a period of 1998-2002 has been used for model calibration and from 2005-2006 used for model validation.

3.5.2.1.1 **Runoff Loss Model**

Soil Conservation Service Curve number (SCS CN) method was used to estimate runoff loss. A relationship between accumulated rainfall and accumulated runoff was derived by SCS from experimental plots for numerous soils and vegetative cover conditions. The SCS runoff equation (Equation 5) was used to estimate direct runoff from 24-hour or 1-day storm rainfall.

$$Q=\frac{(P-Ia)^2}{(P-Ia)+S} \quad (5)$$

Where:

Q = accumulated direct runoff (in)

P = accumulated rainfall or potential maximum runoff (in)

Ia = initial abstraction including surface storage, interception, evaporation, and infiltration prior to runoff (in)

S = potential maximum soil retention (in) = 1000/CN-10

An empirical relationship used in the SCS method for estimating Ia is presented in

Ia = 0.2S

Using soil data of the catchment obtained from Ministry of water, irrigation and energy and Harmonized World Soil Database Sandy Loam, Silt Loam, Clay loam, Loam and Sand are the broad soil divisions mentioned. For the derivation of CN Soil Conservation Service (SCS).Technical Report 55 had classified the soils in to A, B, C, D Hydrological soil groups (HSG's). Accordingly, the catchments soils were classified in to HSG's A, B ,and D. i.e,Sand and Sandy Loam are HSG A, Silt Loam or Loam are HSG B and Clay loam, silty clay loam, sandy clay, silty clay, or clay are HSG D. Soil classified under HSG C was not found in the catchment.

The CN for a watershed can be estimated as a function of land use, soil type and antecedent moisture content of watershed, using tables published by the Soil Conservation Service (SCS). The curve number estimated are for normal antecedent moisture conditions (AMC II).For dry conditions (AMC I) or wet conditions (AMC III),equivalent curve numbers can be computed by equation 6 and 7 respectively.

$$CN(I) = \frac{4.2CN(II)}{10-0.058CN(II)} \qquad (6)$$

$$CN(III) = \frac{23CN(II)}{10+0.13CN(II)} \qquad (7)$$

The range of antecedent moisture conditions for each class is given on Soil Conservation Service, 1972, Table 4.2.P. 4.12.). Weighted curve number estimated for the study area was for normal antecedent moisture conditions (AMC II). However, total 5-day antecedent Rainfall before simulation showed 4.2 mm indicating AMC I as the days are dormant season for the area. Therefore, AMCII CN has to be transformed to AMCI CN using equation (6).

3.5.2.1.2 **Estimating Base flow Model Parameters**

The recession model was used to explain the drainage from natural storage in a watershed. It defines the relationship of Q_t, the base flow at any time t, to an initial value as:

$Q_t=Q_0e^{-\alpha t}$...(8)

The term $e^{-\alpha}$ in this equation can be replaced by K called the recession constant or depletion factor which is commonly used as an indicator of the extent of baseflow (Nathan and McMahon 1990)

$Q_t = Q_0K^t$...(9)

Where: Q_0 = initial base flow (at time zero); α is constant also known as the cut-off frequency. and K= an exponential decay constant

As implemented in the program, K is defined as the ratio of base flow at time t to the baseflow one day earlier. The starting baseflow value, Q_0, is an initial condition of the model.

In Exponential recession model, initial flow, the recession ratio and the threshold flow are parameters. The initial flow is an initial condition. The recession constant K, depends upon the source of baseflow. It was estimated using gauged flow data available. Flows before start of direct runoff identified and the ratio of ordinates spaced one day apart were computed. The computed value of recession constant was about 1. Although, exponential decay of typical undeveloped watersheds must be less than one, may be correct for this watershed as the Cheleleka lake (wetland) regulates the flow at outflow.

The threshold value can be estimated from examination of graph of observed flows versus time. It was estimated to be about 1.726 m^3/sec. Observed flow is shown in Figure 3.7.

K = Q_o present/Q_o one day before present

Peak flow in 1998 was 4.673 m^3/s.

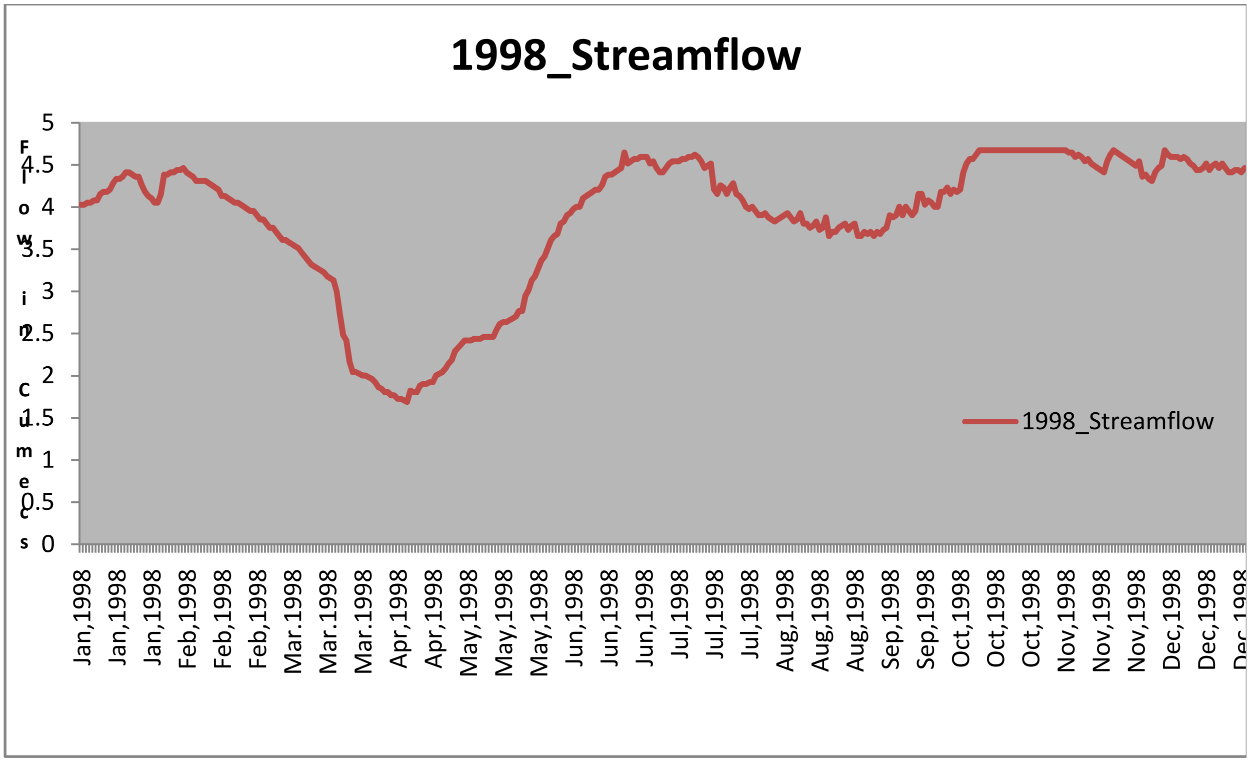

Figure 3.7 Tikur Wuha Observed Stream Flow during Calibration

3.5.2.1.3 **Time of Concentration (Tc) Estimation**

One of the parameter used in transfer model of direct runoff model is time of concentration. Time of concentration for this study was estimated using different methods and appropriate value was selected. Based on the summary of Witham (2006), five empirical equations were used to obtain Time of Concentration for sub catchment.

I. Californian Culverts Practice (1942) (Chow, Maidment and Mays, 1988)

$$T_c = 60\,(11.9\,L^3/H)^{0.385} \quad \text{...(10)}$$

Where: L is length of the longest water course (mi)

H is elevation difference between divide and outlet (ft)

II. SCS Lag Equation (1973) Using Average Values for CN

$$\frac{100L^{0.8}\left(\frac{100}{CN}-9\right)^{0.7}}{1900\,S^{0.5}} \quad \text{..(11)}$$

Where: L is hydraulic length of watershed (longest flow path) (ft)

S is average watershed slope (%)

CN is average SCS curve number for each sub catchment

III. SCS Lag Equation (1973) Using Mode Value for CN

$$\frac{100L^{0.8}(\frac{100}{CN}-9)^{0.7}}{1900\ S^{0.5}} \text{...(12)}$$

Where: L is hydraulic length of watershed (longest flow path) (ft)

S is average watershed slope (%)

CN is mode SCS curve number for each sub catchment

IV. Bransby-Williams (Ministry of Works and Development, 1980)

$$Tc = \frac{0.953\ L^{1.2}}{A^{0.1}H^{0.2}} \text{..(13)}$$

Where: L is maximum flow length (km)

A is watershed area (km^2)

H is elevation difference between the highest and lowest points along the main channel (m)

V. US Soil Conservation Service (Martin et al., 1997).

$$T_c = \left(\frac{0.87\ L^3}{H}\right)^{0.385} \text{...(14)}$$

Where: L is maximum flow length (km)

H is elevation difference between the highest and lowest points along the main channel (m)

All the physical parameters required in the formulas above were derived from the digital elevation model (DEM) for the study area using ArcMap by attributes queries operations and 'Surface Analysis extension'.Time of concentration obtained gives a large variation only with US Soil conservation service equation for sub-basin 7. Therefore, averages of all methods were taken as shown in Table 3.14.

Table 3.14 Time of Concentration estimated for the study area.

SubBasin ID	**Time of Concentration (hr)**				
	Californian Culverts Practice	Bransby-Williams	US Soil Conservation Service	SCS Lag Equation	Average
9	0.904	0.375	0.396	1.165	0.710
8	0.480	0.123	0.106	0.761	0.368
7	0.765	5.764	45.684	1.872	13.521
6	2.954	0.097	0.063	0.825	0.985
5	0.224	0.177	0.150	1.857	0.602
4	1.818	0.272	0.227	1.210	0.882
3	0.337	0.460	0.599	0.462	0.465
2	1.319	0.192	0.099	1.070	0.670
1	5.021	0.351	0.377	0.997	1.687

3.5.2.1.4 **Storage Coefficient (R)**

The basin storage coefficient, R, is an index of the temporary storage of precipitation excess in the watershed as it drains to the outlet point. Clark (1945) indicated that R can be calculated as the flow at the inflection point on the falling limb of the hydrograph divided by the time derivative of flow, so it has the unit of time. Based on Clark's (1945) indication, the storage coefficient of the catchment was estimated.

3.5.2.1.5 **Control Specifications**

Control specifications are one of the main components in a project, even though they do not contain much parameter data. Their principle purpose is to control when simulation start and stop, and what time interval is used in the simulation. Time Steps (simulation interval) used was 24 hours (1Day).

3.5.2.1.6 **Meteorological Model**

Precipitation was one of inputs of meteorological model. Mean precipitation of the rainfall gauging station was used for analysis. The mean was calculated using Theissen polygon method.To create Theissen polygon, delineated Tikur Wuha watershed and the rainfall gage stations from the four stations were located depending on the coordinates obtained from Meteorological Agency. The stations and their coordinate locations are shown in Table 3.15.

Table 3.15. Rainfall gage stations and location coordinate

Name	**Latitude**	**Longitude**
Awassa	$7^{o}03'32''$	$38^{o}28'35''$
Shashemene	$7^{o}12'01''$	$38^{o}36'01''$
Haisawita	$6^{o}33'36''$	$38^{o}25'12''$
Wendo Genet	$7^{o}10'12''$	$38^{o}34'48''$

To create rain gage point layer, Shape file was created in ArcCatalog. Then, table created by the location of the stations was imported and X, Y data were added. i.e. X=easting and Y= northing of the stations. Hydro-ID was assigned to the stations and gage Theissen polygon was created. This was using utility tools in Hec-GeoHMS.

The Thiessen method assumes that at any point in the watershed the rainfall is the same as that at the nearest gage so the depth recorded at a given gage is applied out to a distance halfway to the next station in any direction. The relative weights for each gage are determined from the corresponding areas of application in a Thiessen polygon network.The relative weights for the station were shown in the Table 3.16. Thiessen polygon created for the study area was shown in figure 3.8. From Table 3.16 and Figure 3.8 gage polygon, FID 2 represents Wando Genet station and FID 3 represents Awassa station.

Table 3.16 relative weights of rainfall gages

object ID	FID_gage _poly_p	FID_sub basin	shape_length (km)	shape_area (km^2)	KEY FROM	KEY TO	PCT FROM	PCT TO
1	2	1	58.09	66.63	2	1	17.77	71.39
2	2	2	4.07	0.44	2	2	0.12	24.88
3	2	4	7.03	1.45	2	4	0.39	31.18
4	2	6	67.53	99.06	2	6	26.42	100.00
5	2	7	48.84	29.89	2	7	7.97	54.00
6	2	8	23.31	10.58	2	8	2.82	13.84
7	3	1	34.41	26.71	3	1	2.59	28.61
8	3	2	10.73	1.34	3	2	0.13	75.12
9	3	3	143.01	209.32	3	3	20.29	100.00
10	3	4	19.61	3.19	3	4	0.31	68.82
11	3	5	43.85	27.61	3	5	2.68	100.00
12	3	7	39.41	25.46	3	7	2.47	46.00
13	3	8	61.79	65.91	3	8	6.39	86.16
14	3	9	61.42	59.86	3	9	5.80	100.00

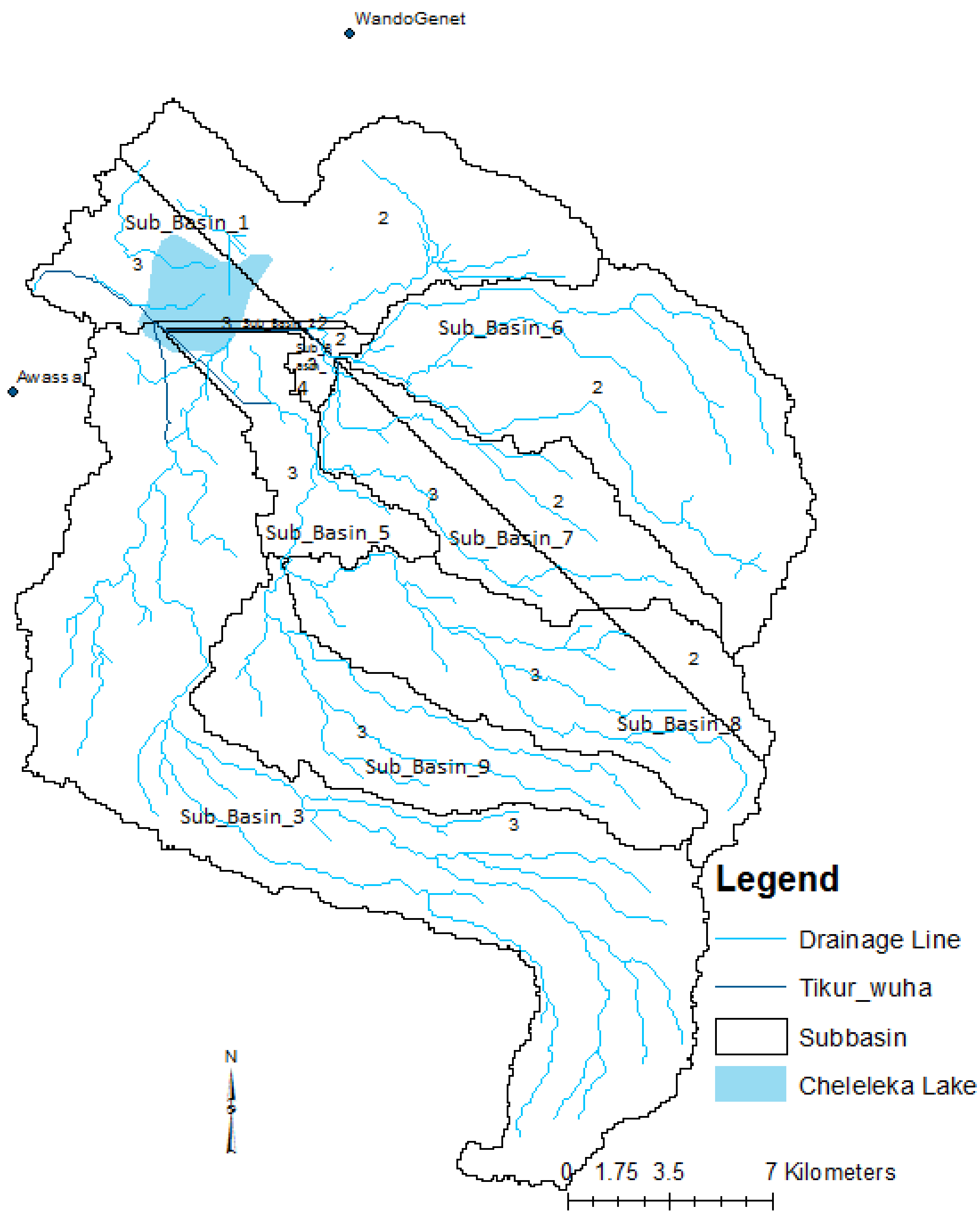

Figure 3.8 Thiessen Polygon of the study area

4 Result and Discussion

Result of image data analysis, climate data analysis and their impact assessment on Tikur Wuha River is presented in this section.

4.1 Land Use Change Impact Analysis

Image classification accuracy assessment and land cover change detection results are discussed as follows.

4.1.1 Image classification

Accuracy assessment

The land cover map of the study area for year 1973, 1986, 2000 and 2005 derived from classified Landsat images are shown in Figure 4.1 (a,b,c,d). The 1973 land-cover map has an overall classification accuracy of 75% and kappa statistic of 0.603 while the 1986 land-cover map obtained 74.28% accuracy and kappa statistic of 0.5565. This figure is interpreted as that the classification of 1973 image is 60.3% better than would have occurred strictly by chance and 1986 image is 55.65% better than would have occurred strictly by chance. Monserud (1990) suggested a kappa value of <40 % as poor, 40–55 % fair, 55–70 % good,70–85 % very good and >85 % as excellent. According to these ranges, the classification in this study has good agreement with the validation data set. Similar Study on "Integrated Landsat Image Analysis and Hydrologic Modeling to Detect Impacts of 25-Year Land-Cover Change on Surface Runoff in a Philippine" had observed that the land-cover maps derived from the classifications are highly accurate, with more than 90% Producer’s and User’s Accuracy for each land-cover class. This may be mainly due to the satisfaction of the assumptions of the MLC for class signatures to be normally distributed, and to the high degree of separability of the class signatures. While this holds true in the present study, in some cases, the number of training samples to obtain class signatures is limited and/or may not have normal distributions, which restricts the MLC to get the ideal result.

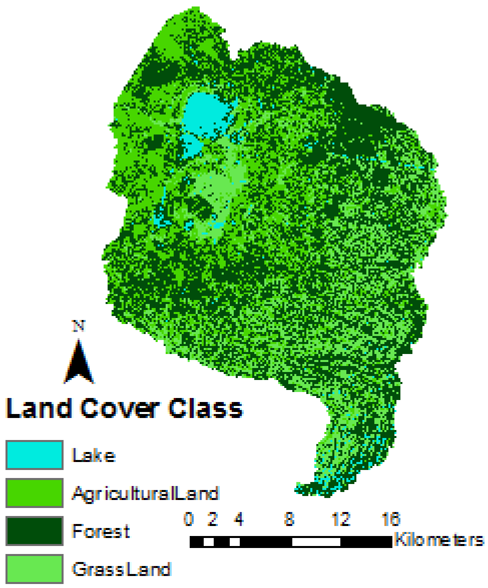

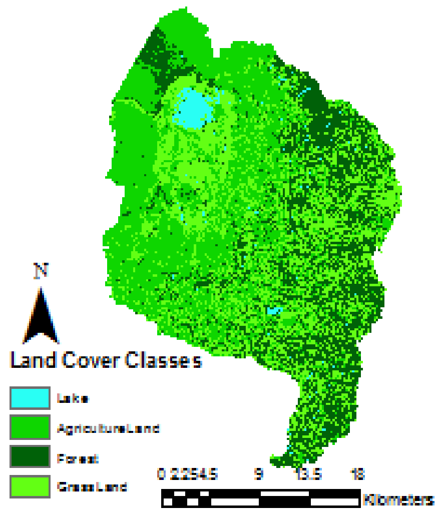

(a) year 1973 **(b) year 1986**

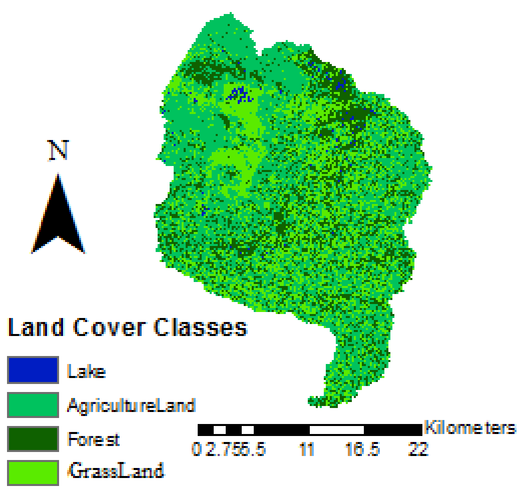

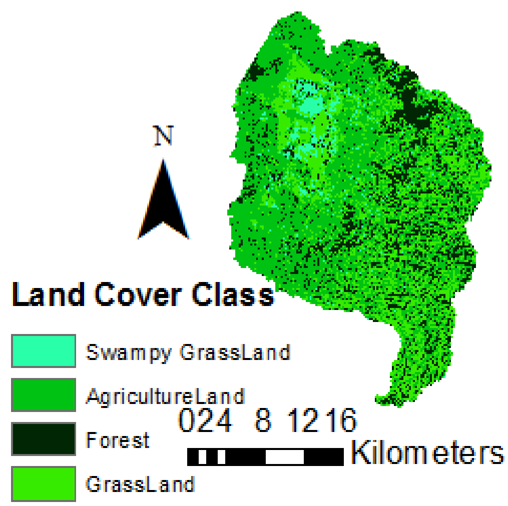

(c) Year 2000 **(d) year 2005**

Figure 4.1 Result of image classification of year 1973 (a), 1986 (b), 2000(c) and 2005 (d)

4.1.2 **Land Cover Change Detection**

Comparing land-cover maps, changes in land-cover from 1973 to 2005 with respect to the total area of the watershed can be determined (Table 4.1). The analysis showed a 28.77% reduction in forest cover, a 3.6% reduction in lake cover, a 23.49% increase in agricultural land, 3.6% increase in marshy land (Swamp) and 5.3% increase in grassland in the study area in the span of 32 years.

The increase in agricultural areas and reduction in forest areas may be because of human settlement and associated expansion of farming, deforestation due to increased demand for fuel, construction wood and charcoal. Site action plan of Rift valley lakes, Awassa project has explained that the forest area is under threat since 1991 because of human settlement. Lake in Tikur wuha sub catchment was disappeared (reduced from 3.6% to 0%).This may be shown as the disappearance of Cheleleka lake because of siltation as explained in other researches done on the area. Study done on Lake Awassa (Shewangizaw and Michael. 2010) showed also natural vegetation decreases by 11,768 ha, the cultivated land increases by 20,661 ha and the urban area increases by 1,310 ha in the period of 1965 to 1998 in Lake Awassa catchment. Land cover change observed can change watershed response to rainfall leading to increased surface runoff volume and sedimentation of Lake Awassa. Another study in Gilgel Abbay catchment (Rientjes et al.2011) concluded forest land decreased from 50.9 % in 1973 to 32.9 % in 1986. Agricultural land increased from 28.2 % in 1973 to 40.2 % in 1986. In the period, 1986–2001 forest land decreased from 32.9 % to 16.7 % while agricultural land increased from 40.2 % to 62.7 %.

Table 4.1 Land cover change statistics of the study area

Land cover classes	1973 % of total area	1986 % of total area	2000 % of total area	2005 % of total area	%Change From 1973 to 2005 with respect to total watershed area
Lake	3.60	2.01	0.72	-	-3.6
Agricultural land	27.7	40.52	49.46	51.19	23.49
Forest	48.29	26.49	22.18	19.52	-28.77
GrassLand	20.39	30.97	27.62	25.69	5.3
MarshyLand (swamp)	-	-	-	3.6	3.6

4.1.1 HEC - HMS Model Calibration and Validation

HEC - HMS model inputs were estimated and used for model calibration. The models used for this particular study were, SCS curve number (CN) for runoff volume model, Clark's unit hydrograph to estimate direct runoff, exponential recession model for base flow estimation. Parameters estimated during calibration and their optimized values were shown in Table 4.2 (a) and (b). The objective function minimization was done to measure the goodness of fit between the computed result from the model and the observed flow. i.e. it measures the degree of variation between computed and observed hydrographs.

Table 4.2 Estimated (a) and Optimized (b) parameters value during calibration

(a)

SubBasn ID	CN	Initial Abstraction in (mm)	Clark Time of Concentration in (HR)	Clark Storage Coefficient in (HR)	Baseflow Initial Flow in (M^3/s)	Recession Constant	Baseflow Threshold Flow in (M^3/S)
9	64	5.76	0.709	4.32	0.36	0.98	0.155
8	88	5.12	0.567	3.84	0.32	0.98	0.138
7	64.77	4.48	13.542	3.36	0.28	0.98	0.121
6	88	3.84	1.201	2.88	0.24	0.98	0.104
5	62	3.2	0.577	2.4	0.2	0.98	0.086
4	55	2.56	0.819	1.92	0.16	0.98	0.069
3	88	1.92	0.586	1.44	0.12	0.98	0.052
2	58.5	1.28	0.634	0.96	0.08	0.98	0.035
1	58.5	0.64	1.654	0.48	0.04	0.98	0.017

(b)

Sub Basin ID	CN	Initial Abstraction in (mm)	Clark Time of Concentration in (HR)	Clark Storage Coefficient in (HR)	Baseflow Initial Flow in (M^3/s)	Recession Constant	Baseflow Threshold Flow in (M^3/S)
9	76	0.5	1.2	8.57	0.481	0.99	1.164
8	90	0.2	0.5	9.852	0.587	0.99	1.21
7	68	1	0.386	8.233	0.452	0.998	1.152
6	91	0.2	0.51	14.57	0.631	0.99	1.6
5	67	1.1	0.37	4.11	0.276	0.99	1.759
4	55	1.2	1	0.7	0.32	0.98	0.4
3	90	0.2	10.54	32.01	0.35	0.98	1.9
2	62	1.1	0.36	0.26	0.3	0.99	0.491
1	62	1.1	0.5	14.14	0.6	0.99	1.6

Using the initial estimation output of the HEC - HMS program peak discharge obtained by simulation was 10.5 m^3/s and observed peak discharge was as 4.7 m^3/s. simulated runoff volume was 827.4 mm and observed runoff volume was 882.1 mm. This shows a very high difference for peak discharge and the model is not good for peak flow estimation using initial estimation of parameters.

To get good agreement with observed values, the program was rerun using optimized parameter and shown in Figure 4.2. Yemane (2004) reported that simulated total runoff from Tikur Wuha sub catchment based on land use map of 1998 was 200Mm^3, which is more than 100% higher than what is measured in the sub catchment outlet, not to mention in accuracy of the river discharge measurement itself. When the relationship of measured discharge and rainfall are evaluated, measured rainfall was about 1037.95mm and stream flow was about 194.71mm on year 1998 while measured rainfall was 707.68mm and stream flow was about 202.7mm on year 1999.

The comparison between the observed and simulated stream flows indicated that there is a good agreement between the observed and simulated discharge which was verified by values of Nash coefficient which is about 0.61. The Nash-Suttcliffe simulation efficiency results fulfilled the requirements suggested by (Santhi et al., 2001) for Nash coefficient > 0.5.The validation result of the model is shown in Appendix Figure D.

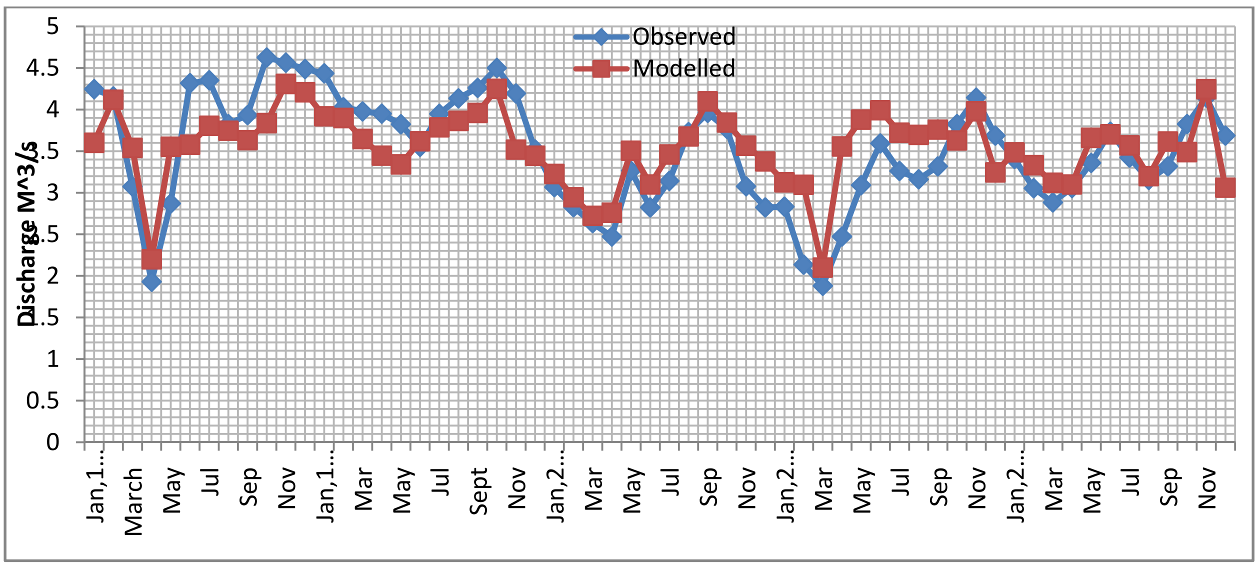

Figure 4.2 Observed and Simulated hydrograph of Tikur Wuha River, Period (1998-2002) – Calibration Period

4.1.1.1 **Sensitivity Analysis**

Sensitivity analysis has been made to all parameters considered in HEC-HMS model. As it is indicated in Figure 4.3, the model is more sensitive to curve number and recession constant. 10% change in the recession constant can cause up to 2.54% reduction or 3.18% increment on runoff volume. Similarly, by changing curve number by -10% a change up to -1.40% was obtained. The variable to which the model is least sensitive is time of concentration and baseflow initial flow.

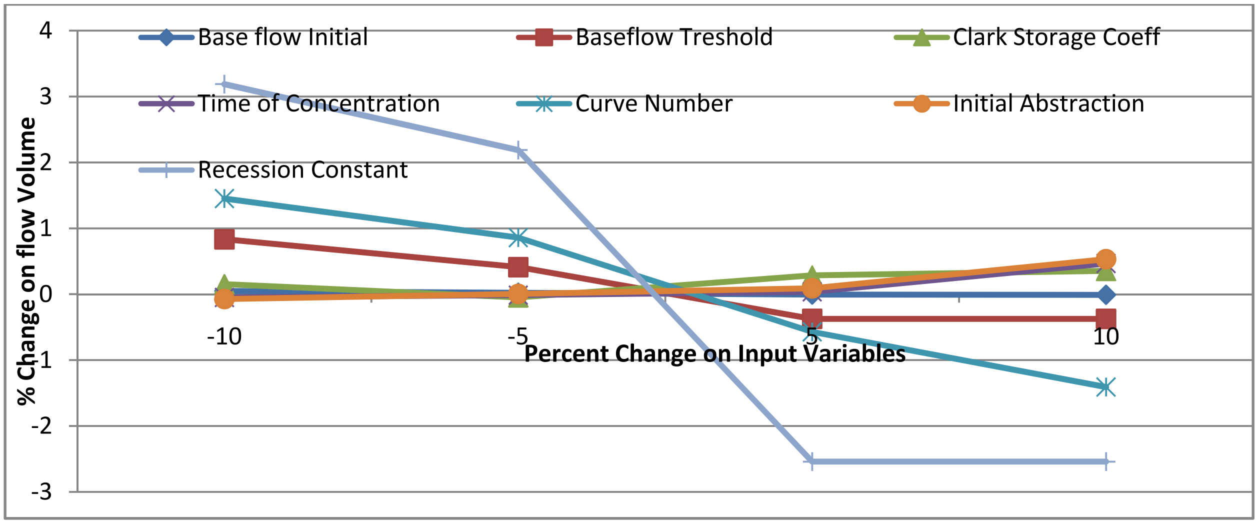

Figure 4.3 Sensitivity analysis of HEC - HMS Model

4.1.2 **Impact of Land use change**

The calibrated and validated hydrologic model was used to simulate surface runoff under three land-cover conditions namely, 2005, 1986; 1973.

When calibrated hydrologic model used to analyse impact of land cover change, as emphasized by the use of the Different land-cover condition scenarios, only the CN parameter of the model that has a direct relationship with land-cover was altered. The same rainfall events used previously for model calibration were utilized again in the simulations. The results of the simulations were then analyzed to determine the runoff responses of the watershed in different land-cover conditions, to identify how different these responses are from one other under the assumption that the same rainfall events will take place. The general assumption here is that the physical and climatological conditions of the study area are constant for the four scenarios except for the land-cover.

Changes such as forest cover reduction through deforestation and conversion for agricultural purposes can alter a watershed’s response to rainfall events, that often leads to increased volumes of surface runoff and greatly increase the incidence of flooding and sedimentation of receiving water bodies (McColl.et.al.2007, Cebecauer.et.al.2008). This study showed that Water shade runoff volume increases from period of 1973 to 2005.Runoff volume was about 318.35 million cubic meters (MCM) in 1973 and was about 337.9MCM in 2005. The result is shown in Table 4.3. This Runoff volume increment might be due to land degradation. Because, forest coverage in the area was about 48.29% and agricultural land was about 27.7% in 1973. Forest land was reduced to 19.52% and agricultural land was increased to 51.19%.in 2005. Studies showed that the lake level of Awassa Lake was rising in the past period. Tikur Wuha River is the only perennial river draining in to Lake Awassa. Therefore, increase in runoff volume in Tikur Wuha catchment has its own contribution in the rise of Awassa Lake level.

Table 4.3 Annual runoff volume of Tikur wuha sub catchment under different land cover conditions.

LandCover Condition	Water Shade Runoff Volume X 10^3 m^3	% difference from 2005 Condition
1973	318357.1	- 5.79
1986	336974.4	- 0.27
2005 (Reference)	337903.5	-

4.2 Climate Change Impact Analysis

In this section result of temperature and precipitation downscaling calibration and validation, downscaling future scenarios and impact of climate change were presented and discussed.

4.2.1 Climate change in the catchment

To see if there is change in rainfall in past Climatological baseline (1961 - 1990) was used as past and periods of 1991 - 2010 were used as current and comparison was done. The analysis showed that the precipitation of the area decreased in all months as compared to the past 30 years (1961 - 1990) as shown in figure 4.4. Interannual variability of rainfall on the sub-catchment is apparent that the annual rainfall ranges from 707.6 mm on driest year 1999 to 1289.85 mm on the wettest year of 2006.

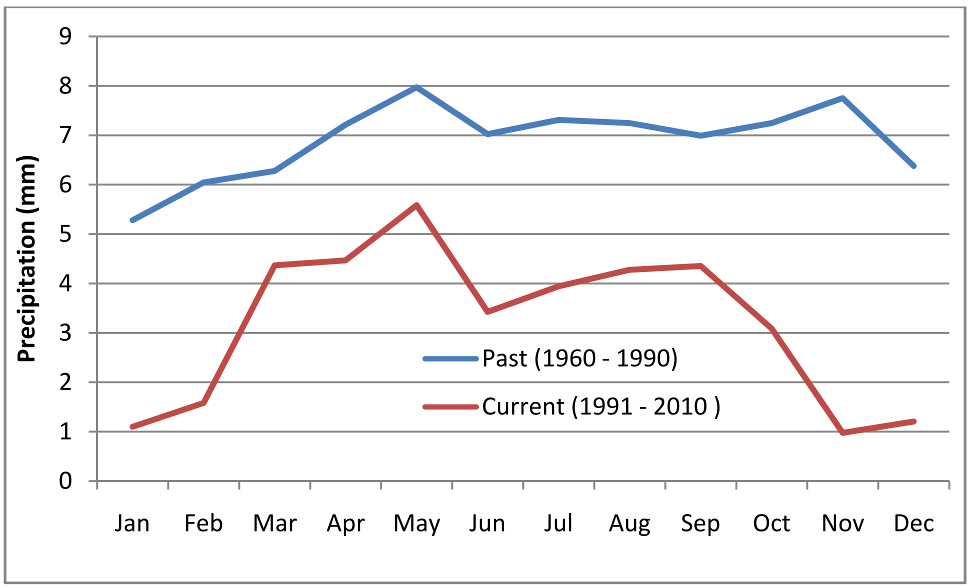

Figure 4.4 Change in precipitation of the study area.

4.2.2 Climate Downscaling Model

4.2.2.1 Climate Downscaling Model Efficiency Evaluation

Nash-Sutcliffe efficiencies can range from -∞ to 1. An efficiency of one (E = 1) corresponds to a perfect match between model and observations. An efficiency of 0 indicates that the model predictions are as accurate as the mean of the observed data, whereas an efficiency less than zero (-∞ < E < 0) occurs when the observed mean is a better predictor than the model.

Essentially, the closer the model efficiency to 1, the more accurate the model is. Model efficiency during downscaling was evaluated. Different trials were done to get good Nash value and variable combinations, which show best efficiency during calibration and validation, were used to downscale climate model. Trials selected for maximum temperature downscaling showed Nash value of 0.842 during calibration and o.73 during validation which is better than other trials. However, for precipitation downscaling the model efficiency is not good as that of temperature downscaling though it is between 0 and 1 (0<E<1) for all stations. Trials selected for precipitation downscaling was with Nash value of 0.7 for Wando Genet station,0.642 for Shashemene station,0.669 for Awassa station and 0.704 for Hasiwaita station. Nash value during model calibration of minimum temperature was 0.807.

4.2.2.2 **Bias-correction**

In this section, the application of the bias-correction technique to the precipitation and temperature downscaling output is detailed.

Bias corrections were performed over the 30-year period from 1961 to 1990, against the observed precipitation (considered as the reference precipitation for bias-correction) at the station of interest. Table 4.4 and 4.5 shows the statistics of the observed precipitation and temperature that reproduced by the downscaling model before and after the application of bias-correction. As can be seen from the table both temperature and precipitation downscaling efficiency is improved with the application of bias correction in all stations considered.The scatter plots of precipitation and temperature downscaled before and after bias correction is shown in appendix E.

Table 4.4 Statistics of precipitation before and after bias-correction

Station	statistic	Before Bias Correction	After Bias Correction
Awassa	R^2	0.722	0.732
	NSE	0.67	0.692
Wondo Genet	R^2	0.716	0.724
	NSE	0.7	0.715
Shashemene	R^2	0.663	0.71
	NSE	0.642	0.682
Haisawita	R^2	0.708	0.781
	NSE	0.704	0.7802

Where: - R^2=coefficient of determination, NSE=Nash–Sutcliffe efficiency

Table 4.5 Statistics of Temperature before and after bias-correction

Variable	statistic	Before Bias Correction	After Bias Correction
Maximum temperature	R^2	0.873	0.893
	NSE	0.842	0.852
Minimum temperature	R^2	0.807	0.842
	NSE	0.8	0.841

Where: - R^2=coefficient of determination, NSE=Nash–Sutcliffe efficiency

4.2.2.3 Calibration and Validation of Downscaling Model

The base line scenarios downscaled for base period for all stations, were 30-year period from 1961-1990 to represent baseline for this study and also used as calibration period. The rest of the years were considered for model validation. Thus, CGCM3 GCM was downscaled for the base period for three emission scenarios (A2a, A1B and B1) and some of the statistical properties of the downscaled data were compared with observed data. The downscaled base line for both maximum and minimum temperatures shows good agreement with observed data. There were variation between downscaled and observed data as precipitation downscaling is necessarily more problematic than temperature. Because daily precipitation amounts at individual sites are relatively poorly resolved by regional–scale predictors, and precipitation is a conditional process (i.e., both the occurrence and amount processes must be specified). Downscaled climate variables (precipitations, maximum and minimum temperatures) and observed data are shown in the Figure 4.5 to 4.8, For Awassa Station and in Appendix B for other stations.

I. Maximum Temperature

When compared with observed maximum temperature, the statistical downscaling model showed a good fit in all months with Nash value of 0.842 during calibration and 0.73 during validation. In other words, the patterns and trend of the downscaled maximum temperature showed good agreement with observed values.

Similar study done by Girma et.al (2009) on Upper Blue Nile showed that observed and simulated mean daily maximum temperature showed good agreement for all months of the year. Calibration and Validation result of maximum temperature are shown in Figure 4.5 and Figure 4.6 respectively.

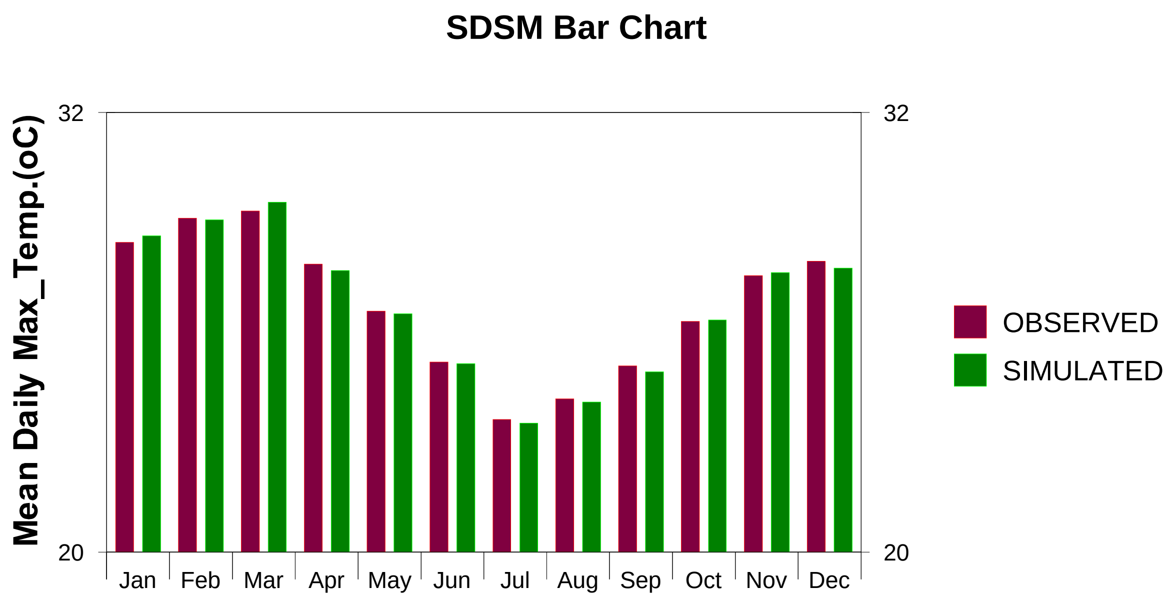

Figure.4.5. Calibration result of SDSM model downscaling (1961-1990) of daily maximum temperature at Awassa Station

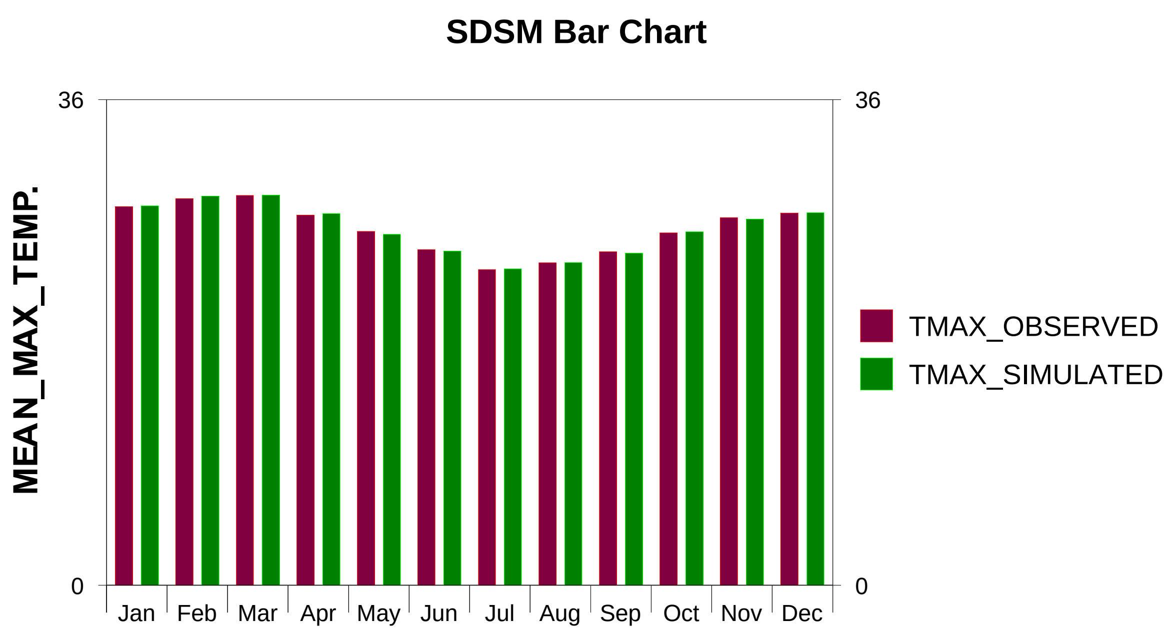

Figure.4.6. Validation result of SDSM model downscaling (1991-2000) of daily maximum temperature at Awassa Station

II. Minimum Temperature

The monthly minimum temperature downscaled for CGCM3 for Awassa station showed good agreement, except months of February, March, September and October in which it showed slight deviation from the observed values (see Figure.4.7). Similar study done by Girma et.al (2009) on Upper Blue Nile showed that observed and simulated mean daily minimum temperature showed good agreement for all months of the year. Nash value during model calibration of minimum temperature was 0.8 and 0.78 during model validation.

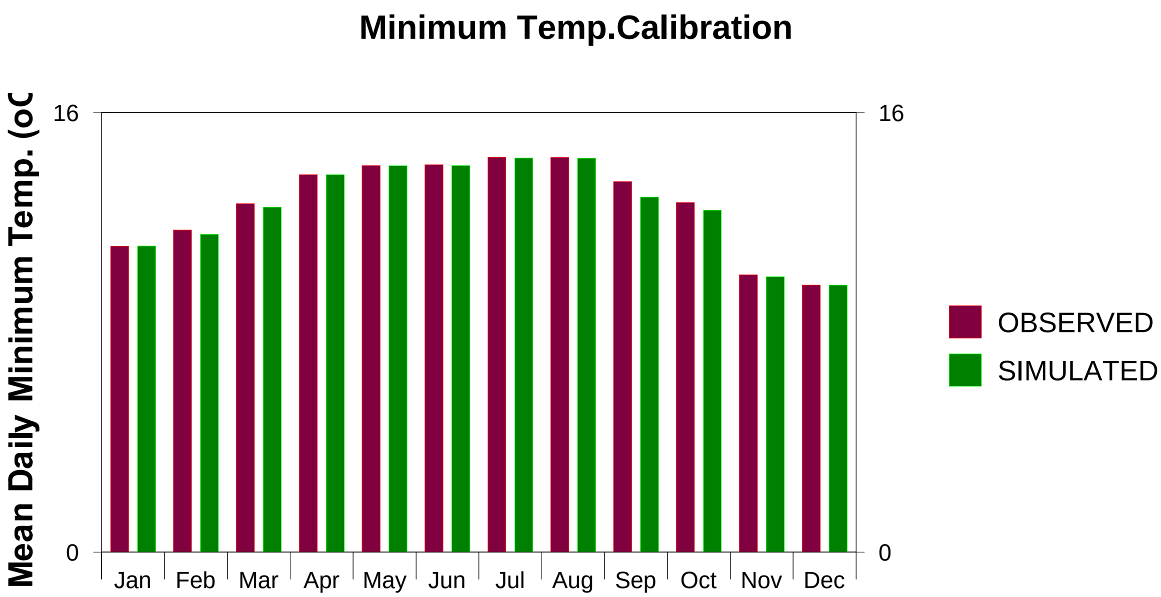

Figure.4.7 Calibration result of SDSM model downscaling (1961-1990) of daily minimum temperature at Awassa Station.

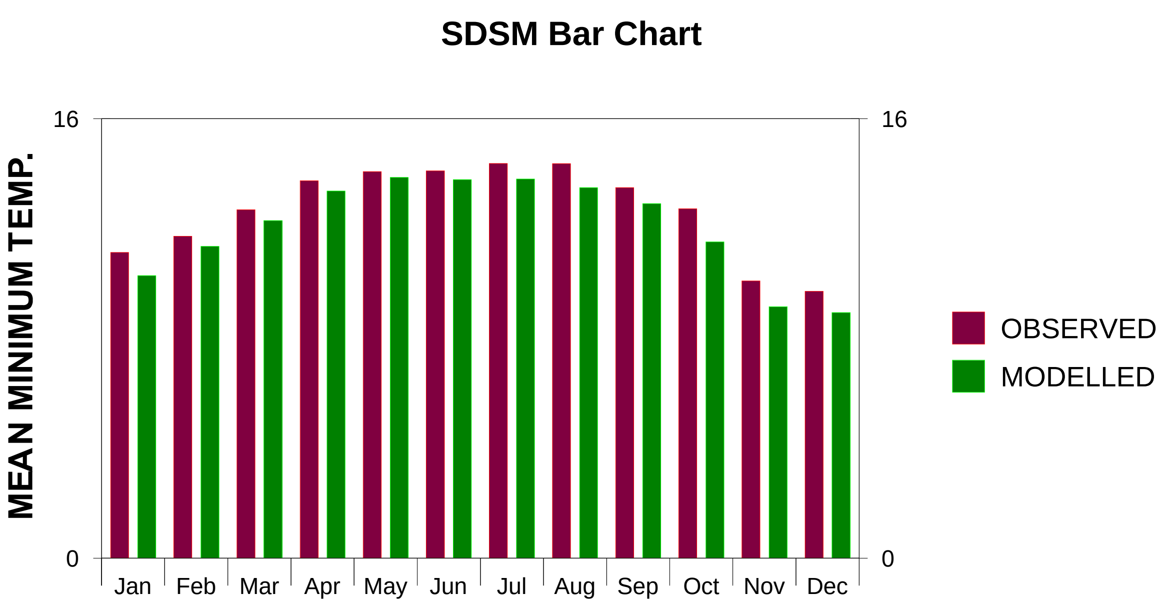

Figure.4.8 Validation result of SDSM model downscaling (1991-2000) of daily minimum temperature at Awassa Station

III. Precipitation

For Awassa station, from the 27 years of data, representing the current climate condition, the first 17 years of data (1973-1990) were considered during calibration while the remaining 10 years (1991-2000) were used to validate the model. For Wondo Genet station, years (1965 -1990) was used for calibration and (1991 -2000) for Validation, for Shashemene station years (1980-1990) for calibration and years (1991-2001) for validation and years (1970 -1990) for calibration and years (1991 - 2000) was used for validation of Haisawita station.

Time periods of 1961 to the start of period when the gage data obtained were given -999 to show missing value during calibration in all stations. For example for Awassa station time period of 1961 to 1973 were given -999 value. This is because of the baseline selected was time period of 1961 to 1990 and was also used as model calibration period.

Some of the SDSM setup parameters for event threshold, bias correction and variance inflation were adjusted during calibration to obtain a good statistical agreement between the observed and simulated climate variables. During the calibration of precipitation, downscaling models, in addition to the mean daily precipitation, monthly average dry and wet-spell lengths were used as performance criteria. Figure 4.9, 4.10 and 4.11 shows the performance of the model during validation period for Awassa Station while graphs for other stations are shown in appendix B. The graph shows a good agreement between the observed and simulated mean daily precipitation for all months of the year except January, October, November and December. Unlike temperature, precipitation is a conditional process that depends on other intermediate process like occurrence of humidity, cloud cover, and /or wet-days. For that reason, it is identified by many researchers as one of the most problematic variable in downscaling.

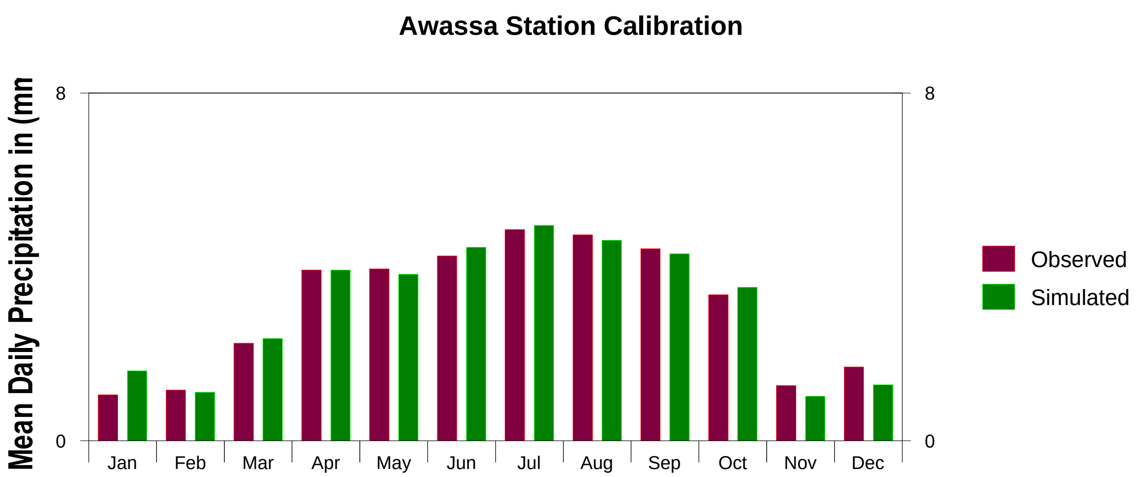

(a)

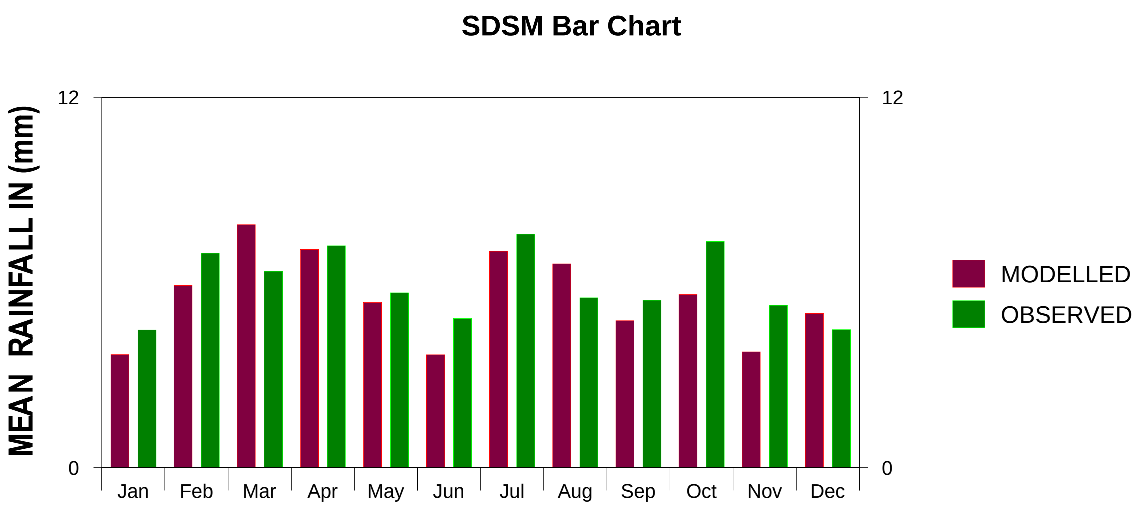

(b)

Figure.4.9 (a) Calibration 1961 - 1990 and (b) Validation 1991-2000 of daily precipitation at Awassa station

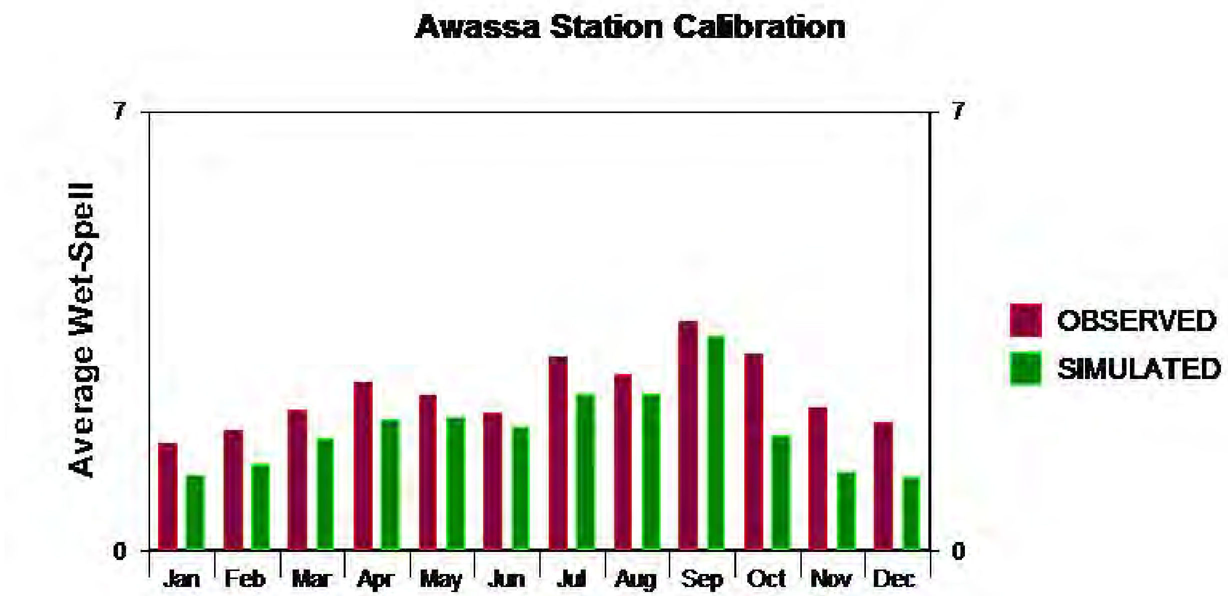

Figure.4.10 Validation Result of SDSM Model Downscaling of daily precipitation (1991- 2000) at Awassa station

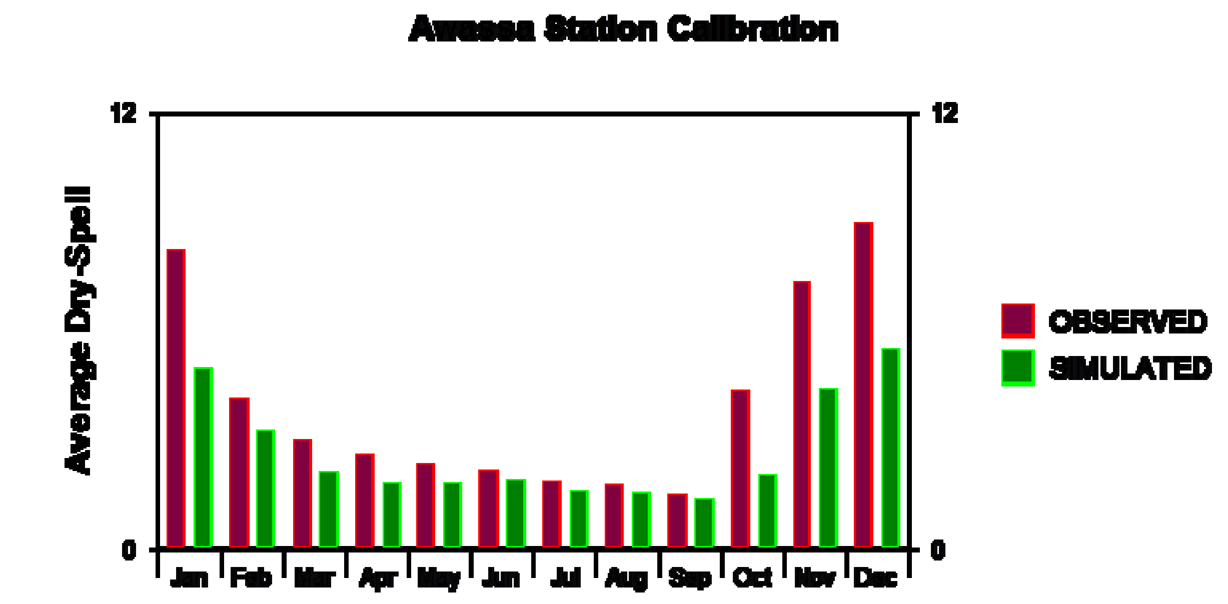

Figure.4.11.Validation Result of SDSM Model Downscaling of daily precipitation (1991- 2000) at Awassa station

4.2.2.4 **Downscaling Future Scenarios**

After calibrating the SDSM model, using observed data and large-scale predictors originating from Canadian Centre for Climate Modeling and Analysis (IPCC 20-th Century Experiment with CGCM3.1/T63), the same empirical relationship with predictors, supplied by GCMs, were tuned to downscale the future climate change scenario simulated by GCMs.

Future climate scenarios downscaled for three climate variables (precipitation, maximum and minimum temperature) are shown in the Figure 4.12- 4.14. With the aid of statistical downscaling model (SDSM) the GCMs global predictors were used for development of future climate scenarios. The scenarios were analyzed for future periods of 2020’s (2015 -2035), 2050's (2040 - 2060) and 2080's (2080 - 2100) for A2, A1B and B1 emission scenarios.

I. Maximum and Minimum Temperature

20 ensembles of synthetic daily time series were generated for A2, A1B and B1 emission scenarios for the period of 19 years (2015 -2035) , (2040 - 2060) and (2080-2099). Fig.4.12 and 4.13 shows the general trend in the mean daily maximum and minimum temperature at Awassa station corresponding to future climate change scenarios downscaled with SDSM. From these figures, it could be seen that increasing trend is evident for maximum temperature throughout the seasons. Maximum and minimum temperature change for period 2080 s was about 3.16 ^oC and 0.28 ^oC for SRES A2 ,1.46 ^oC and 0.34 ^oC for SRES A1B ,2.03 ^oC and 0.342 ^oC for SRES B1 respectively. Average increase in maximum and minimum temperature for 2050 s was about 1.37 ^oC and 0.43 ^oC for SRES A2, 1.43 ^oC and 0.35 ^oC for SRES A1B and 1.39 ^oC and 0.33 ^oC for SRES B1 respectively. Study on Upper Blue Nile Girma et.al (2009) showed that the average increase in minimum and maximum temperature between the current climate and that of 2050 s was about 2.5 ^oC and 2.3 ^oC , respectively. Maximum temperature downscaling for SRES A2 do not show consistent increment for period 2050 s. It decreases in May, June and September. Lowest maximum temperature was observed in July for all emission scenarios and highest maximum temperature was observed in February and March in all periods considered. This is also true for current maximum temperature.

Minimum temperature decreased in months January, April, May, October and November for all Scenarios in all periods considered. Minimum temperature increased in months February, March, June, July and August for all emission scenarios and periods considered.

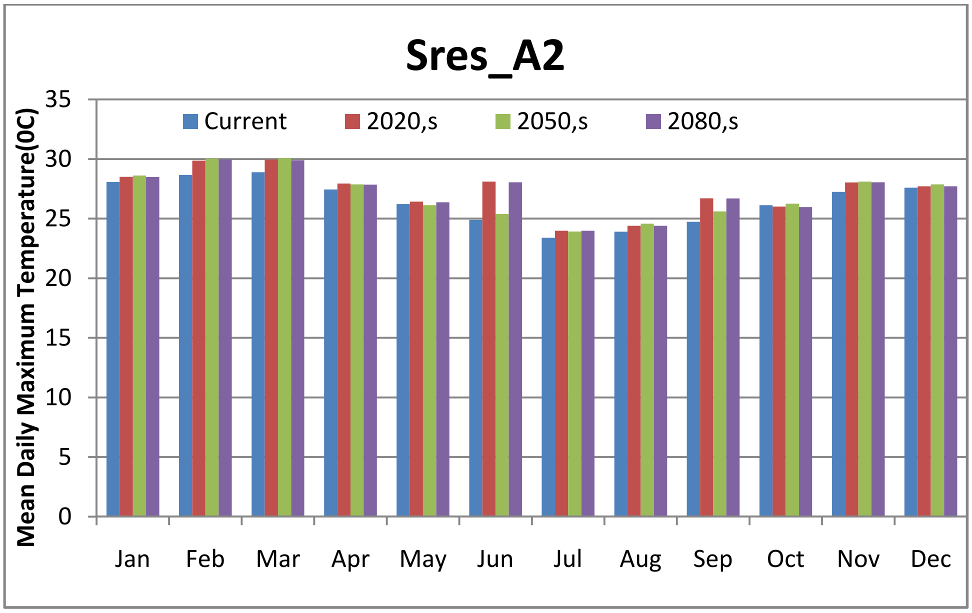
Sres_A2
Current
2020,s
2050,s
2080,s
Mean Daily Maximum Temperature(0C)
0
5
10
15
20
25
30
35
Jan
Feb
Mar
Apr
May
Jun
Jul
Aug
Sep
Oct
Nov
Dec

(a)

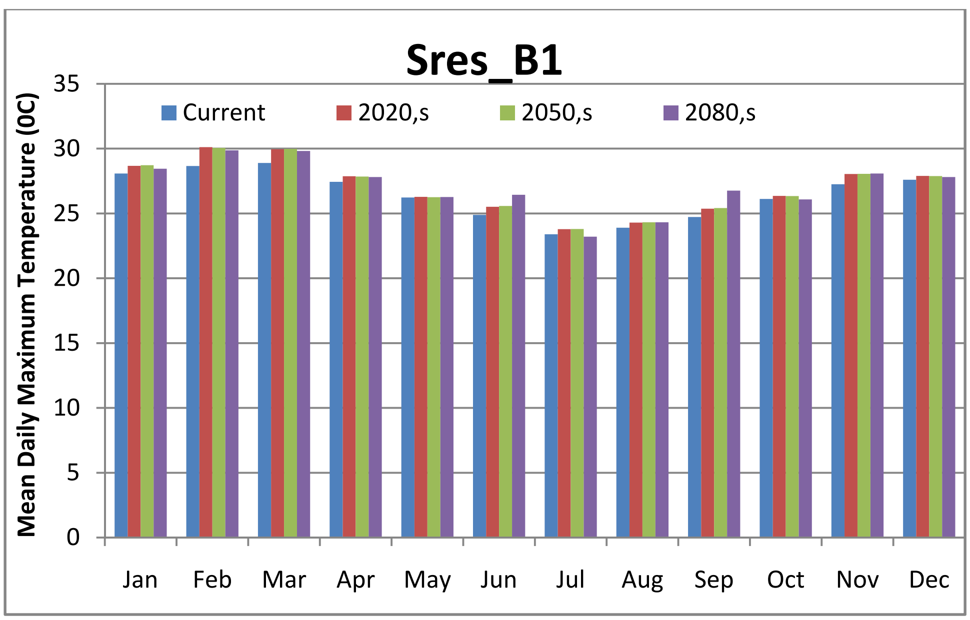
Sres_B1
Current
2020,s
2050,s
2080,s
Mean Daily Maximum Temperature (0C)
0
5
10
15
20
25
30
35
Jan
Feb
Mar
Apr
May
Jun
Jul
Aug
Sep
Oct
Nov
Dec

(b)

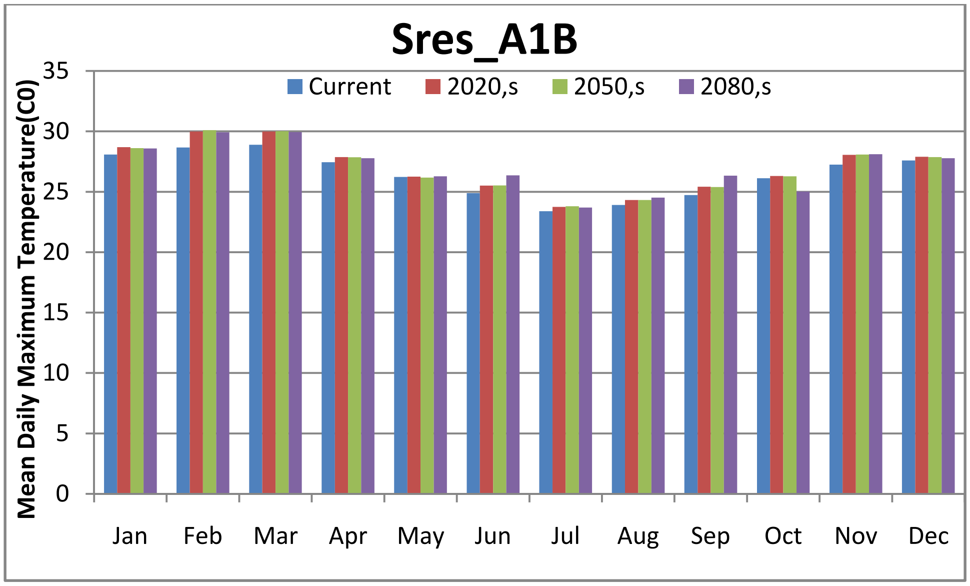

(c)

Figure .4.12 Change in maximum temperature at Awassa Station corresponding to climate scenario downscaled with SDSM (a) sres_A2 ,(b) sres_B1 and (c) Sres_A1B

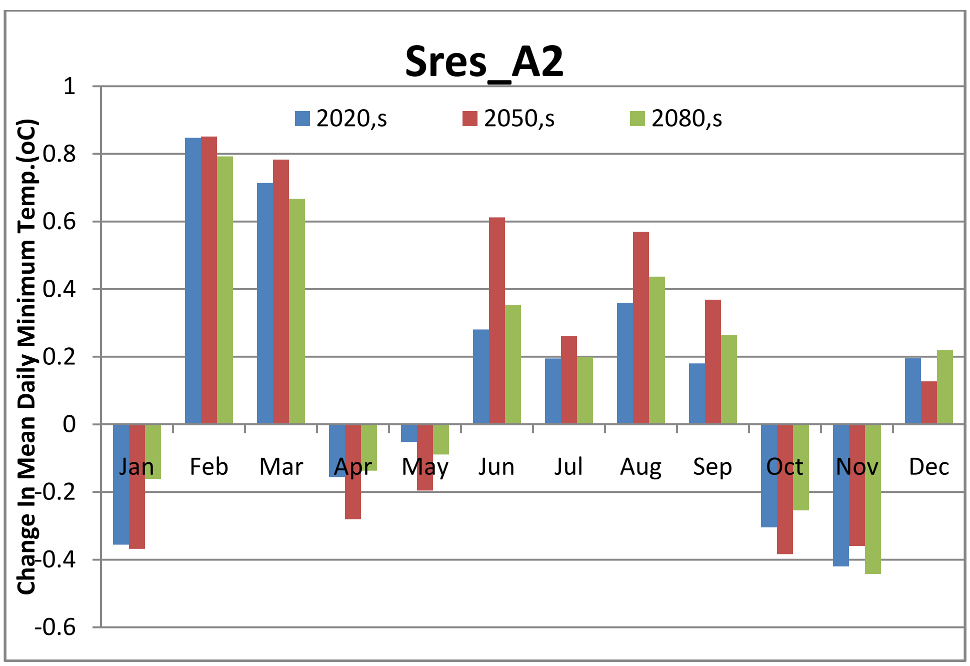

(a)

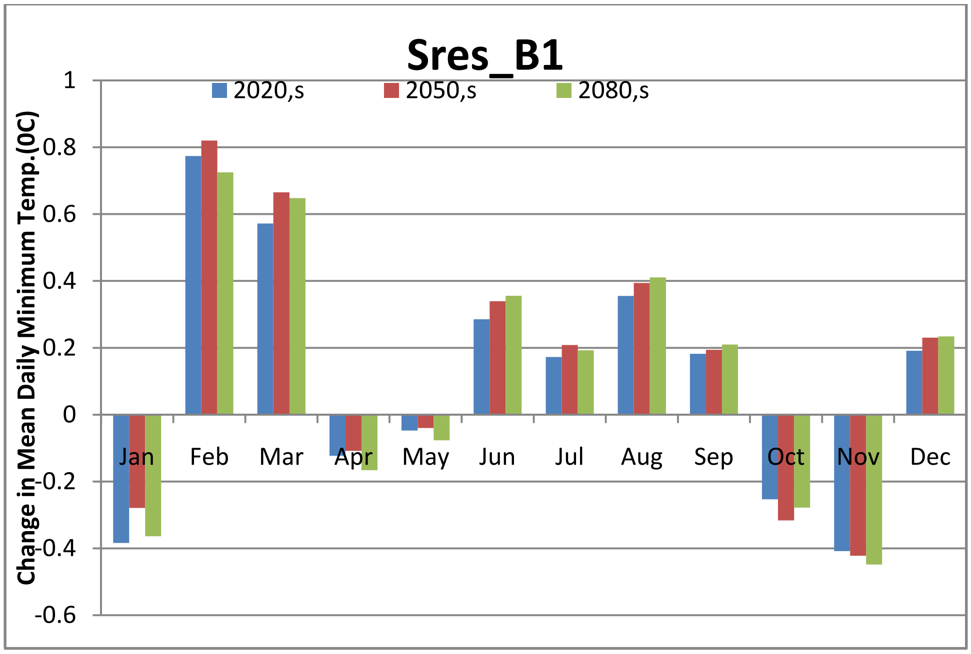

(b)

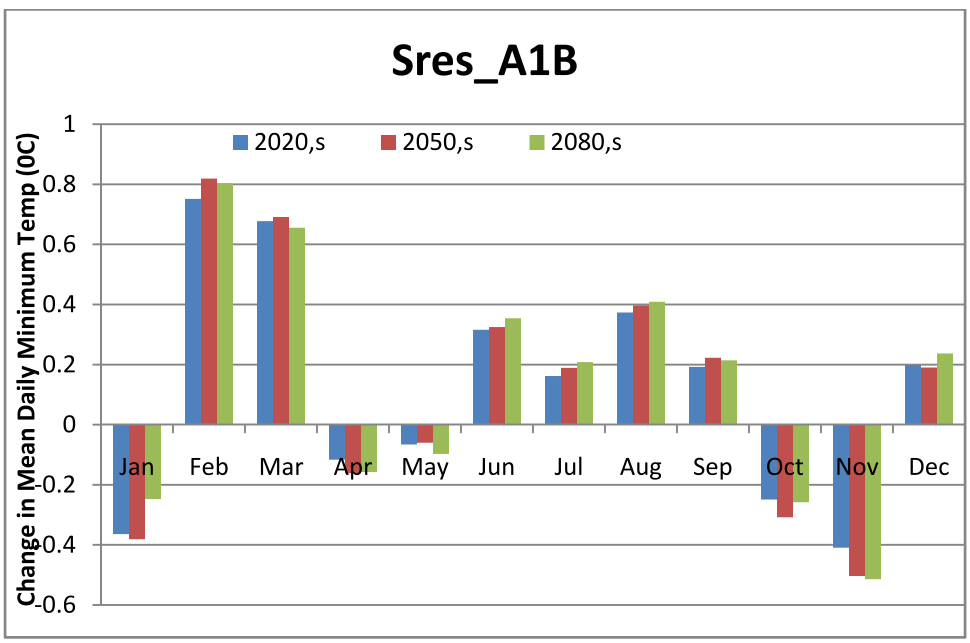

(c)

Figure .4.13 Change in minimum temperature at Awassa Station corresponding to climate scenario downscaled with SDSM (a) sres_A2 ,(b) sres_B1 and (c) Sres_A1B

II. precipitation

The future precipitation projections showed increasing trend from February to April using all three scenarios as shown in Figure 4.14. However, the change is not consistent for time period (2040 - 2060) in scenarios A2 and A1B. When compared to the current situation (1991-2010), 2080s periods shows decreasing trends for all months except January, February, August and September for all scenarios. For Kiremt months, (June, July and August) rainfall will experience a decrease in amount for scenarios A2 and B1 in all periods considered. At the end of rainy season precipitation increases for all scenarios in future. The study compares precipitation change dividing the data into a wet-season (June to September) and a dry-season (October to May) so that the results are easier to interpret from the perspective of possible impacts. Change in precipitation for SRES A2 in period 2020s,2050s and 2080s was estimated to be about 0.7%, -10.13% and -3.54% in wet season at Wando Genet station respectively. For SRES B1 change in precipitation projected was 5.24%, 0.8% and -0.483 in period 2020s, 2050s and 2080s at Wando Genet station respectively during wet season. For Dry season Change in precipitation for SRES A2 in period 2020s, 2050s and 2080s was estimated to be about 3.38%, 5.14% and 17.04% at Wando Genet station respectively.

For SRES B1 change in precipitation projected was -3.2%,7.57% and 10.56% in period 2020s,2050s and 2080s at Wando Genet station respectively in dry season. In all cases, the projected rainfall changes were less than 30%.Similar Study done on upper Blue Nile Girma et.al (2009) showed rainfall decrease in future for rainy season. In contrast, study by Shimelis G.et.al showed that the GCM's do not give confident picture of rainfall change in their study. Firstly, approximately half of the models suggest increases in rainfall, and half suggest decreases, so there is no consensus between 15 GCMs considered. Further, in most cases the projected rainfall changes are less than three (3) standard deviations; even though some of the changes are large in absolute terms (greater than 50%).The study noted that the larger changes are projected in the GCMs with the largest inter-annual variations (S.G. Setegn et al.2011). For several of the models the study considered changes are similar for all three scenarios (A2, A1B and B1); that is, they appear to be independent of the emission scenario. For this study figures for other stations, which shows future precipitation are shown in appendix B.

The Analysis showed Tikur Wuha sub catchment could experience reduced precipitation for period 2050s and 2080s during rainy season, which would reduce rain-fed agricultural productivity.

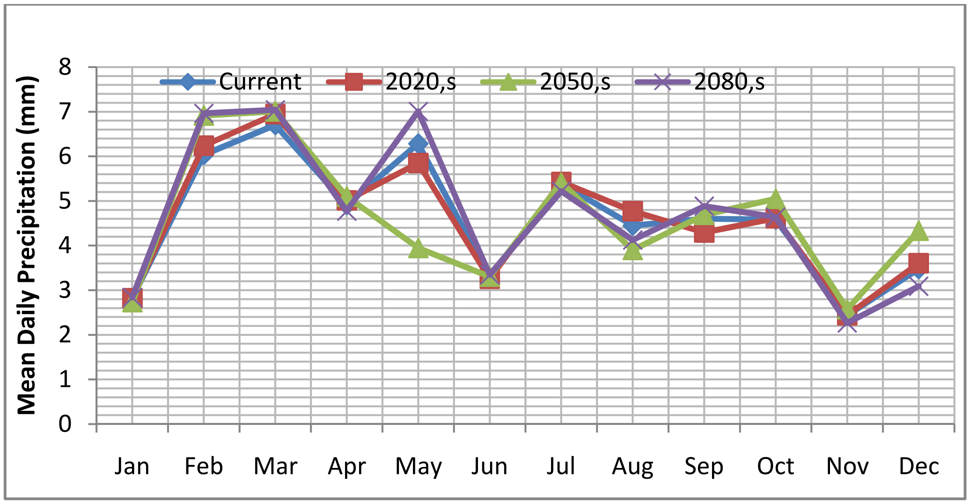

(a)

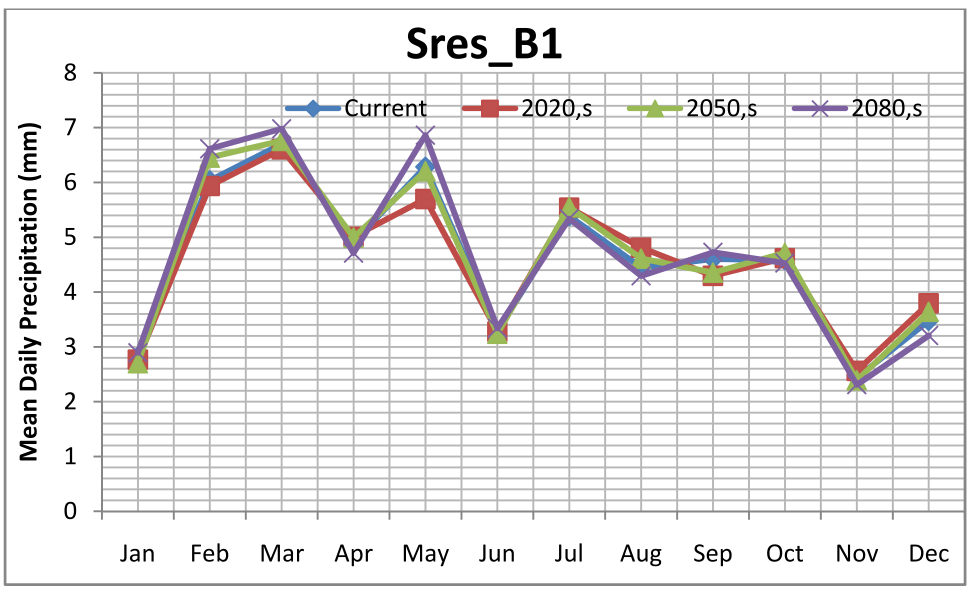

(b)

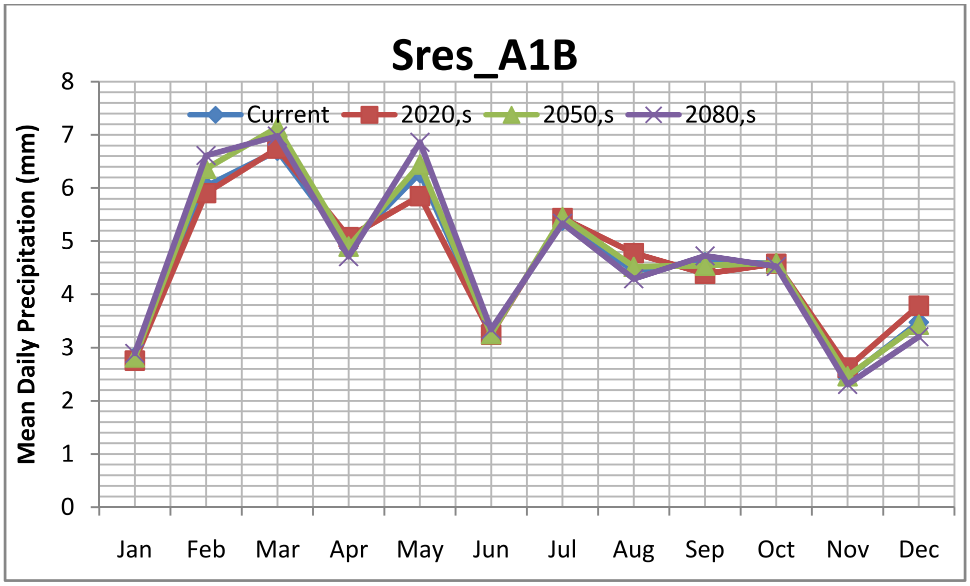

(c)

Figure.4.14 Downscaled mean daily Precipitation of Wondo Genet station for future period, (a) for A2, (b) for B1 and (c) for A1B emission scenarios.

4.2.3 **Impact of Future Climate change**

After calibrating the hydrological model with the historical data, the next step was assessing impact of climate change. Downscaled precipitation data of A2, B1 and A1B emission scenario was used for stream flow estimation in hydrologic model. The future estimation was carried out with the downscaled precipitation data by taking average of 20 ensembles produced by scenario generator.

Figure 4.15 shows the change in average monthly mean flows of Tikur Wuha River corresponding to the downscaled precipitation data of present (1961-2001) and future(2015 - 2035 , 2040 - 2050 and 2080-2099) climate. Annual mean stream flow for all time periods and scenarios considered showed that the flow will increase in future though the precipitation downscaled was not consistent. The River flow would increase by 20.5% in period 2080s for SRES A2 scenario which is highest emission scenario. Hydrologically Awassa Lake is closed lake. Small closed lakes are most vulnerable to a change in climate; there are indications that even relatively small changes in inputs can produce large fluctuations in water level and salinity in small closed lakes in western North America (Laird *et al.*, 1996).

It is thus very likely that changes in river inflow would also change the volume of the lake and the water balance, which could ultimately adversely impact the lake ecosystem of Lake Awassa as Tikur wuha is a main input to this Lake. The percentage of change in stream flow is shown in Table 4.6.

Table 4.6 Simulated Tikur Wuha stream flow change in future

Scenarios	% change in 2020's	% change in 2050's	% change in 2080's
SRES A2	32.65	27.76	20.5
SRES B1	30.06	51.67	35.88
SRES A1B	30.0	29.81	47.2

Study done on Hydrological Response of a Catchment to Climate Change in the Upper Beles River Basin, Upper Blue Nile, showed a decrease in the mean annual flow by 5.7 % during the period between the present and the future (2050). (Girma Y.et.al.2009). Though both studies used the same hydrologic model (HEC - HMS) the high difference in annual flow percentage may be because of the runoff model used in the studies. The study on the Upper Beles River uses continuous soil moisture accounting model where as SCS CN method was used in this study.

In addition, GCM model output used in both studies are different as some GCM model estimates better for some regions and poor estimation for some regions.

Another study on north highlands of Ethiopia Using downscaled data from the CCMA, MPI and GFDL models, showed a reduction on the stream flow under all SRES scenarios for time periods (2046–2065 and 2080–2100). But with the NCAR models there was an increase in stream flow forA2 and B1 scenarios during the two time periods. It also showed that Wet season stream flow is significantly reduced in the downscaled cccma_cgcm3_1 model for all scenarios for both time periods. For the downscaled gfdl_cm2_1 model there are reductions of around 20% for the 2046–2065 period, and around 50% for the 2080–2100 period, with little variation between scenarios. Results from the downscaled mpi_echams5 model show little change. (Shimelis G.et.al.2011).

Precipitation would increase by 7.73%, 7.62% and 6.75% and stream flow will increase by 32.65 %, 27.76% and 20.5% in periods 2020s, 2050s and 2080s respectively for SRES A2.

The variation of rainfall and stream flow increment is may be because of the interannual variability of precipitation. For SRES B1 precipitation would increase by 8.75%, 6.23%, 20.13% while stream flow will increase by 30.06%,51.67% and 35.88% for periods 2020s,2050s and 2080s respectively.

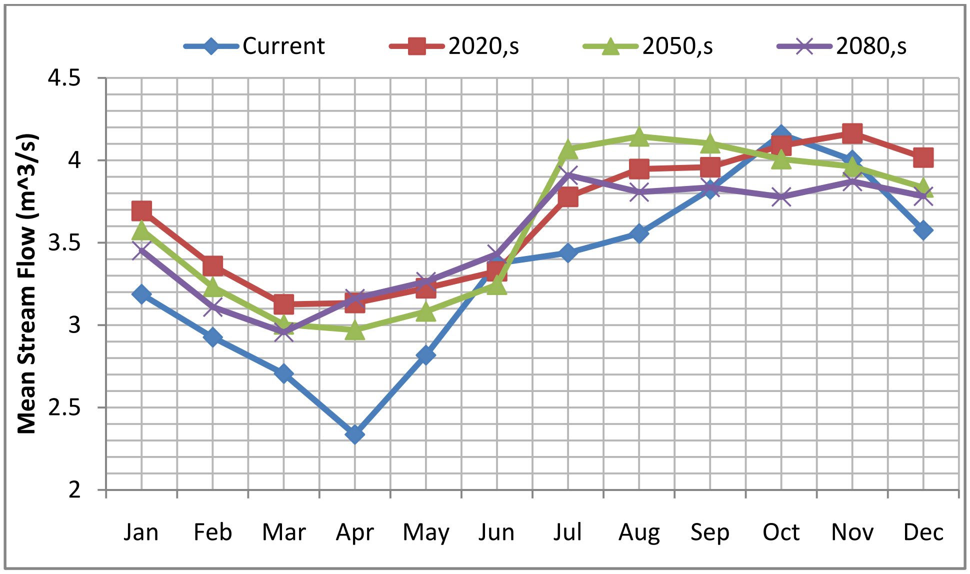

(a)

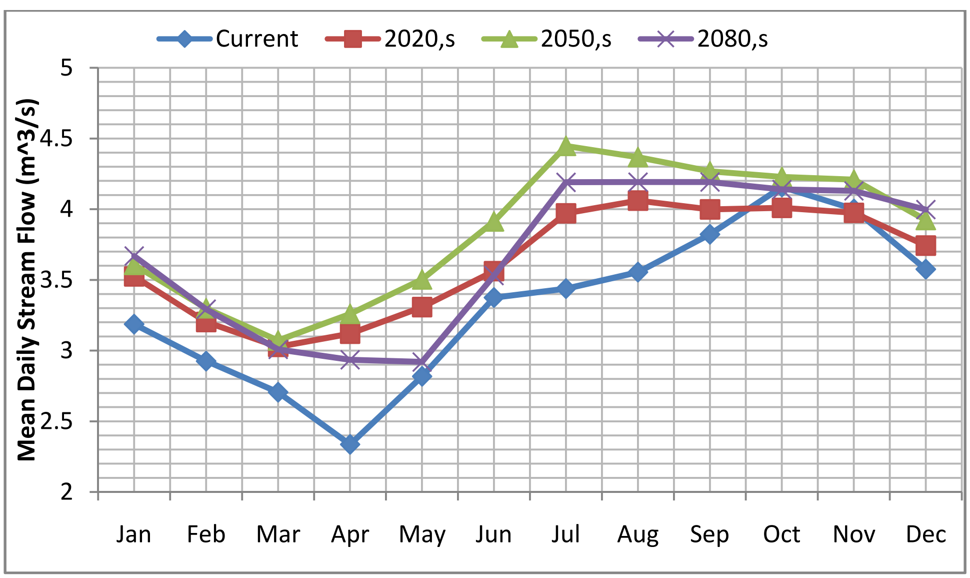

(b)

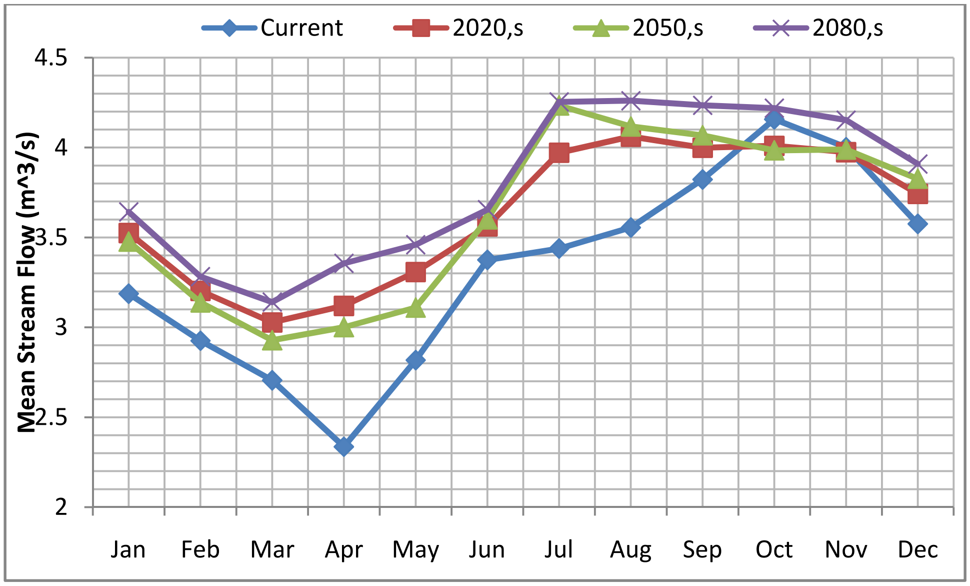

(c)

Figure 4.15: Comparison of simulated change in the average monthly mean flows in Tikur Wuha River corresponding to the downscaled precipitation of the present (1961-2000) and future (a) for A2,(b) for B1 and (c) for A1B emission scenarios.

4.3 Model Uncertainties

During Landsat image classification, pattern recognition skills and prior knowledge of the data are useful. To select reliable samples, the user should apply information (either spatial or spectral) about the pixels that they want to classify. The location of a specific characteristic, such as a land cover type, may be known through field observations that acquire knowledge about the study area from first-hand observation, analysis of aerial photography, personal experience, etc. Field data are considered to be the most accurate (correct) data available about the area of study. They should be collected at the same time as the remotely sensed data, so that the data correspond as much as possible. However, all field data may not be completely accurate because of observation errors, instrument inaccuracies, and human shortcomings. Quality of LandSat images are also the source of uncertainties. Among classifiers available the classifier used in this study was Maximum Likelihood. The limitation with Maximum Likelihood is its assumption of normal distribution of class signatures.

Climate and land use change impact assessment on Tikur Wuha River consider climate model analyses and out puts, which depends on simplified assumptions. Hence, it is unquestionable that the uncertainties presented in the model and model outputs kept on cumulating while progressing towards the final output. These Uncertainties include: Uncertainty Linked to Data quality, General circulation Model (GCMs), Emission scenarios, Downscaling Method, and Hydrological model. The uncertainty related to data used for Downscaling model and Hydrological model consists of problem with data quality and Missing data.

GCM outputs have also many uncertainties. There are considerable uncertainties in the radiative forcing changes, especially aerosol forcing, associated with changes in atmospheric concentrations (Mearns et al., 2001). The IPCC report on emission scenarios, SRES, (IPCC, 2001) clustered these scenarios into six groups. Despite their equal probability, model results based on these scenarios may vary noticeably. Hence, choosing among the scenarios adds to the uncertainty. The coarser resolutions make GCMs not to be used directly for impact studies.

Though “downscaling” is a solution towards narrowing the temporal and spatial resolution disparity, the techniques involved are still another source of uncertainty. The SDSM statistical downscaling technique used in this study needed the screening of weather parameters (predictors).

Finding good predictors-Predictand correlation was a core part of the downscaling process. However, even after several trial and errors, the correlation coefficients found were very small especially for the precipitation and minimum temperature Predictand variables. The knowledge gap related to the atmospheric physics of the local climatic process may be one of the obstacles in choosing the best predictor combinations. Beyond that, SDSM downscaling is based on the assumption that the predictor -Predictand relationships under the current condition remain valid for future climate conditions too, which might not be the case and hence another source of uncertainty.

Predictive hydrologic modeling is normally carried out on a given catchment using a specific model under the supervision of individual hydrologist. The usefulness of the results depends in large measure on the talents and experience of the hydrologist. (League and Freeze 1985).

Implementing distributed rainfall- runoff models is critical to get more reliable model analysis in watershed. SCS CN model was developed with data with small agricultural watersheds in mid western US, so applicability with elsewhere is uncertain.

Exponential recession model used in the study to estimate baseflow needs recession constant K, which depends on the source of baseflow. This needs deep study on ground water of the study area or can be estimated if gauged flow data are available. In this study it was estimated from the gauged data. Another, baseflow parameter "threshold value" is also estimated from a graph of observed flow versus time. Therefore, uncertainty of stream flow data highly affects the estimation of this parameter and baseflow estimation.

Understanding the hydrology of wetlands is very important and this involves understanding the characteristics of wetlands; this can aid in the model selection process. Impact of Cheleleka wetland on flood control is not considered in this study.

Tikur Wuha river is used for irrigation and bore holes for water supply purpose is found in the study area. But, the abstraction of water from the river and ground water is not taken in account during the assessment which will also affect the result of the analysis.

5 Conclusion and Recommendations

5.1 Conclusion

The study have presented an analysis of land-cover change and climate change in Tikur Wuha Watershed in Awassa, Ethiopia using post-classification comparison analysis of Maximum Likelihood-classified Landsat images for land cover change detection. The study expanded the analysis by incorporating the detected changes in land-cover to a GIS-based hydrologic model. This allowed the researcher to better understand the impacts of the land-cover change to the increase in surface runoff during rainfall events in the Tikur wuha Watershed. Land cover analysis was done using Landsat image obtained in time periods of 1976.1986,2000 and 2005.

The analysis showed a 28.77% reduction in forest cover, a 3.6% reduction in lake cover, a 23.49% increase in agricultural land areas, 3.6% increase in marshy land and 5.3% increase in grassland in the study area in the span of 32 years from 1976 to 2005.

The hydrologic model simulations indicate that with the land-cover changes that have occurred, there is a change in stream. The study reveals that watersheds run off is lower by 5.79 % in time period 1973, 0.27% in 1986 compared to time period of 2005 as reference. This shows that the runoff increases from period 1973 to 2005.This also agrees with the land cover change of the area.

In addition to land cover change, the study has also assessed the impact of climate change on watershed runoff. Statistical downscaling model was applied to downscale GCM data and application of the downscaled data in hydrological models was demonstrated to assess the future impact of climate change. The downscaling, in this study, was performed by using one GCM model output (CGCM3) only. Previous studies showed that data taken from different GCMs could differ significantly. Therefore, the methods described in this paper could be used to provide an indication to the likely impact of climate change in the Tikur wuha River. Consequently, care should be taken in interpreting the results for further impacts assessments.

This study reaches to the following conclusion from climate change analysis.

- Rainfall of the study area decreased currently (1991 - 2010) compared to past time period (1961 -1990)

- SDSM model simulated maximum and minimum temperature more accurately than precipitation. This is because the maximum and minimum temperatures are highly affected by large-scale variables. Accordingly, the major large scale predictors highly affect local maximum temperature.
- Maximum and minimum temperature change for period 2080 s was about 3.16 ^{o}C and 0.28 ^{o}C for SRES A2 ,1.46 ^{o}C and 0.34 ^{o}C for SRES A1B ,2.03 ^{o}C and 0.342 ^{o}C for SRES B1 respectively.
- Average increase in maximum and minimum temperature for 2050 s was 1.37 ^{o}C and 0.43 ^{o}C for SRES A2, 1.43 ^{o}C and 0.35 ^{o}C for SRES A1B and 1.39 ^{o}C and 0.33 ^{o}C for SRES B1 respectively.
- The result of projected rainfall indicated that there is a probability of decreasing in precipitation during the main rainy season (JJA).
- The downscaled precipitation data used with HEC - HMS model indicates that the runoff in the Tikur Wuha River will increase in the future.
- Average mean flow is increased in the future (2015 - 2035, 2040 - 2050 and 2080-2099). SDSM downscaling data resulted in a increase in the mean annual flow by 32.65 %,27.76 % and 20.5 % for A2 emission scenario, by 30.06 % ,51.67% and 35.88 % for B1 emission scenario and by 30 % ,29.81 % and 47.2 % for A1B emission scenario during the time period 2020 s (2015 - 2035),2050 (2040 -2050) and 2080 (2080 - 2100) respectively.
- precipitation would increase by 7.73% , 7.62% and 6.75% and stream flow will increase by 32.65%,27.76% and 20.5% in periods 2020s,2050s and 2080s respectively for SRES A2. For SRES B1 precipitation would increase by 8.75%, 6.23%,20.13% while stream flow will increase by 30.06%,51.67% and 35.88% for periods 2020s,2050s and 2080s respectively.
- The result of hydrological model calibration and validation indicated that the HEC - HMS model is capable to simulate the stream flow volume appreciably than peak discharge for the study area.

5.2 Recommendation

Depending on the analysis undertaken in this study, the following is recommended.

1. Land use change detection in the area indicates that the Cheleleka Lake was converted to wet land. Some wetlands are the source of ground water recharge while others act as detention areas and other wetlands are able to store surface water over the long term, thus allowing for the maintenance of fish habitat during periods of dry weather. Another important hydrologic function of some wetlands is their ability to maintain the water table at a high level. This allows hydrophytic communities to be maintained, thus sustaining bio-diversity in the area. The reduction of downstream flood peaks due to a wetland's short-term surface water storage capability has also been accredited as one of their benefits. Therefore, to conserve fish habitat and biodiversity in this catchment measure should be taken. To keep Surface water storage capability of the lake effective land use management should be applied in the catchment.
2. This study showed that land cover change affects the stream flow of Tikur Wuha River. Volume of runoff in the sub catchment increases over past 32 years. Tikur Wuha River is the only perennial river, which feeds Awassa Lake. Lake level of Awassa Lake may increase due to increase in runoff and likely sedimentation of Lake Awassa because of Land cover change. This will also damage areas near the lake by flooding. Therefore, effective land use management is needed to alleviate this problem.
3. Climate change impact analysis also showed increase in Tikur Wuha river flow. This will also damage areas near the lake by flooding. Therefore, measures should have to be taken to avoid threat of climate change impact on this catchment and Lake Awassa water quantity.

5.2.1 Suggestion For Further Study

1. Recent topographic map of the area and field collected land cover data is not available to detect land use change more accurately. Therefore, a research which uses recent topographic map and field collected data have to be done to understand land cover change in detail.

2. Implementing Continuous Simulation of rainfall- runoff models is critical to get more reliable model analysis in watershed. The runoff method used in this study was SCS, which is not continuous rainfall- runoff method.
3. The abstraction of water from the river is not taken in account during the assessment, which will also affect the result of the analysis. Therefore, further study that considers evapotranispiration,and water abstraction should be done.
4. Output of this study is based on a single GCM output. To get indication of consistency in projected changes using different (more than one) GCM model gives us a good comparison. i.e. using different GCM models the comparison of the outputs whether they increase or decrease together.(in the same direction)

6 References

Casey Brown, Arthur Greene, Paul Block, Alessandra Giannini. Review of downscaling methodologies for Africa climate applications. IRI Technical Report 08-05: IRI Downscaling Report. (2008).

Cebecauer, T.; Hofierka, J. The consequences of land-cover changes on soil erosion distribution in Slovakia. Geomorphology, 98, 187-198. 2008

Cherill, A.J.; Lane, A.; Fuller, R.M. The use of classified Landsat 5 Thematic Mapper imagery in the characterization of landscape composition: A case study in Northern England. J. Environ. Manage., 40, 357-377. 1994

Cingolani, A.M.; Renison, D.; Zak, M.R.; Cabido, M.R. Mapping vegetation in a heterogeneous mountain rangeland using Landsat data: An alternative method to define and classify land-cover units. Remote Sens. Environ., 92, 84-97. 2004

CHONG-YU XU (1999). Climate Change and Hydrologic Models: A Review of Existing Gaps and Recent Research Developments. Water Resources Management13: 369–382, 1999.

Chow,V.T.,Maidment,D.R., and Mays,L.WApplied Hydrology .McGraw-Hill,New York,NY.1988.

Daniel Shewangizaw1 and Yonas Michael2, Nile Basin Water Science& Engineering Journal, Vol.3, Issue2, 2010

Dokken DJ, McFarland M (Eds.) Prepared in collaboration with the Scientific Assessment Panel to the Montreal Protocol on Substances that Deplete the Ozone Layer. Cambridge University Press, Cambridge, UK. p 373

General guidelines on the use of scenario data for climate impact and adaptation assessment Version 2 Task Group on Data and Scenario Support for Impact and Climate Assessment (TGICA) Intergovernmental Panel on Climate Change. June 2007

Girma Yimer , Andreja Jonoski and Ann Van Griensven. Hydrological Response of a Catchment to ClimateChange in the Upper Beles River Basin, Upper Blue Nile, Ethiopia Nile Basin Water Engineering Scientific Magazine, Vol.2, 2009.

Gleick PH, Chalecki EL the impacts of climatic changes for water resources of the Colorado and Sacramento-San Joaquin River basins. J Am Water Resour Assoc 35: 1429–1441. 1999

Hagner, O.; Reese, H. A method for calibrated maximum likelihood classification of forest types. Remote Sens. Environ., 110, 438-444. 2007

Houghton, J. T., Jenkins, G. J. and Ephraums, J. J. (eds):,Climate Change. The IPCC Assessment, Cambridge University Press. 1990

http://www.cics.uvic.ca/scenarios/sdsm/select.cgi SDSM predictor data files are downloaded from the Canadian Institute for Climate Studies (CICS) website accessed October ,20,2014

IPCC (Intergovernmental Panel on Climate Change) In: Penner JE, Lister DH, Griggs DJ. 1999

IPCC (Intergovernmental Panel on Climate Change) (2007) In: Parry ML et al (eds) Climate change: impacts, adaptation, and vulnerability—contribution of working group II to the third assessment report of the Intergovernmental Panel on Climate Change. Cambridge University Press, Cambridge, UK. 2007

Linsley,R.K.,Kohler,M.A.,and Paulhus,J.L.H..Hydrology For Engineers. McGraw-Hill,New York,NY. 1982

McColl, C.; Aggett, G. Land-use forecasting and hydrologic model integration for improved land-use decision support. J. Environ. Manage, 84, 494-512 . 2007

O'Connell, P.E.; Ewen, J.; O'Donnell, G.; Quinn, P. Is there a link between agricultural land-use management and flooding? Hydrol. Earth Syst. Sci., 11, 96-107. 2007

Ponce, V.M,and Hawkins,R.H.,"Runoff curve number:Has it reached maturity?"Journal of Hydrologic engineering,ASCE,1(1)11-19. 1966

Randall, D.A., R.A. Wood, S. Bony, R. Colman, T. Fichefet, J. Fyfe, V. Kattsov, A. Pitman, J. Shukla, J. Srinivasan, R.J. Stouffer, A. Sumi and K.E. Taylor,: Cilmate Models and Their Evaluation. In: Climate Change : The Physical Science Basis. Contribution of Working Group I to the Fourth Assessment Report of the Intergovernmental Panel on Climate Change[Solomon, S., D. Qin, M. Manning, Z. Chen, M. Marquis, K.B. Averyt, M.Tignor and H.L. Miller (eds.)]. Cambridge University Press, Cambridge, United Kingdom and New York, NY, USA.2007

Robert L. Wilbymand Christian W. Dawson, SDSM 4.2 a decision support tool for the assessment of regional climate change impacts. August 2007.

Shimelis G. Setegn, David Rayner, Assefa M. Melesse, Bijan Dargahi,Ragahavan Srinivasan, and Anders Wörman. Climate Change Impact on Agricultural Water Resources Variability in the Northern Highlands of Ethiopia.2011

Swain, P.H.; Davis, S.M. Remote Sensing: The Quantitative Approach; McGraw-Hill: New York, NY, USA, 1978.

Tammy E. Parece James B. Campbell Remote Sensing Analysis in an ArcMap Environment, ,2013

Tenalem..The Hydrological System of the lake district basin, central Main Ethiopian Riftvalley PH.D thesis.International institute for geographic Information Science and Earth Observation(ITC) Enschede.1998

The impact of wetlands on flood control in the red river valley of manitoba. Final Report to International Joint Commission September 1999

U. S. Army Corps of Engineers (USACE). Geospatial modeling extension. HEC-GeoHMS, User's Manual. Davis, CA: U.S. Army Corps of Engineers, Hydrologic Engineering Center. 2000

U. S. Army Corps of Engineers (USACE).. Hydrologic Modeling System: Technical Reference Manual. Davis, CA: U.S. Army Corps of Engineers, Hydrologic Engineering Center. 2000

Vafeidis, A.T.; Drake, N.A.; Wainwright, J. A proposed method for modelling the hydrologic response of catchments to burning with the use of remote sensing and GIS. Catena , 70, 396-409.2007

Wilby, R. L. and Wigley, T. M. L.:, Downscaling general circulation model output: a review of methods and limitations,Progress in Physical Geography21, 530–548. 1997

Wilby, R. L., and Dawson, C. W. SDSM 4.2 — A decision supporttool for the assessment of regional climate change impacts,User Manual . 2007

Wilby, R. L., and Wigley, T. M. L. Precipiation Predictors for Downscaling: Observed and General Circulation Model Relationships. International Journal of Climatology. 1999

WWDSE, , The study of Lake Awassa level rise, Southern Nations Nationalities and peoples Regional State, Water, Mines and Energy Resources Development Bureau. Unpublished report of the Water Works Design and Supervision Enterprise (main report volume II), Addis Ababa, Ethiopia. 2001

Appendix A

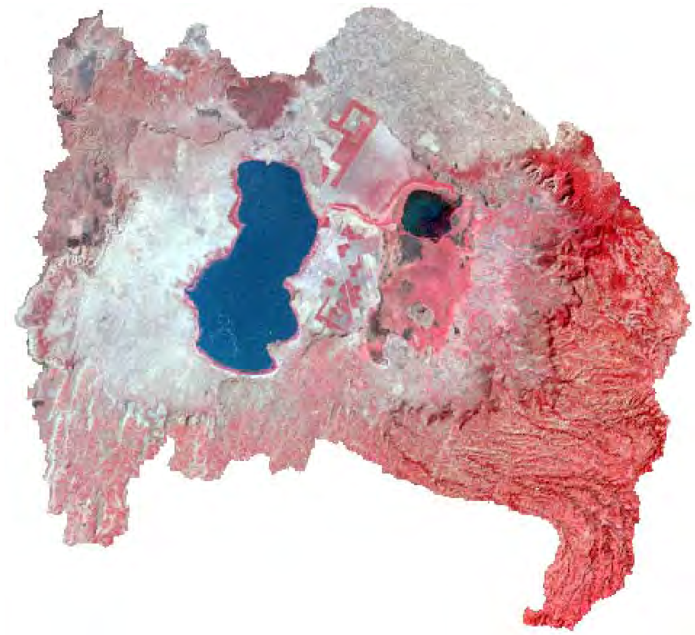

Figure A.1 Color Combination of band 4,2,1 of year1973 image of Awassa Catchment

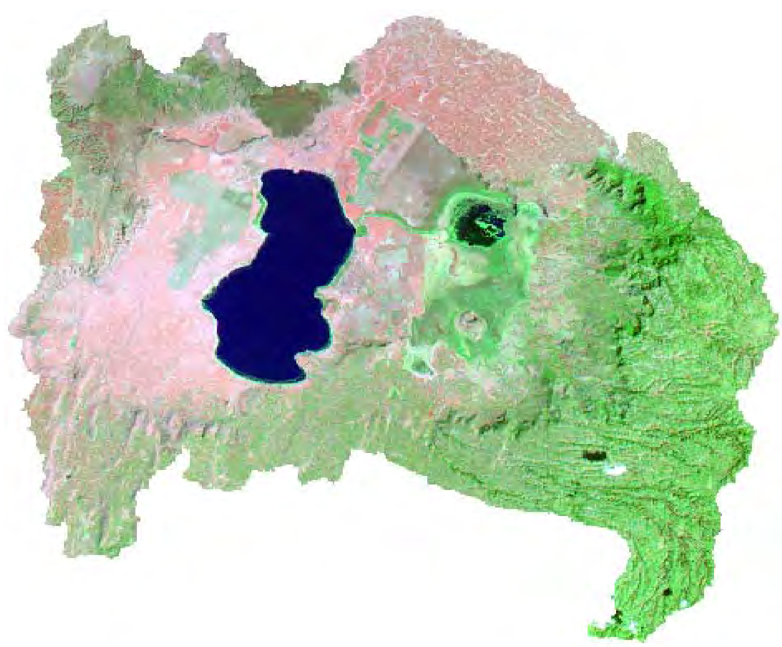

Figure A.2 .Color Combination of band 7,4,2, of year 1986 image of Awassa Catchment

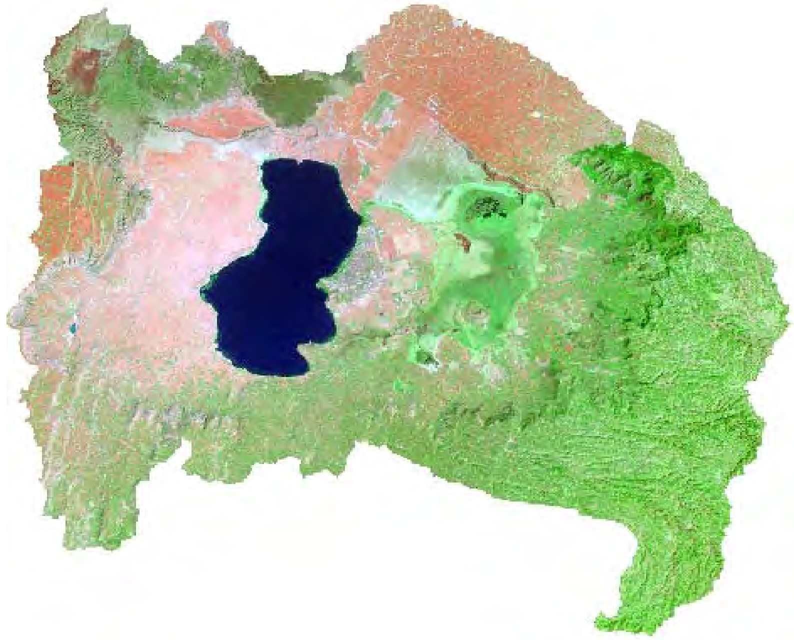

Figure A.3 .Color Combination of band 7,4,2, of year 2000 image of Awassa Catchment

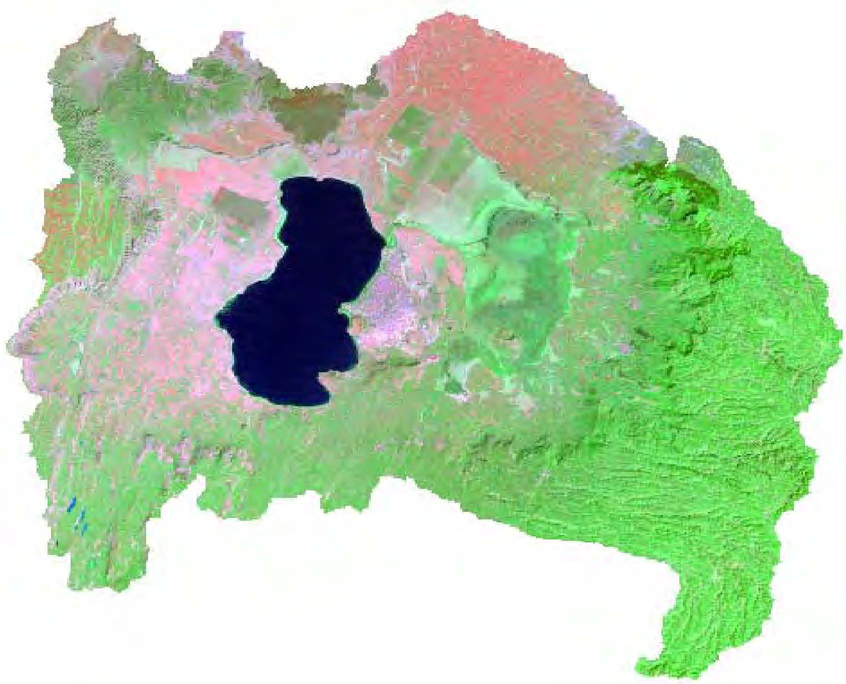

Figure A.4 Color Combination of band 7,4,2, of year 2005 image of Awassa Catchment

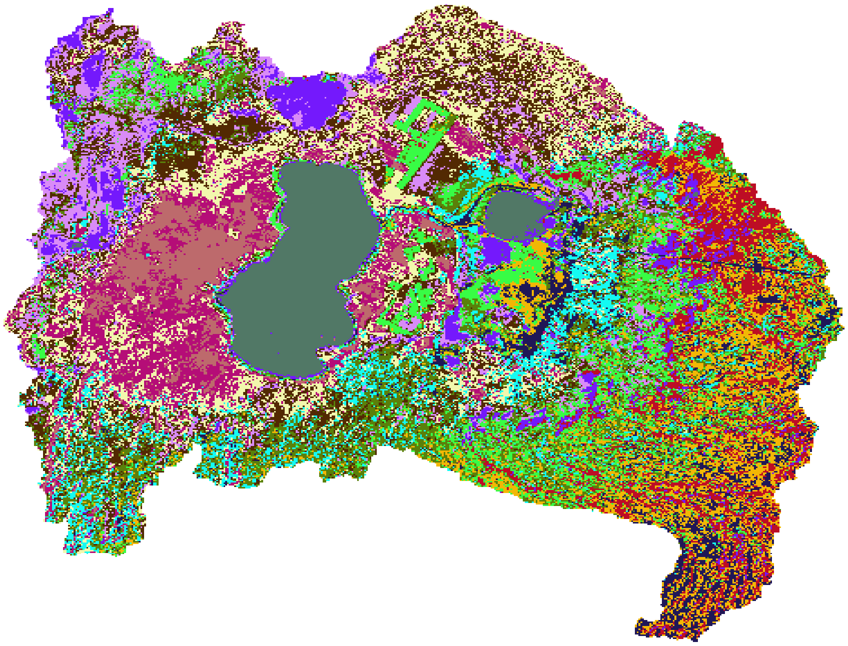

Figure A.5 Unsupervised classification of year 1973 Images

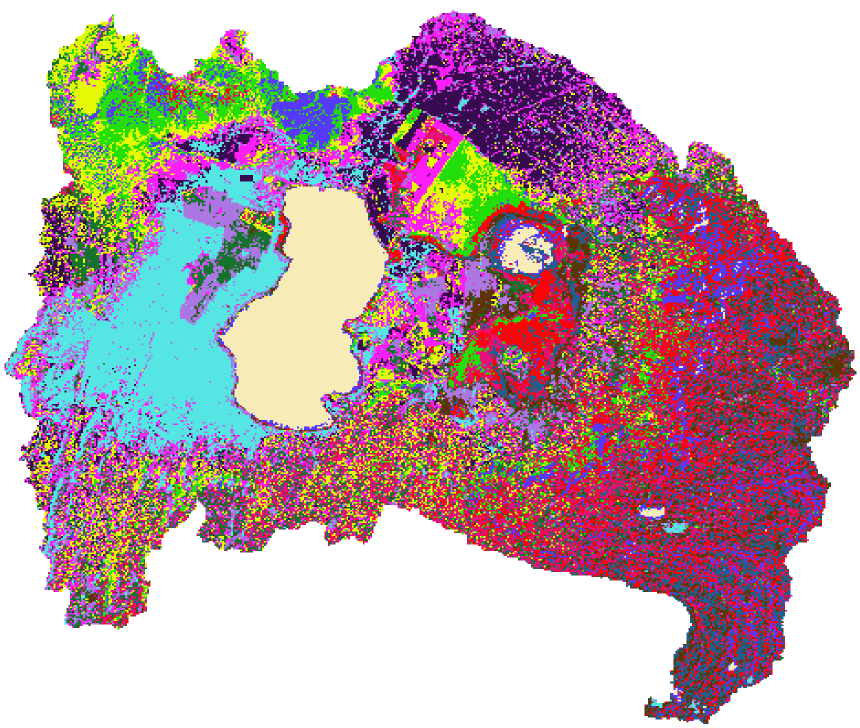

Figure A.6 Unsupervised classification of year 1986 Images

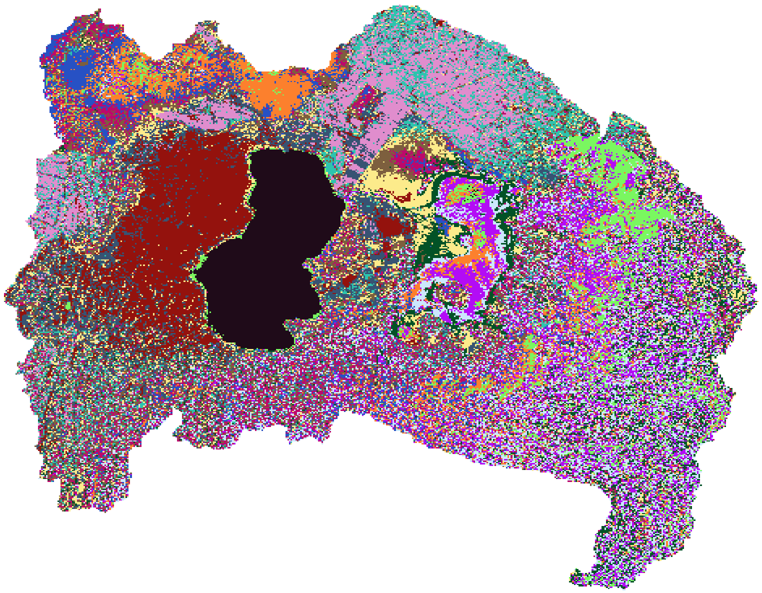

Figure A.7 Unsupervised classification of year 2000 Images

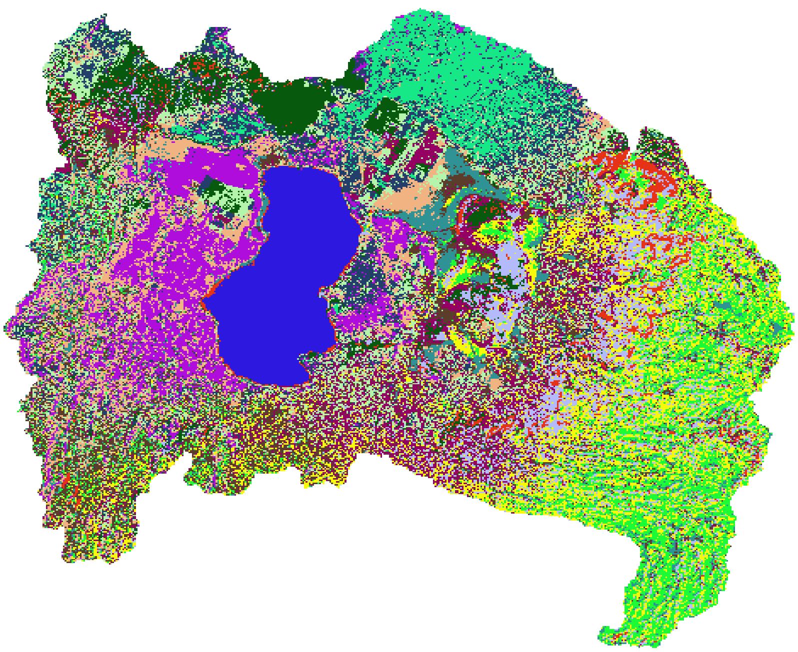

Figure A.8. Unsupervised classification of year 2005 Images

Table A.1 Year 1973 Training sample Covariance partly.

Statistics

Lakes

Statistics	Band_1	Band_2	Band_3	Band_4
Minimum	3.00	0.00	14.00	22.00
Maximum	14.00	111.00	30.00	39.00
Mean	5.52	8.11	16.58	25.75
Std.dev	0.88	6.76	1.11	1.15
Covariance				
Band_1	0.77	-0.04	0.24	0.20
Band_2	-0.04	45.64	0.01	0.66
Band_3	0.24	0.01	1.23	0.74
Band_4	0.20	0.66	0.74	1.33

Forest_8

Statistics	Band_1	Band_2	Band_3	Band_4
Minimum	10.00	1.00	8.00	14.00
Maximum	46.00	40.00	15.00	22.00
Mean	29.86	25.93	11.47	18.36
Std.dev	10.71	9.62	1.84	1.68
Covariance				
Band_1	114.74	95.42	17.86	16.20
Band_2	95.42	92.61	15.50	14.03
Band_3	17.86	15.50	3.40	2.69
Band_4	16.20	14.03	2.69	2.82

Grass L...

Statistics	Band_1	Band_2	Band_3	Band_4
Minimum	30.00	7.00	17.00	23.00
Maximum	47.00	83.00	41.00	39.00
Mean	36.58	37.99	26.33	29.17
Std.dev	2.90	7.25	4.72	2.92
Covariance				
Band_1	8.39	8.93	7.80	5.21
Band_2	8.93	52.52	11.65	7.56
Band_3	7.80	11.65	22.25	12.93
Band_4	5.21	7.56	12.93	8.50

Table A.2 Year 1986 Training sample Covariance partly.

Statistics

Lake 3

Statistics	Band_1	Band_2	Band_3	Band_4	Band_5	Band_6	Band_7
Minimum	132.00	150.00	41.00	65.00	54.00	57.00	54.00
Maximum	139.00	164.00	82.00	78.00	73.00	114.00	130.00
Mean	136.16	158.63	65.86	72.47	65.92	85.36	105.54
Std.dev	1.57	2.72	5.36	2.24	2.77	6.17	13.16
Covariance							
Band_1	2.47	4.02	1.32	1.02	1.78	-0.02	8.68
Band_2	4.02	7.37	2.01	1.85	3.25	-0.29	17.38
Band_3	1.32	2.01	28.70	2.33	6.03	20.78	23.53
Band_4	1.02	1.85	2.33	5.03	3.26	-0.60	16.99
Band_5	1.78	3.25	6.03	3.26	7.69	3.08	28.77
Band_6	-0.02	-0.29	20.78	-0.60	3.08	38.12	-3.66
Band_7	8.68	17.38	23.53	16.99	28.77	-3.66	173.24
Band_8	5.79	11.30	12.36	11.08	17.64	-5.88	104.37

Agricultur...

Statistics	Band_1	Band_2	Band_3	Band_4	Band_5	Band_6	Band_7
Minimum	151.00	184.00	44.00	73.00	60.00	52.00	88.00
Maximum	171.00	221.00	99.00	117.00	115.00	91.00	191.00
Mean	164.95	210.51	63.86	86.94	78.47	66.79	159.57
Std.dev	3.32	6.04	8.81	7.47	10.17	7.28	16.57
Covariance							
Band_1	10.99	19.76	-1.96	2.48	2.84	-4.08	39.18
Band_2	19.76	36.52	-3.10	4.40	4.93	-7.75	72.04
Band_3	-1.96	-3.10	77.65	52.62	74.20	53.22	41.46
Band_4	2.48	4.40	52.62	55.84	73.28	47.65	52.38
Band_5	2.84	4.93	74.20	73.28	103.34	67.95	71.63
Band_6	-4.08	-7.75	53.22	47.65	67.95	53.06	23.04
Band_7	39.18	72.04	41.46	52.38	71.63	23.04	274.56
Band_8	42.92	79.05	1.98	21.70	25.94	-15.83	256.22

Grass La...

Statistics	Band_1	Band_2	Band_3	Band_4	Band_5	Band_6	Band_7
Minimum	128.00	144.00	29.00	62.00	54.00	47.00	67.00

Table A.3 year 2000 Training sample Covariance partly.

Statistics

Lake 2

Statistics	Band_1	Band_2	Band_3	Band_4	Band_5	Band_6	Band_7
Minimum	127.00	142.00	25.00	62.00	43.00	24.00	19.00
Maximum	139.00	162.00	81.00	77.00	68.00	105.00	123.00
Mean	131.67	150.47	51.59	71.22	58.53	60.96	77.38
Std.dev	2.40	4.18	10.27	3.20	4.86	16.09	21.74
Covariance							
Band_1	5.77	9.80	15.19	3.15	7.04	26.05	32.29
Band_2	9.80	17.50	25.92	5.46	12.18	43.59	56.34
Band_3	15.19	25.92	105.57	15.54	38.83	141.65	166.29
Band_4	3.15	5.46	15.54	10.22	11.67	25.28	53.21
Band_5	7.04	12.18	38.83	11.67	23.58	63.73	97.93
Band_6	26.05	43.59	141.65	25.28	63.73	258.97	270.29
Band_7	32.29	56.34	166.29	53.21	97.93	270.29	472.53
Band_8	15.43	27.38	81.64	31.45	53.20	126.65	261.56

Forest 1

Statistics	Band_1	Band_2	Band_3	Band_4	Band_5	Band_6	Band_7
Minimum	121.00	131.00	28.00	55.00	40.00	29.00	33.00
Maximum	155.00	191.00	90.00	90.00	90.00	112.00	161.00
Mean	133.20	153.29	53.83	63.64	53.00	70.04	82.11
Std.dev	8.17	14.63	10.75	5.35	8.01	14.48	31.02
Covariance							
Band_1	66.83	119.36	58.16	31.04	50.49	73.56	205.03
Band_2	119.36	214.13	104.46	55.50	90.20	131.92	366.72
Band_3	58.16	104.46	115.54	38.97	67.04	133.42	256.14
Band_4	31.04	55.50	38.97	28.58	39.15	45.32	144.38
Band_5	50.49	90.20	67.04	39.15	64.20	85.32	226.22
Band_6	73.56	131.92	133.42	45.32	85.32	209.63	323.60
Band_7	205.03	366.72	256.14	144.38	226.22	323.60	962.01
Band_8	128.69	230.23	150.78	93.32	142.41	180.16	600.18

Agricultur...

Statistics	Band_1	Band_2	Band_3	Band_4	Band_5	Band_6	Band_7
Minimum	151.00	184.00	44.00	73.00	60.00	52.00	88.00

Table A.4 year 2005 Training sample Covariance partly.

Statistics

Forest 1

Statistics	Band_1	Band_2	Band_3	Band_4	Band_5	Band_6	Band_7
Minimum	121.00	131.00	28.00	55.00	40.00	29.00	33.00
Maximum	155.00	191.00	90.00	90.00	90.00	112.00	161.00
Mean	133.20	153.29	53.83	63.64	53.00	70.04	82.11
Std.dev	8.17	14.63	10.75	5.35	8.01	14.48	31.02
Covariance							
Band_1	66.83	119.36	58.16	31.04	50.49	73.56	205.03
Band_2	119.36	214.13	104.46	55.50	90.20	131.92	366.72
Band_3	58.16	104.46	115.54	38.97	67.04	133.42	256.14
Band_4	31.04	55.50	38.97	28.58	39.15	45.32	144.38
Band_5	50.49	90.20	67.04	39.15	64.20	85.32	226.22
Band_6	73.56	131.92	133.42	45.32	85.32	209.63	323.60
Band_7	205.03	366.72	256.14	144.38	226.22	323.60	962.01
Band_8	128.69	230.23	150.78	93.32	142.41	180.16	600.18

grass Lan...

Statistics	Band_1	Band_2	Band_3	Band_4	Band_5	Band_6	Band_7
Minimum	141.00	168.00	28.00	65.00	48.00	29.00	54.00
Maximum	166.00	213.00	98.00	95.00	93.00	108.00	188.00
Mean	147.67	179.42	75.47	85.46	82.08	85.88	162.64
Std.dev	4.40	7.96	12.50	5.44	9.03	14.58	25.07
Covariance							
Band_1	19.39	34.76	-39.84	-17.25	-30.47	-51.48	-77.42
Band_2	34.76	63.43	-73.48	-31.48	-55.92	-94.33	-142.12
Band_3	-39.84	-73.48	156.18	58.18	103.48	169.79	275.69
Band_4	-17.25	-31.48	58.18	29.61	45.32	72.00	118.91
Band_5	-30.47	-55.92	103.48	45.32	81.54	127.39	208.68
Band_6	-51.48	-94.33	169.79	72.00	127.39	212.61	336.65
Band_7	-77.42	-142.12	275.69	118.91	208.68	336.65	628.26
Band_8	-29.71	-54.80	115.15	51.36	88.94	139.17	280.87

Agricultur...

Statistics	Band_1	Band_2	Band_3	Band_4	Band_5	Band_6	Band_7
Minimum	161.00	204.00	63.00	88.00	87.00	67.00	165.00

Appendix B

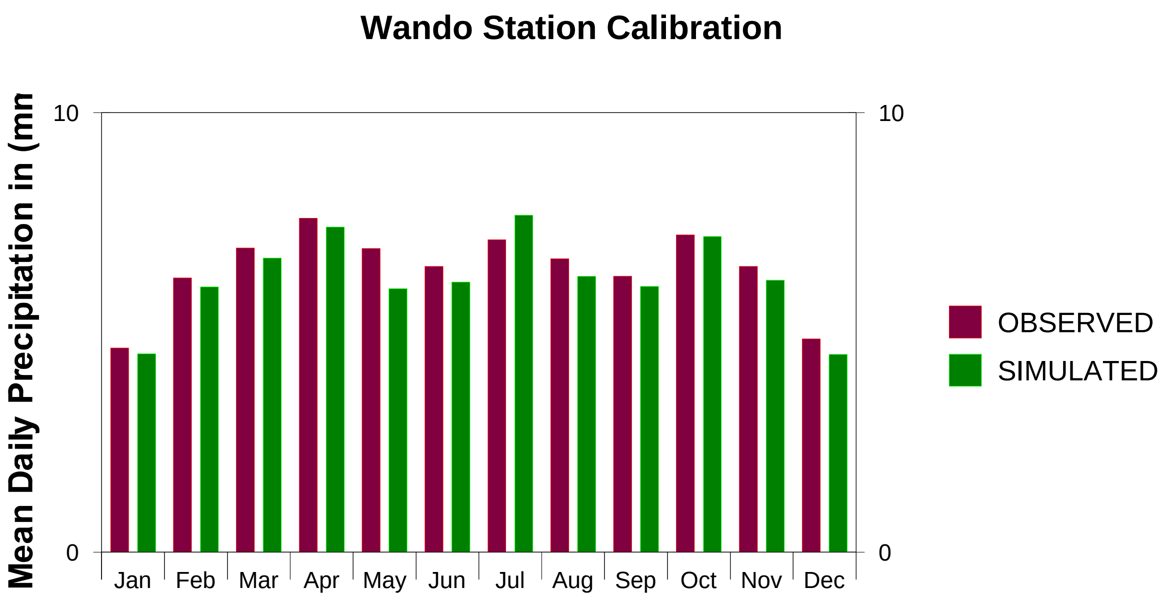

(a)

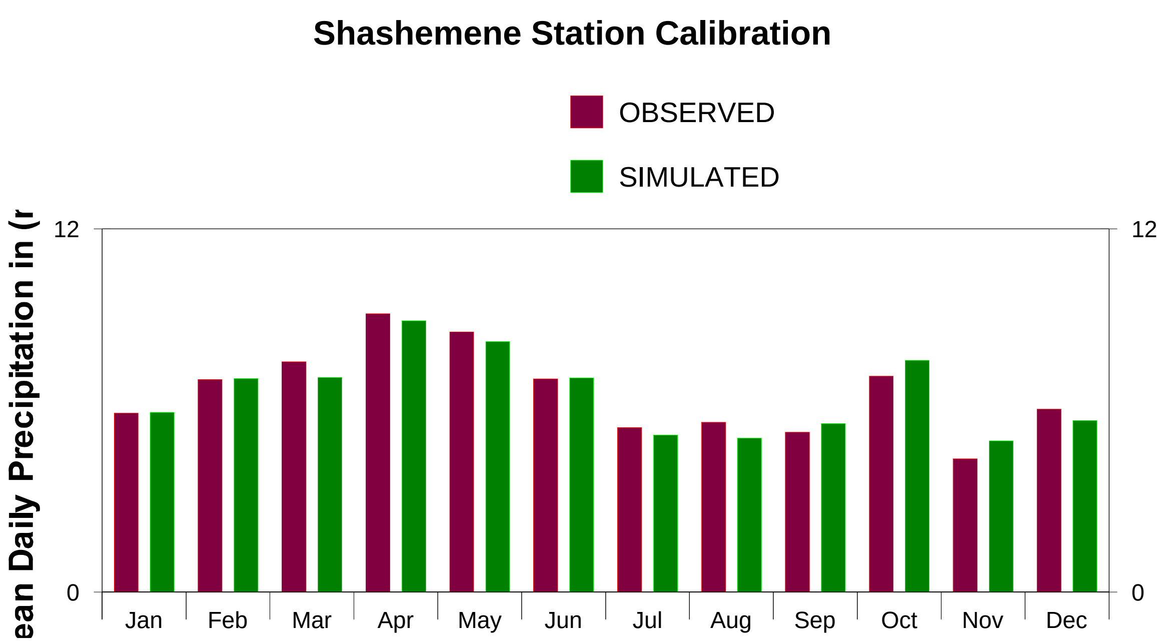

(b)

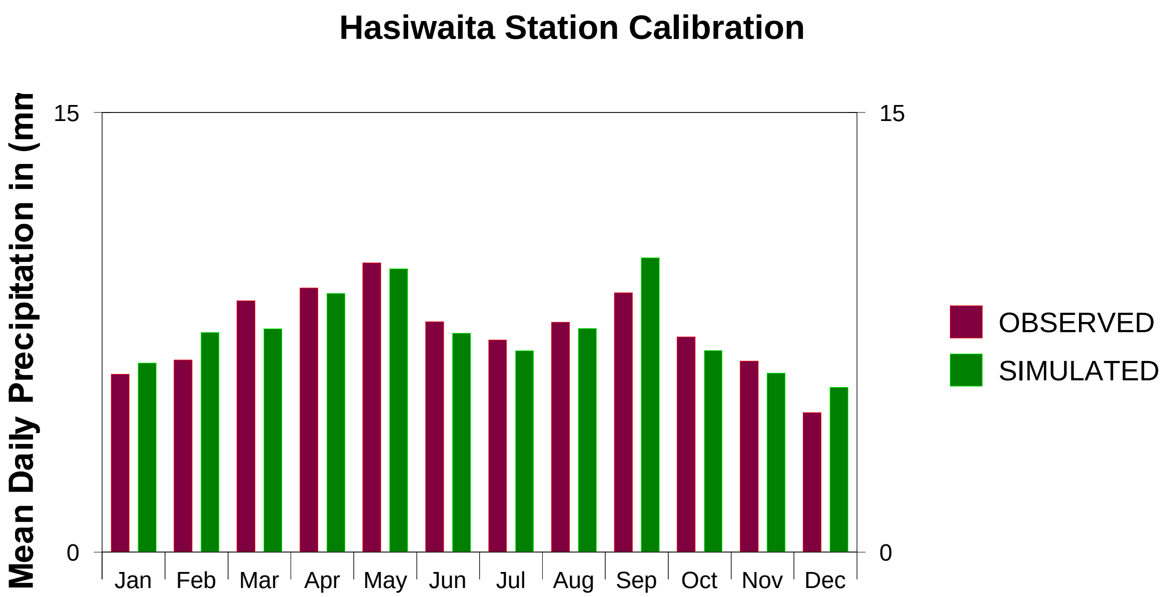

(c)

Figure B.1 Calibration Result of SDSM Model Downscaling of daily precipitation(1961- 1990) for Rainfall Stations (a) Wando Genet (b)Shashemene and (c) Haisawita

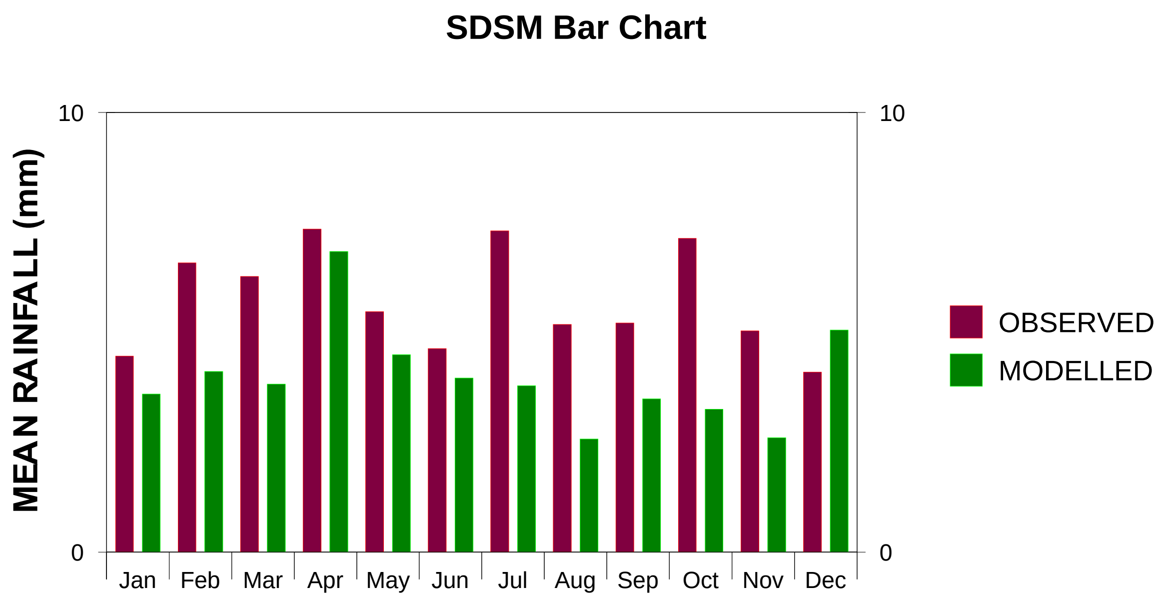

Figure B.2 Validation Result of SDSM Model Downscaling of daily precipitation(1990- 2000) at Shashemene station

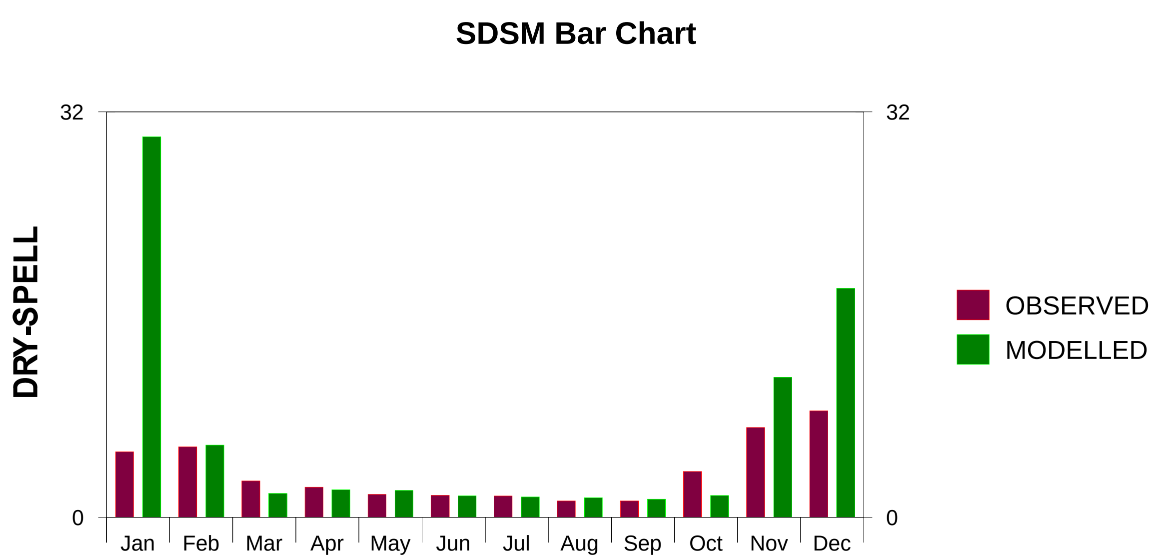

Figure B.3 Validation Result of SDSM Model Downscaling of daily precipitation(1990- 2000) at Shashemene station

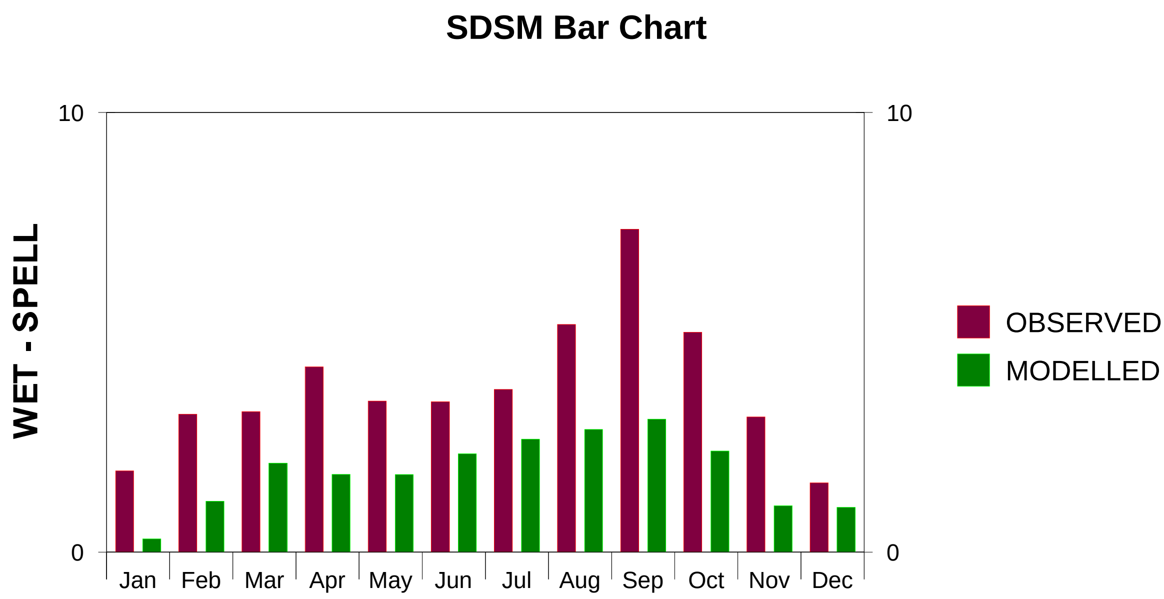

Figure B.4 Validation Result of SDSM Model Downscaling of daily precipitation(1990- 2000) at Shashemene station

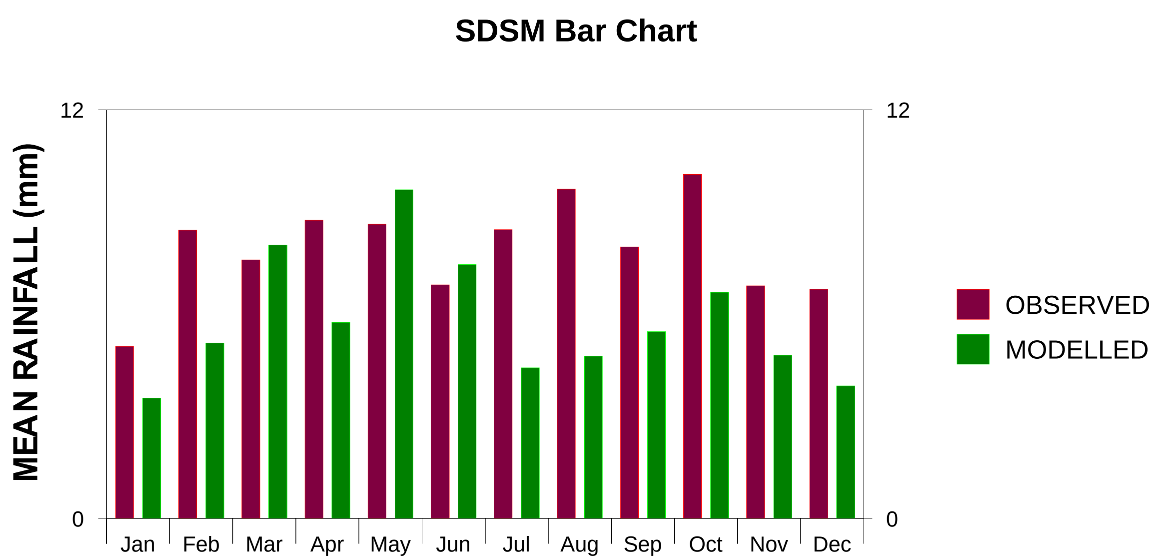

Figure B.5 Validation Result of SDSM Model Downscaling of daily precipitation(1990- 2000) at Haisawita station

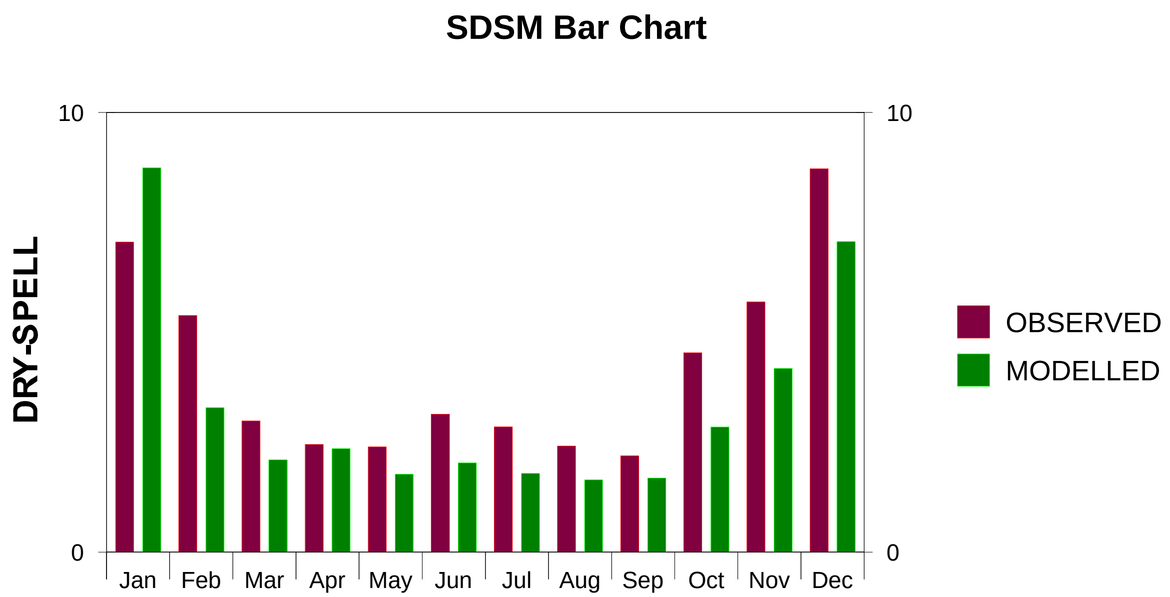

Figure B.6 Validation Result of SDSM Model Downscaling of daily precipitation(1990- 2000) at Haisawita station

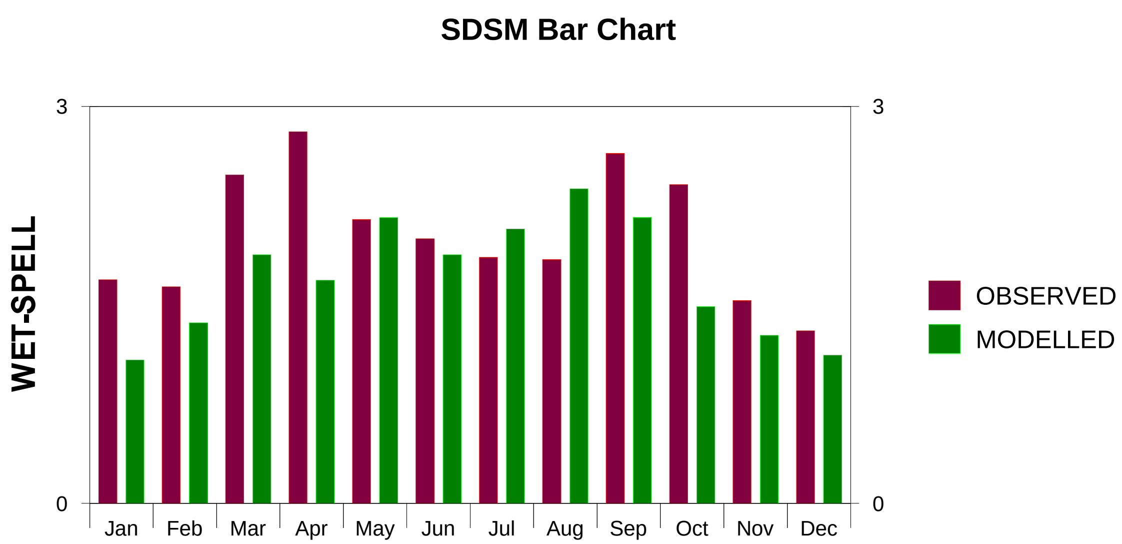

Figure B.7 Validation Result of SDSM Model Downscaling of daily precipitation(1990- 2000) at Haisawita station

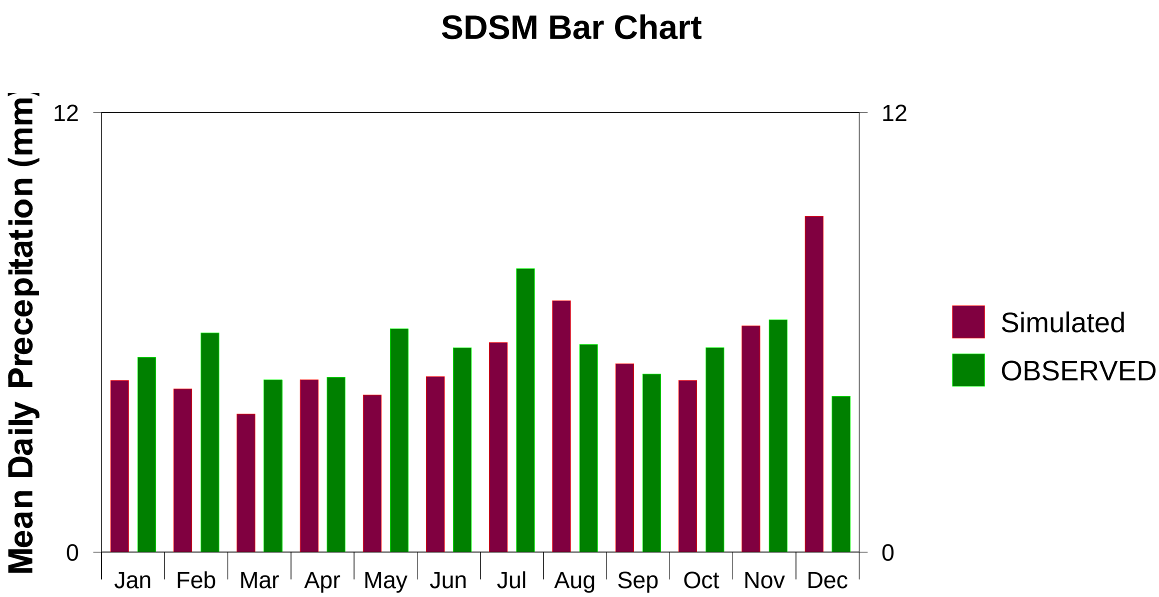

Figure B.8 Validation Result of SDSM Model Downscaling of daily precipitation(1990- 2000) at Awassa station

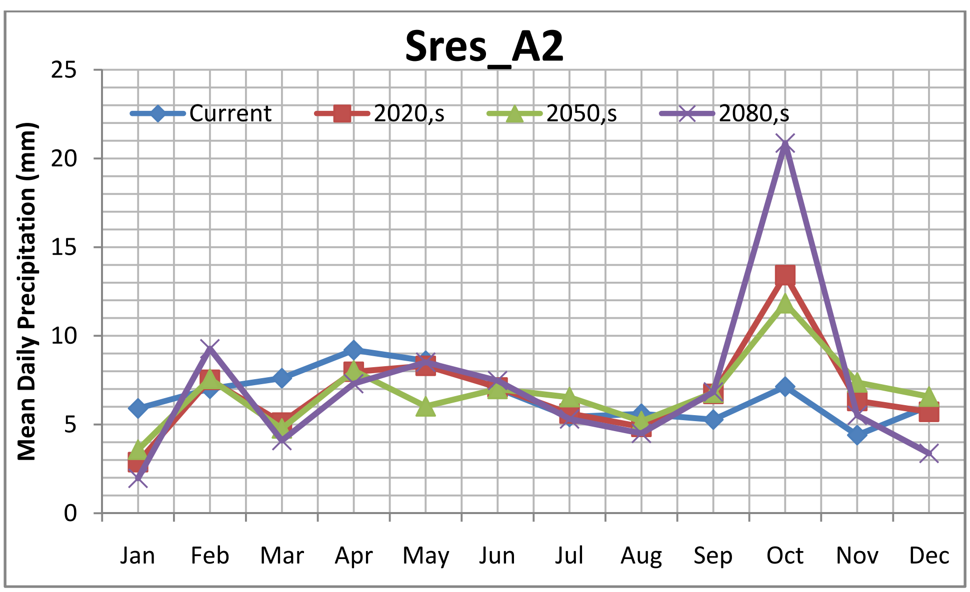

(a)

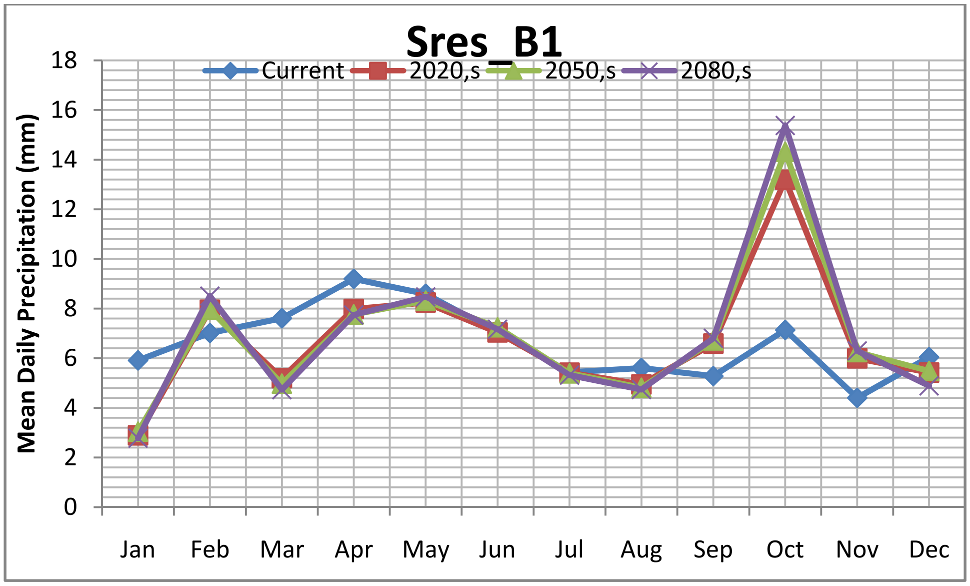

(b)

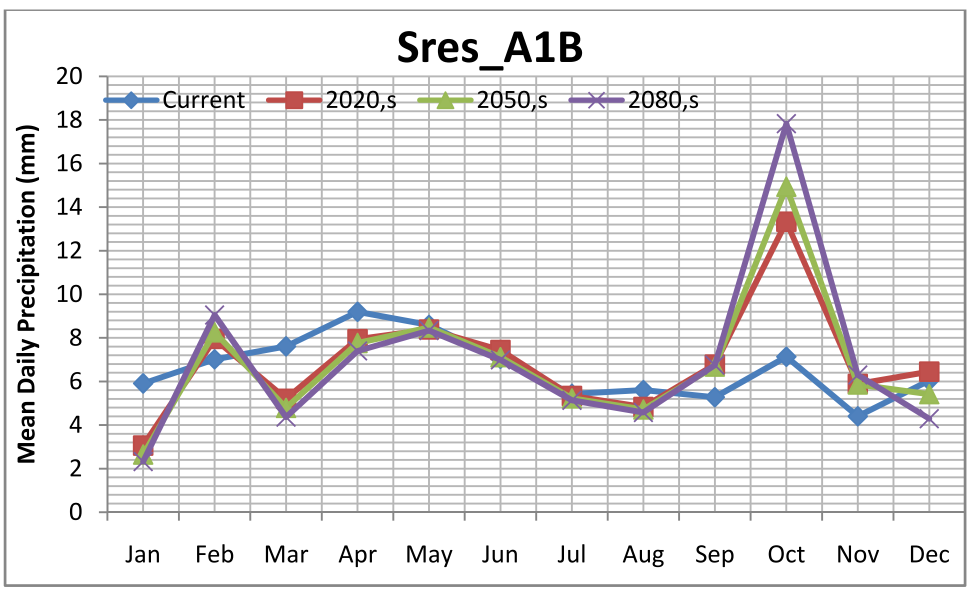

(c)

Figure B.9 General trend in the mean daily precipitation at Shashemene corresponding to climate change scenario downscaled with SDSM ,(a) for sres_A2,(b) for sres_B1 and (c) for sres_A1B

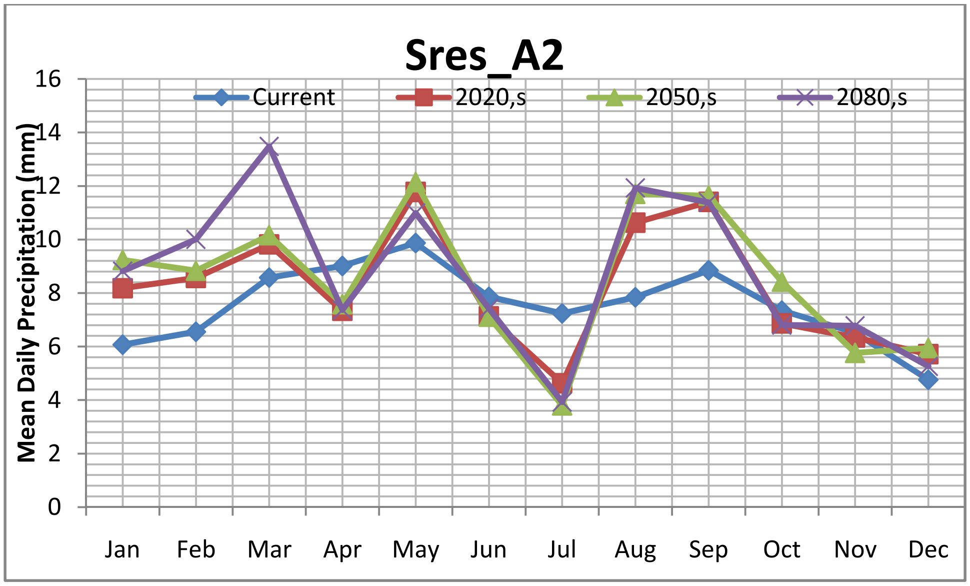
Sres_A2
Current
2020,s
2050,s
2080,s
Mean Daily Precipitation (mm)
16
14
12
10
8
6
4
2
0
Jan
Feb
Mar
Apr
May
Jun
Jul
Aug
Sep
Oct
Nov
Dec

(a)

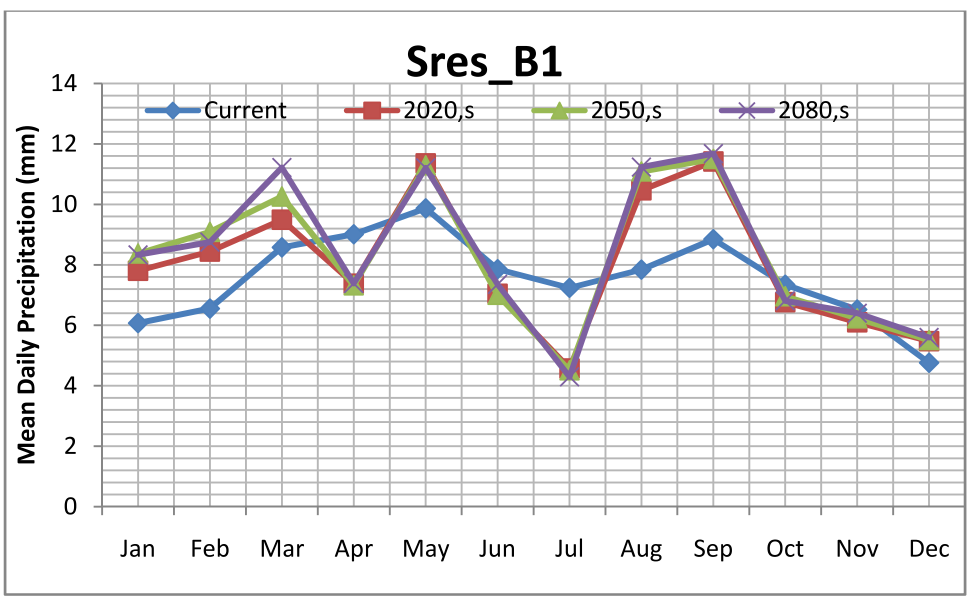
Sres_B1
Current
2020,s
2050,s
2080,s
Mean Daily Precipitation (mm)
14
12
10
8
6
4
2
0
Jan
Feb
Mar
Apr
May
Jun
Jul
Aug
Sep
Oct
Nov
Dec

(b)

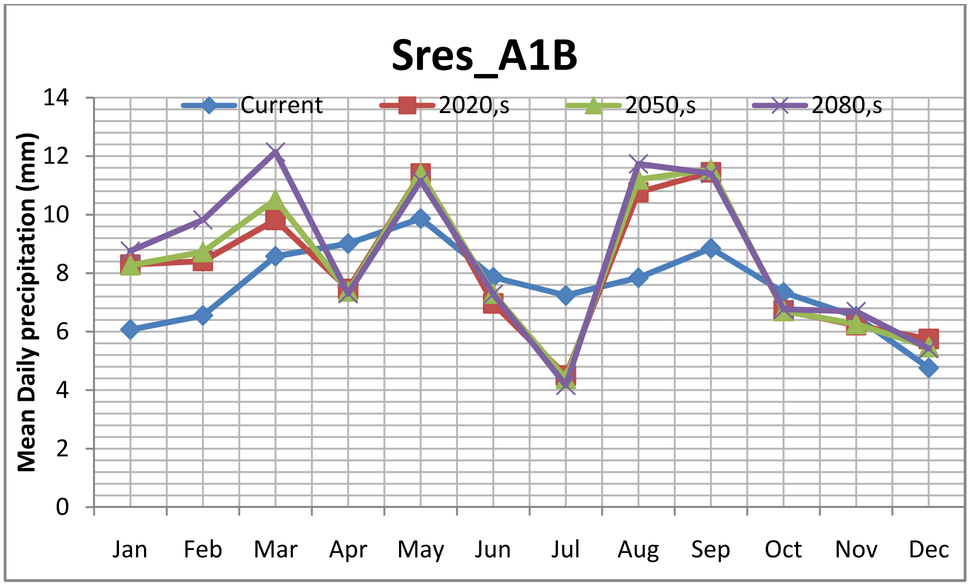

(c)

Figure B.10 Figure B.8 General trend in the mean daily precipitation at Haisawita corresponding to climate change scenario downscaled with SDSM, (a) for sres_A2,(b) for sres_B1 and (c) for sres_A1B

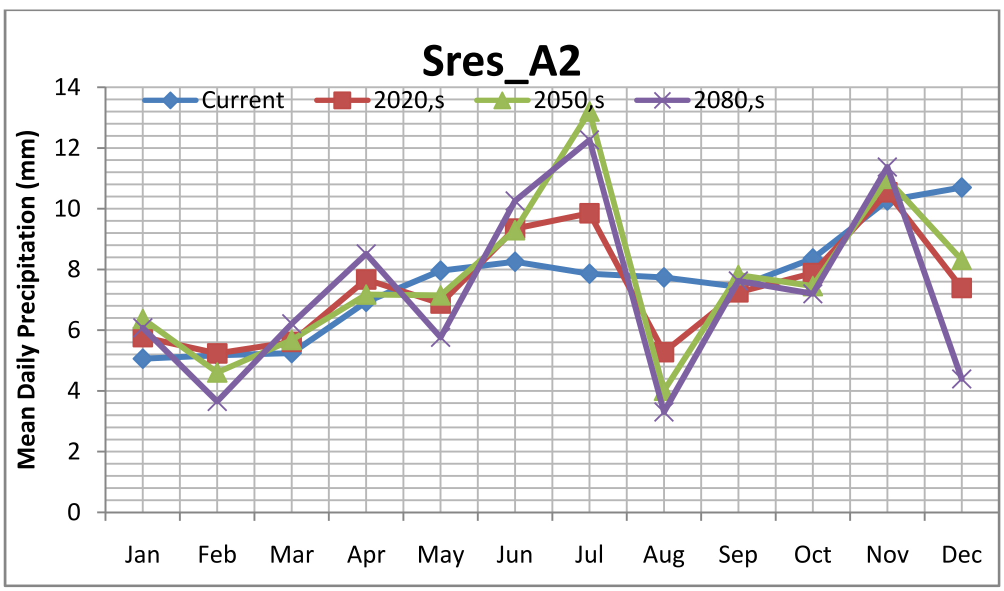

(a)

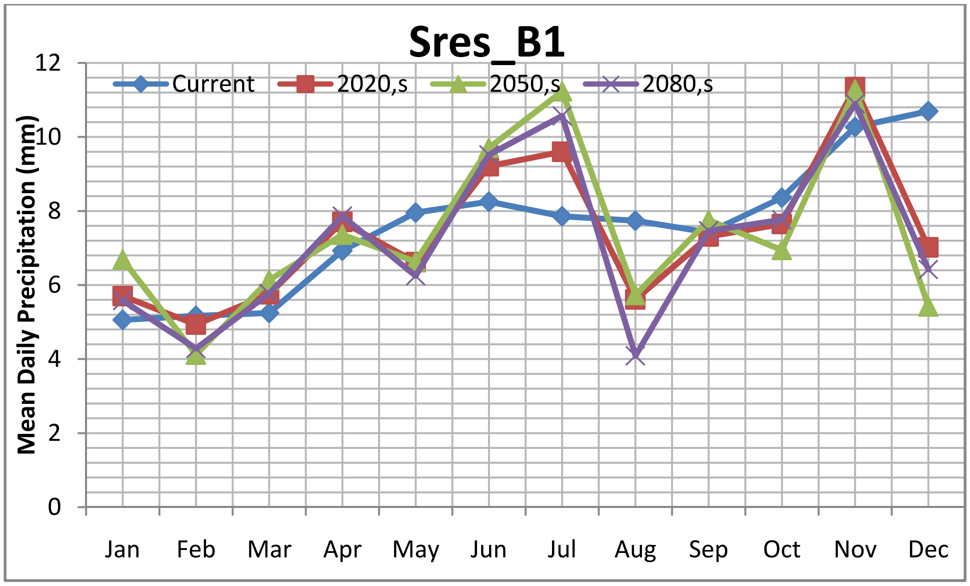

(b)

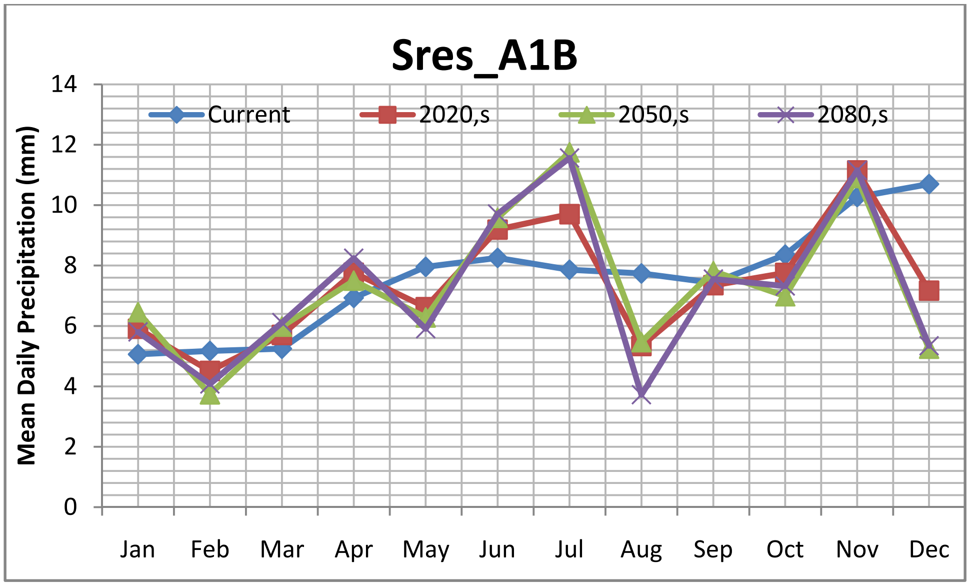

(c)

Figure B.11 Figure B.9 Figure B.8 General trend in the mean daily precipitation at Awassa corresponding to climate change scenario downscaled with SDSM ,(a) for sres_A2,(b) for sres_B1 and (c) for sres_A1B

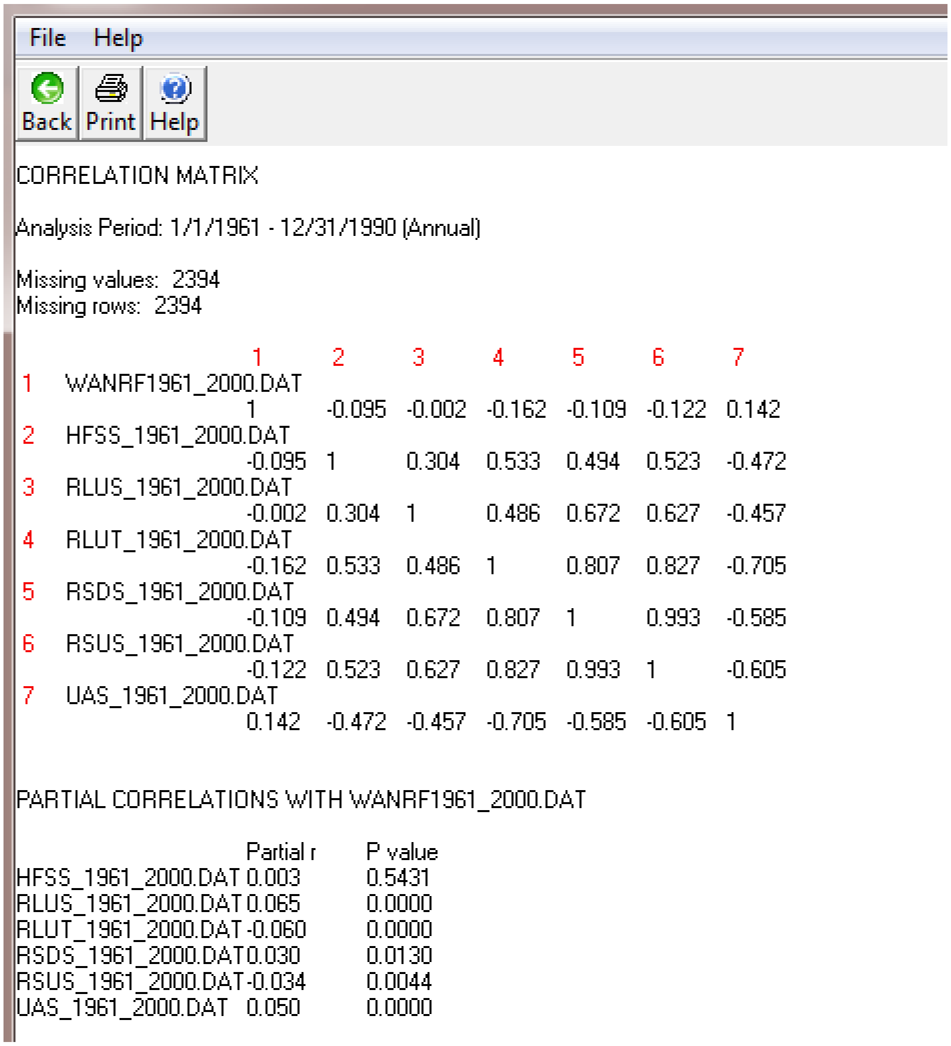

File Help

Back Print Help

CORRELATION MATRIX

Analysis Period: 1/1/1961 - 12/31/1990 (Annual)

Missing values: 2394
Missing rows: 2394

		1	2	3	4	5	6	7
1	WANRF1961_2000.DAT	1	-0.095	-0.002	-0.162	-0.109	-0.122	0.142
2	HFSS_1961_2000.DAT	-0.095	1	0.304	0.533	0.494	0.523	-0.472
3	RLUS_1961_2000.DAT	-0.002	0.304	1	0.486	0.672	0.627	-0.457
4	RLUT_1961_2000.DAT	-0.162	0.533	0.486	1	0.807	0.827	-0.705
5	RSDS_1961_2000.DAT	-0.109	0.494	0.672	0.807	1	0.993	-0.585
6	RSUS_1961_2000.DAT	-0.122	0.523	0.627	0.827	0.993	1	-0.605
7	UAS_1961_2000.DAT	0.142	-0.472	-0.457	-0.705	-0.585	-0.605	1

PARTIAL CORRELATIONS WITH WANRF1961_2000.DAT

	Partial r	P value
HFSS_1961_2000.DAT	0.003	0.5431
RLUS_1961_2000.DAT	0.065	0.0000
RLUT_1961_2000.DAT	-0.060	0.0000
RSDS_1961_2000.DAT	0.030	0.0130
RSUS_1961_2000.DAT	-0.034	0.0044
UAS_1961_2000.DAT	0.050	0.0000

Figure B.12 One of Correlation value during potential predictor selection for calibration of Wando Genet Rainfall

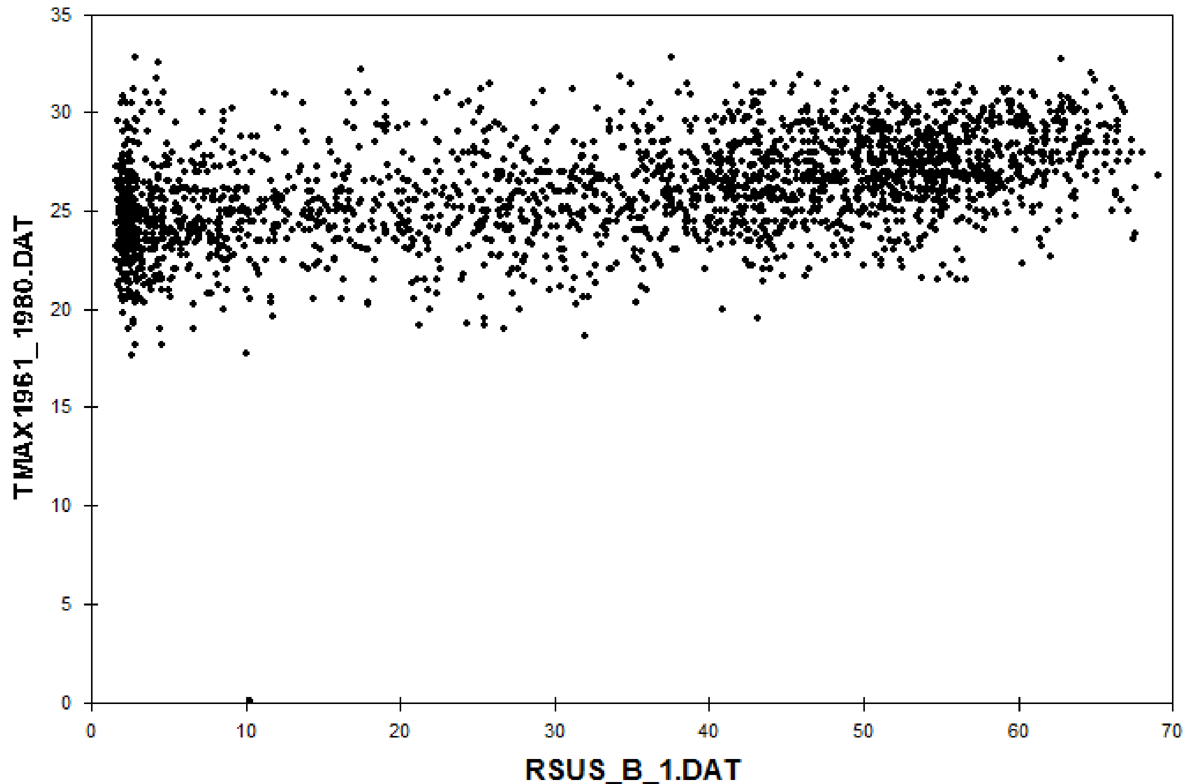

Figure B.13 One of Scatter plot during potential predictor selection for calibration of Maximum Temperature

Appendix C

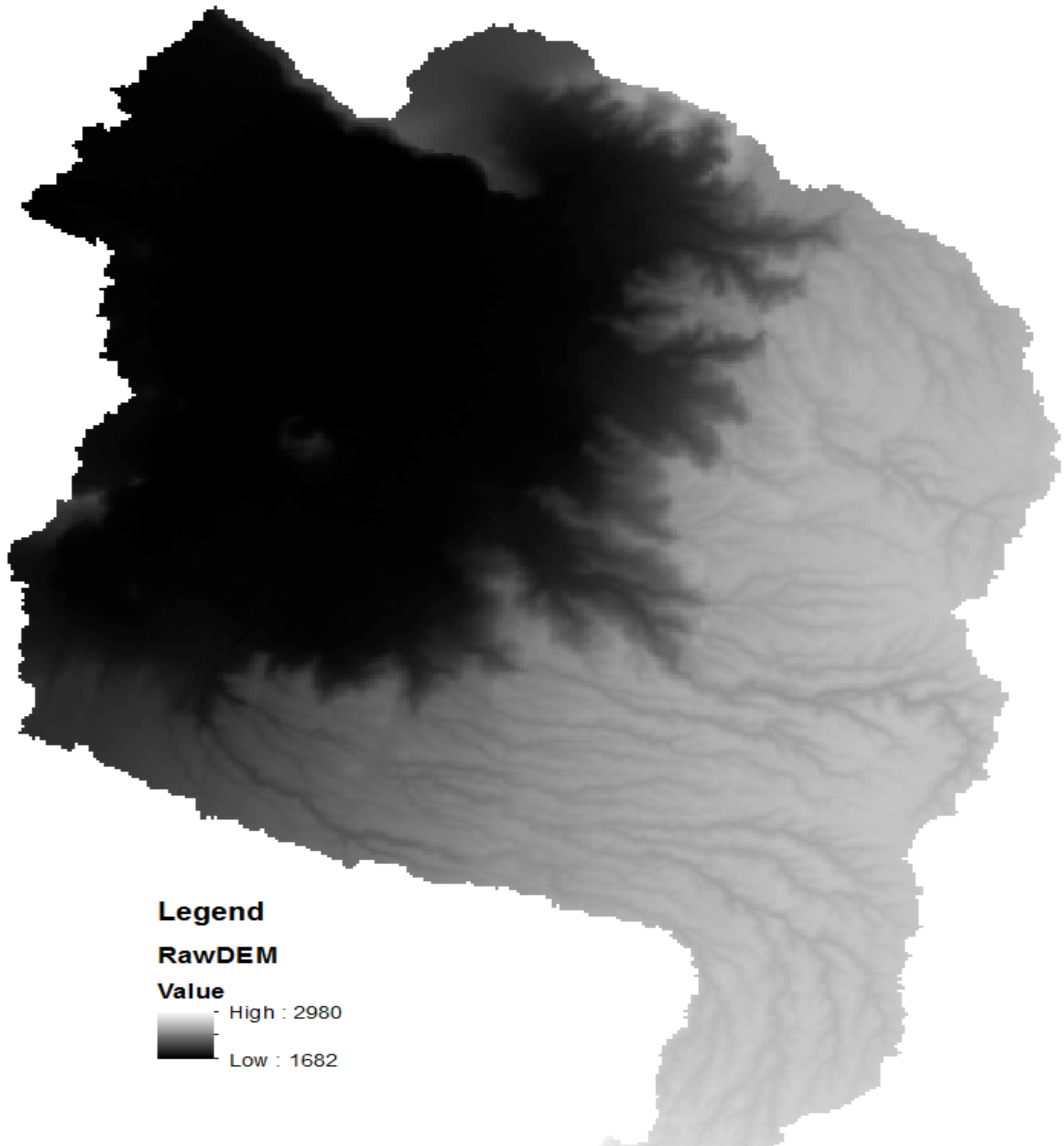

Figure C.1Tikur wuha Sub-catchment DEM

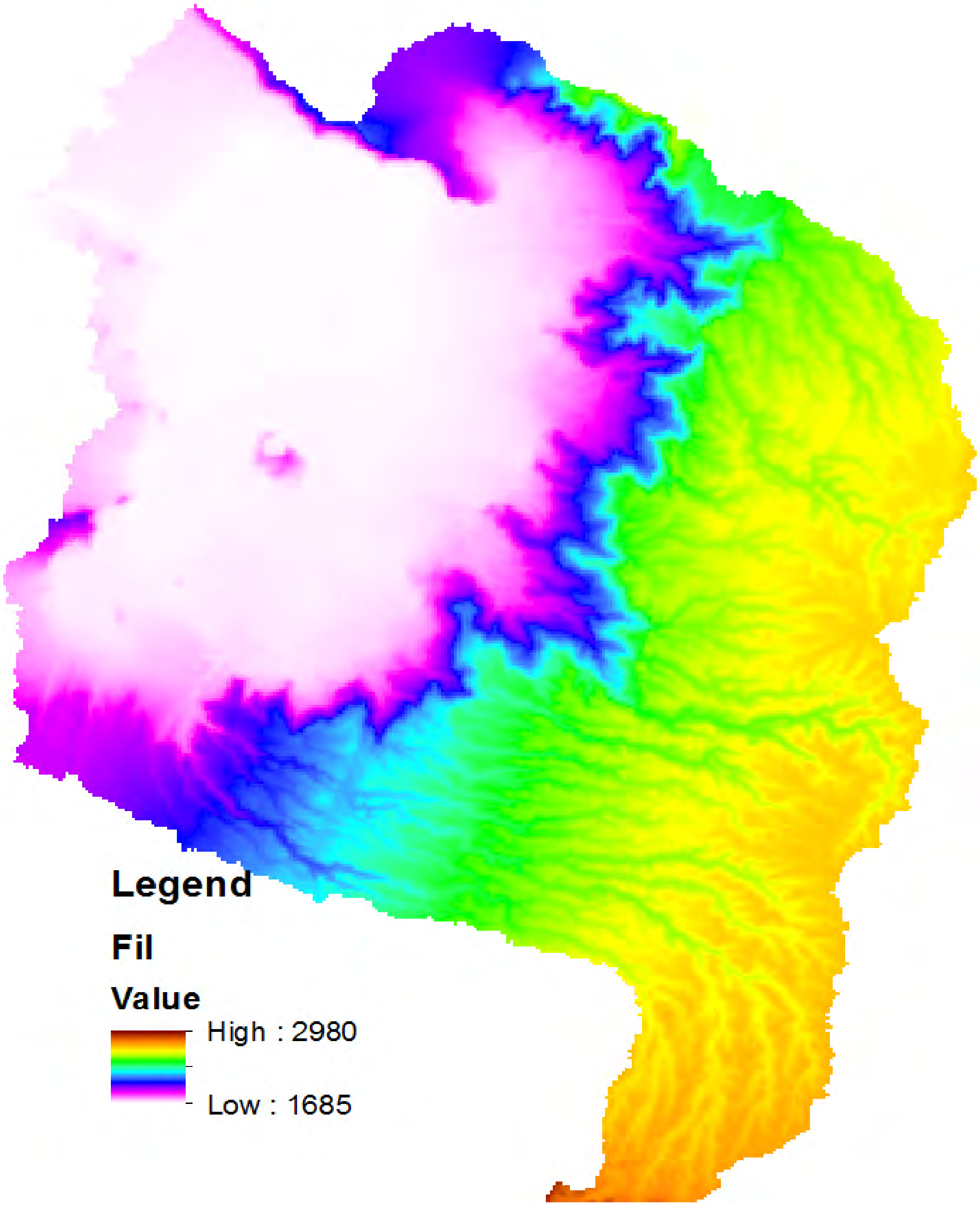

Figure C.2 . Filled DEM

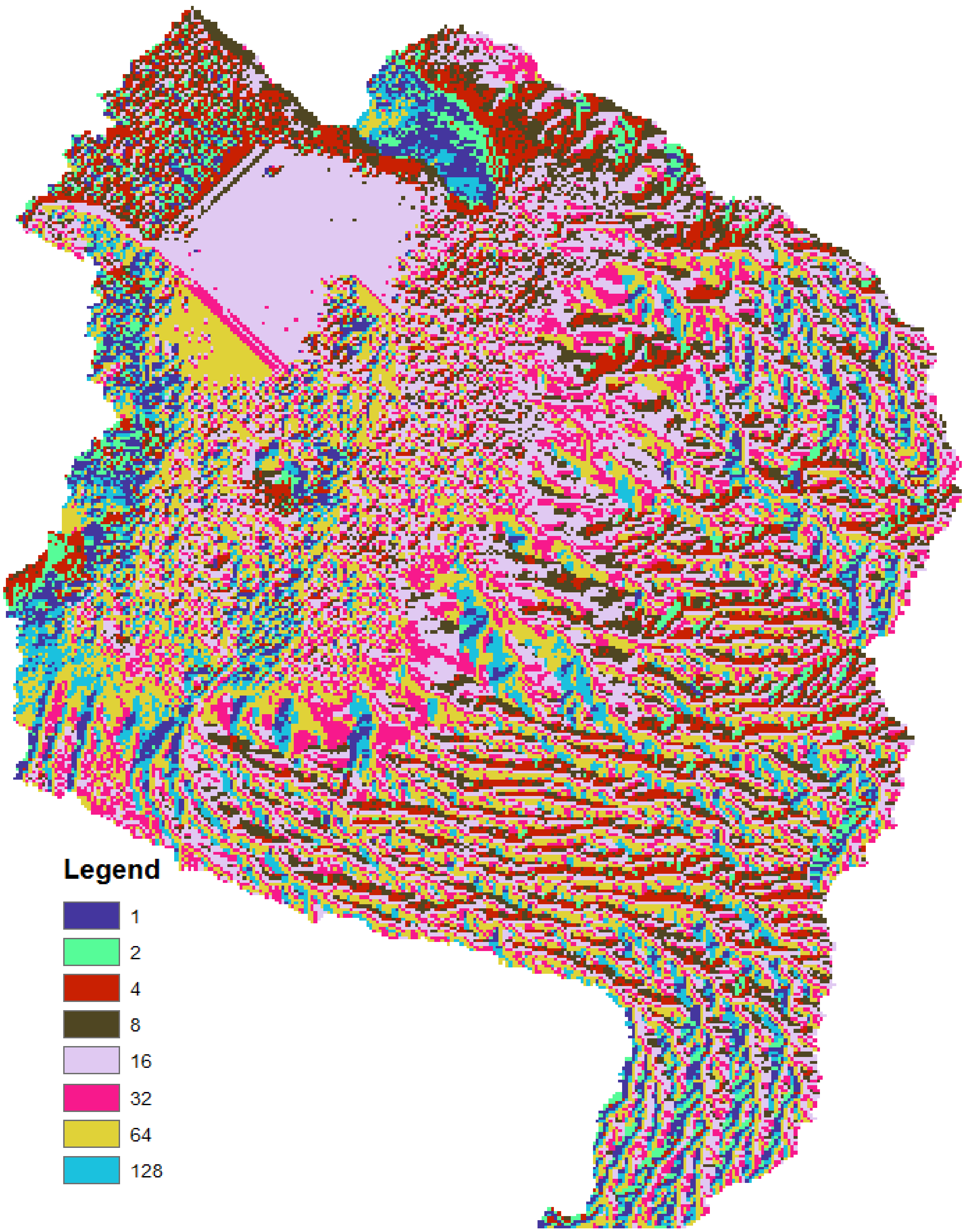

Figure C.3Flow Direction

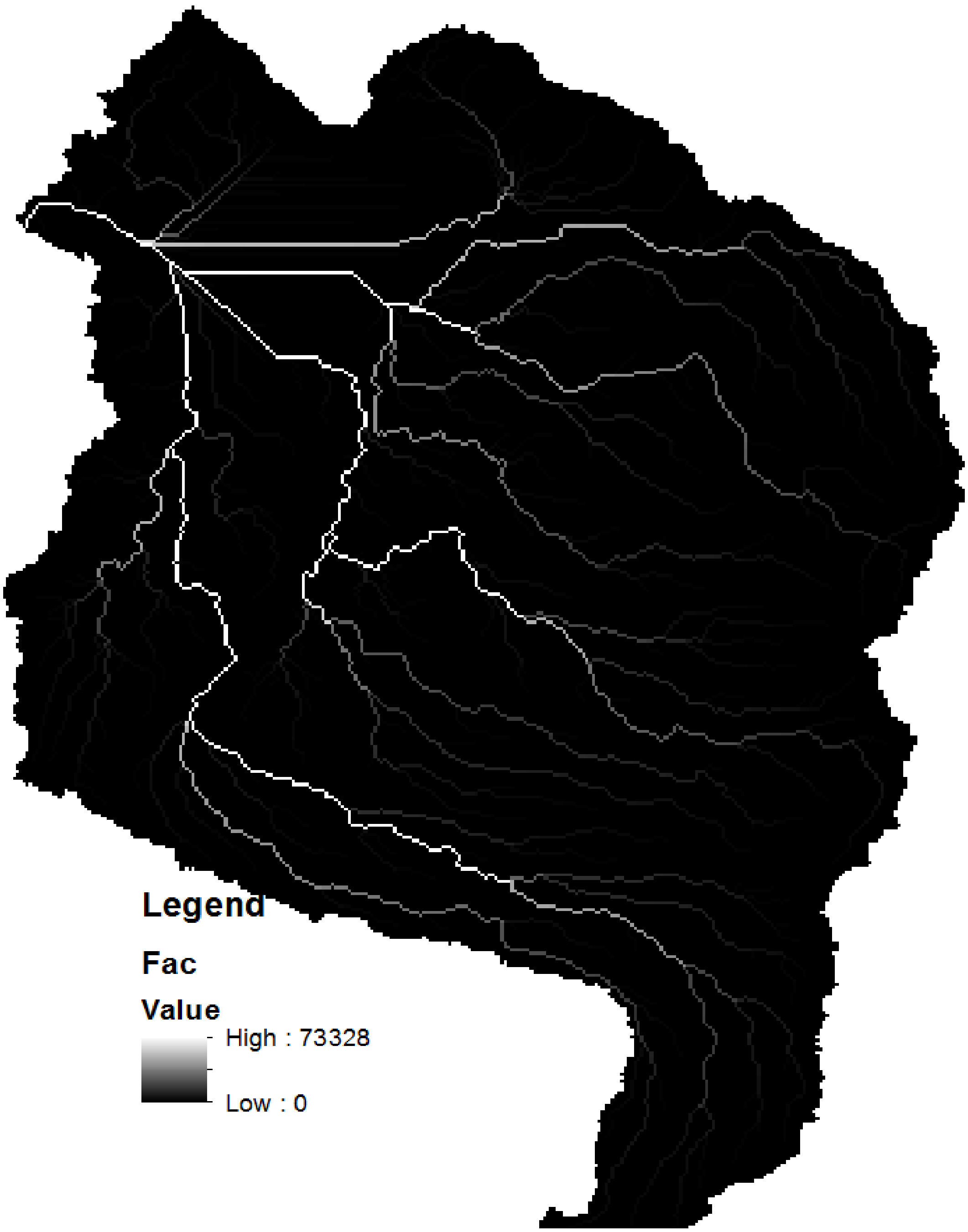

Figure C.4 Flow Accumulation

Appendix D

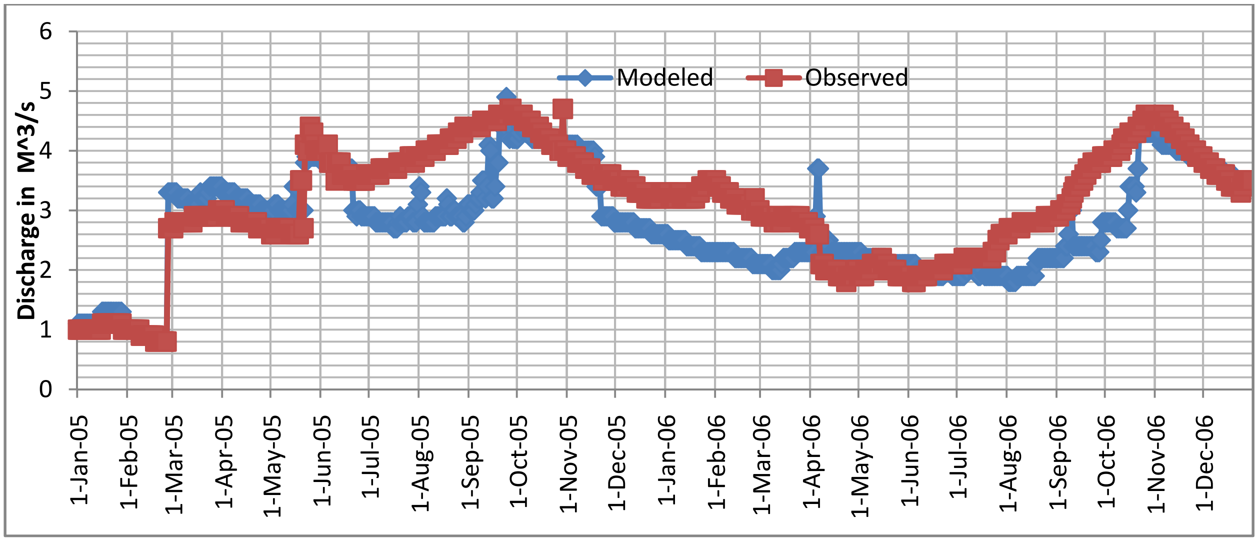

Figure D.1 Validation result of HEC- HMS for Year 2005 and 2006

Appendix E

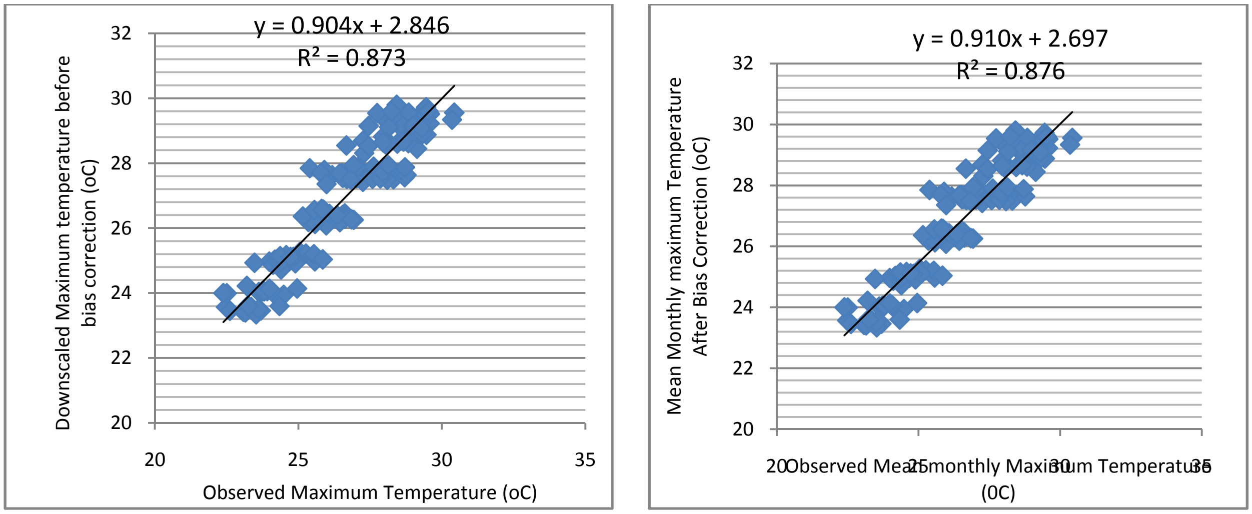

Figure E.1 scatter plots for temperature downscaled before and after bias-correction

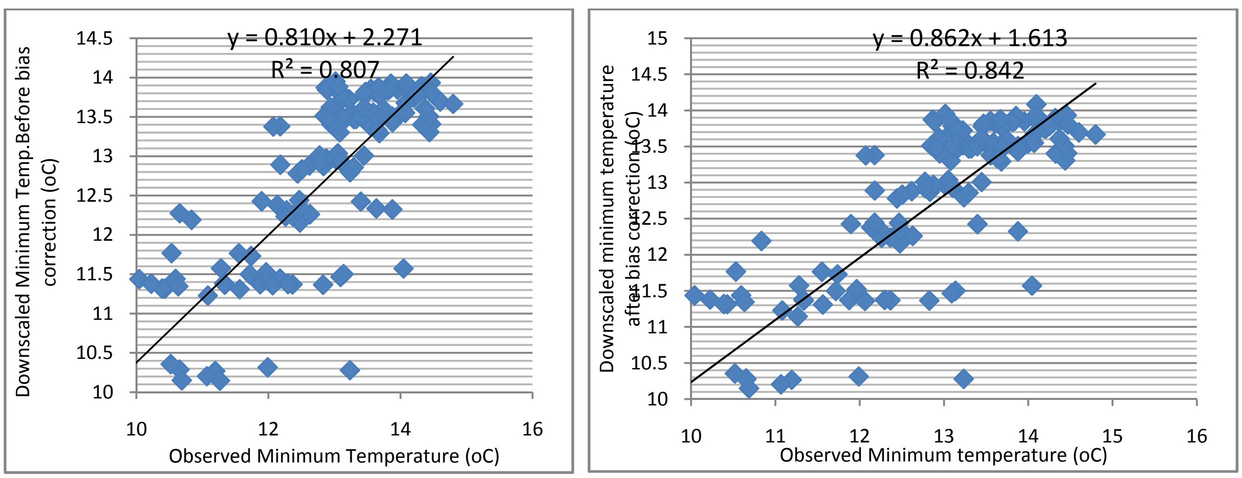

Figure E.2 scatter plots for temperature downscaled before and after bias-correction

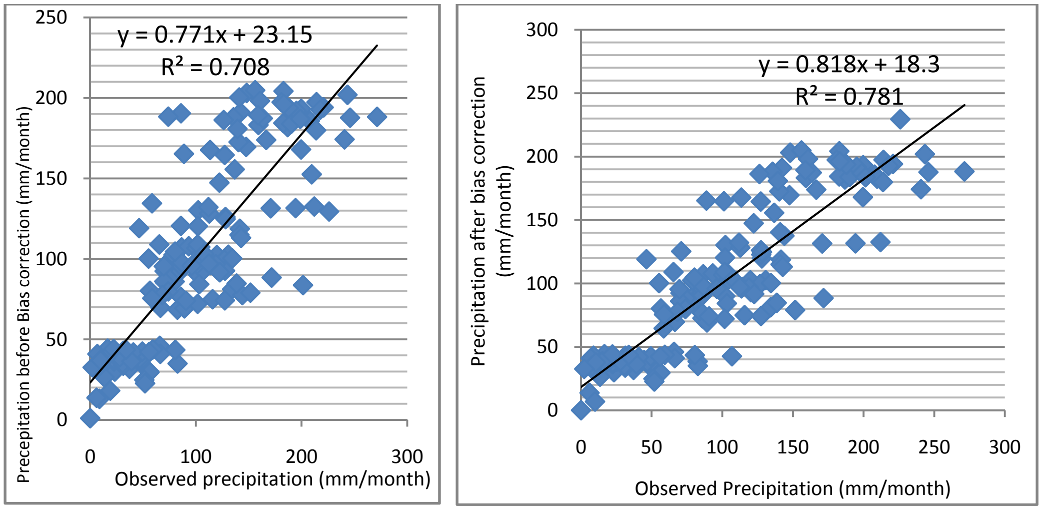

Figure E.3 scatter plots for precipitation downscaled before and after bias-correction (Haisawita Station)

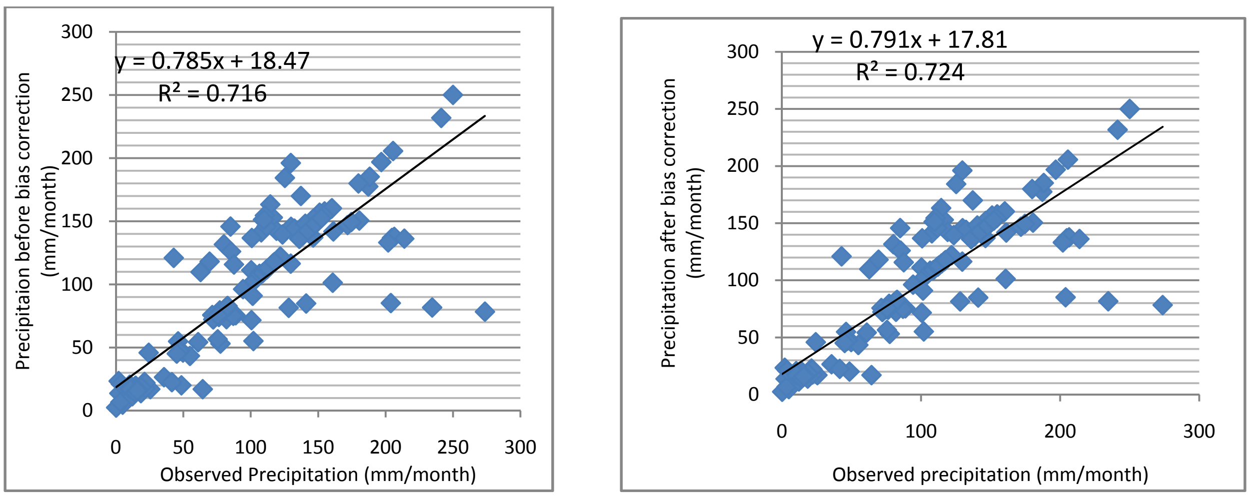

Figure E.4 scatter plots for precipitation downscaled before and after bias-correction (Wondo Genet Station)

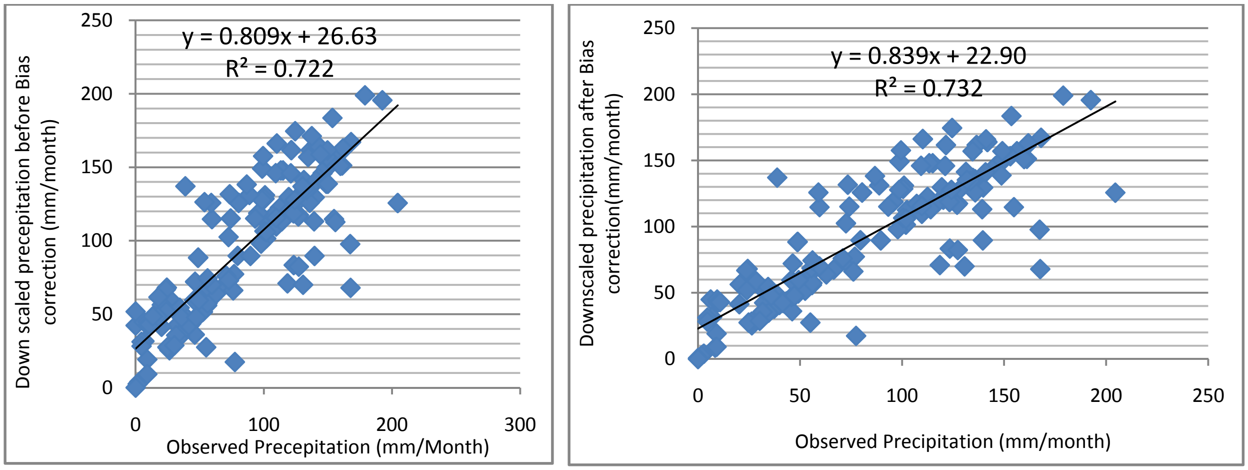

Figure E.5 scatter plots for precipitation downscaled before and after bias-correction (Awassa Station)

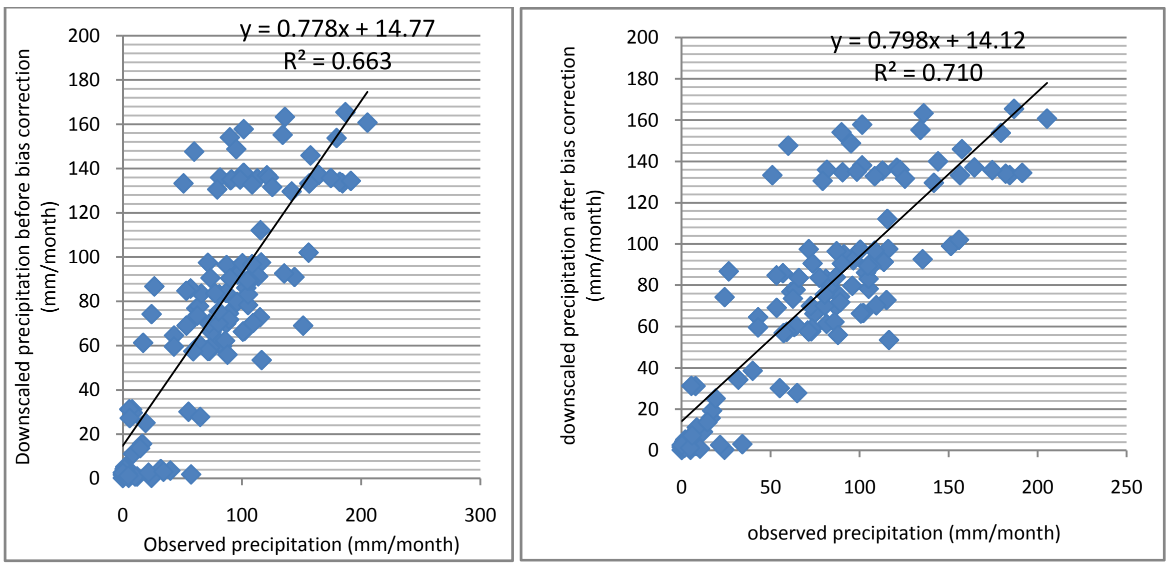

Figure E.6 scatter plots for precipitation downscaled before and after bias-correction (Shashemene Station)